Current detectors, noise and control.

E. Majorana - I.N.F.N. Roma
ettore.majorana@roma1.infn.it
http://www.virgo.infn.it/

VESF school on gravitational waves

Sexten Centre for Astrophysics, July 26th, 2010

World map of ground-based interferometric detectors

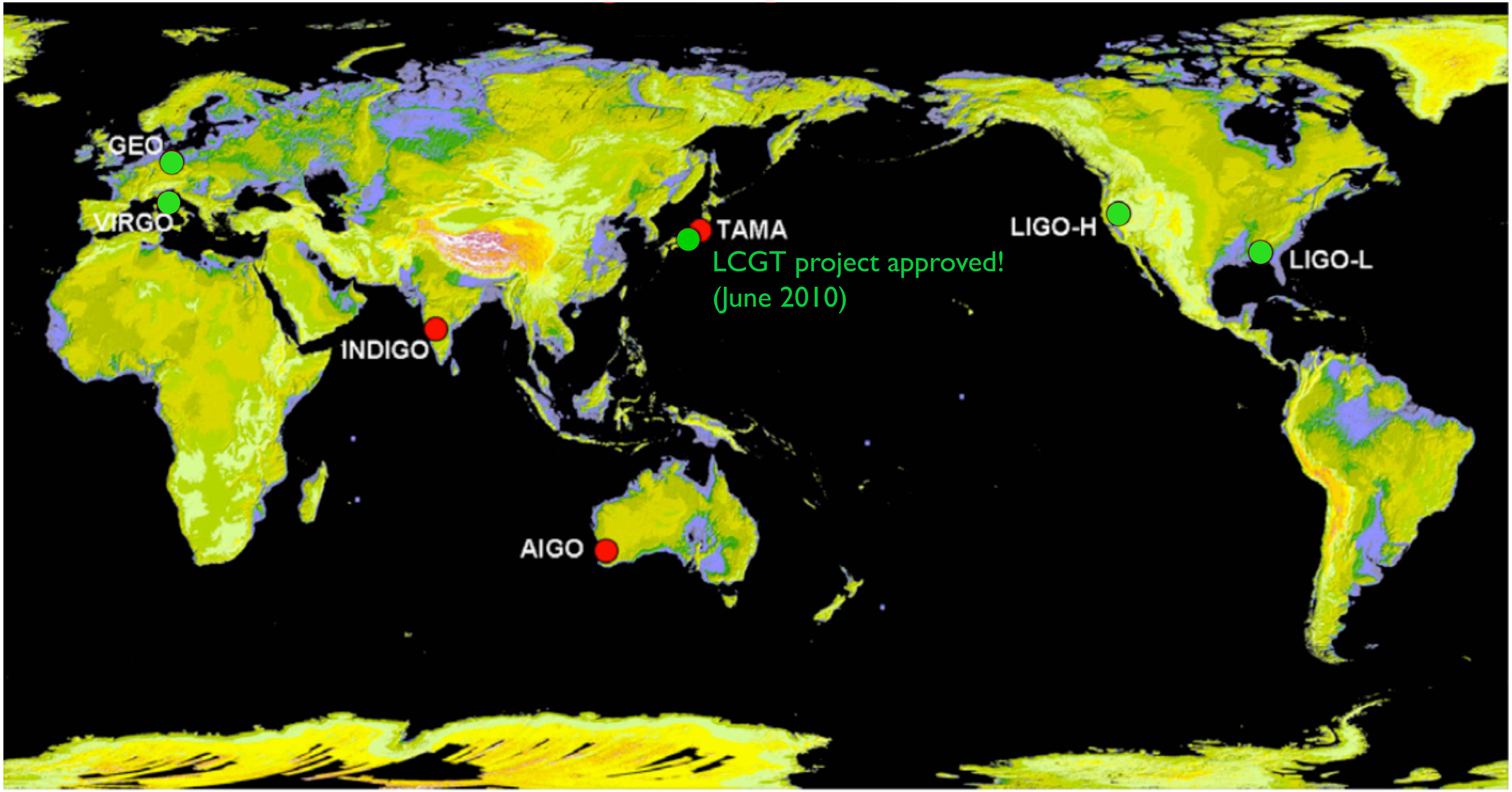

Outline

I) Basic elements
II) External mechanical disturbance: suspended Optics
III) Feednack control basics
IV) Locking
V) Noise hunting and performance
VI) Enjoying digital control in practice
VII) Noise hunting and performance
VIII) Focus on monolithic suspension

First generation of interferometric GW detectors

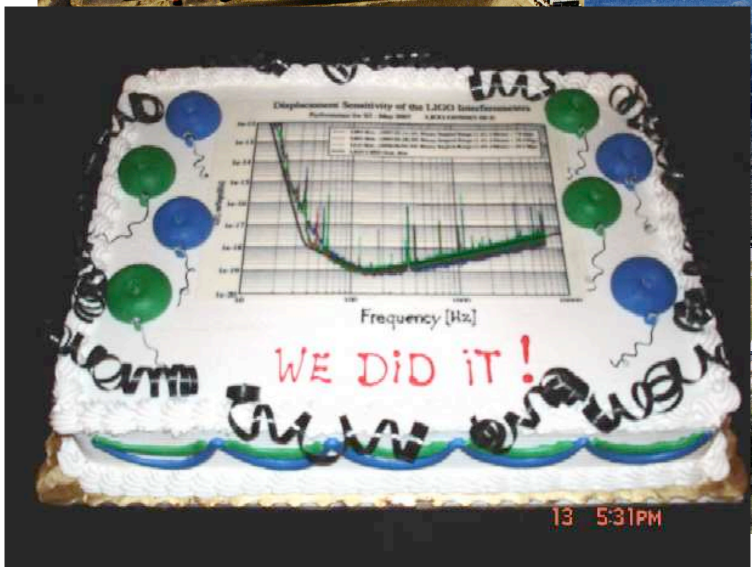

Basic elements

I) Free-test-mass differential detector in practice

Wide-band detection

(=> **more detectable sources !!**)

possible through interferometry.

Interference fringes

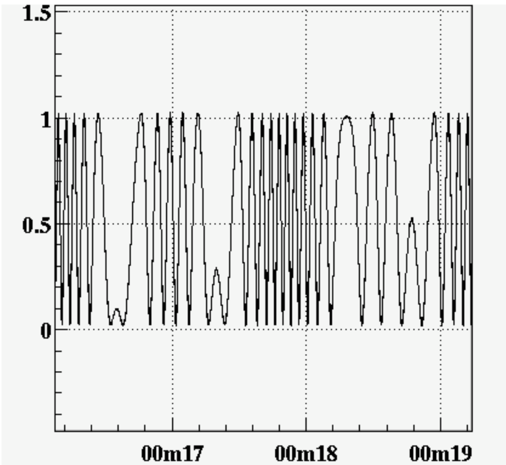

(Next page)

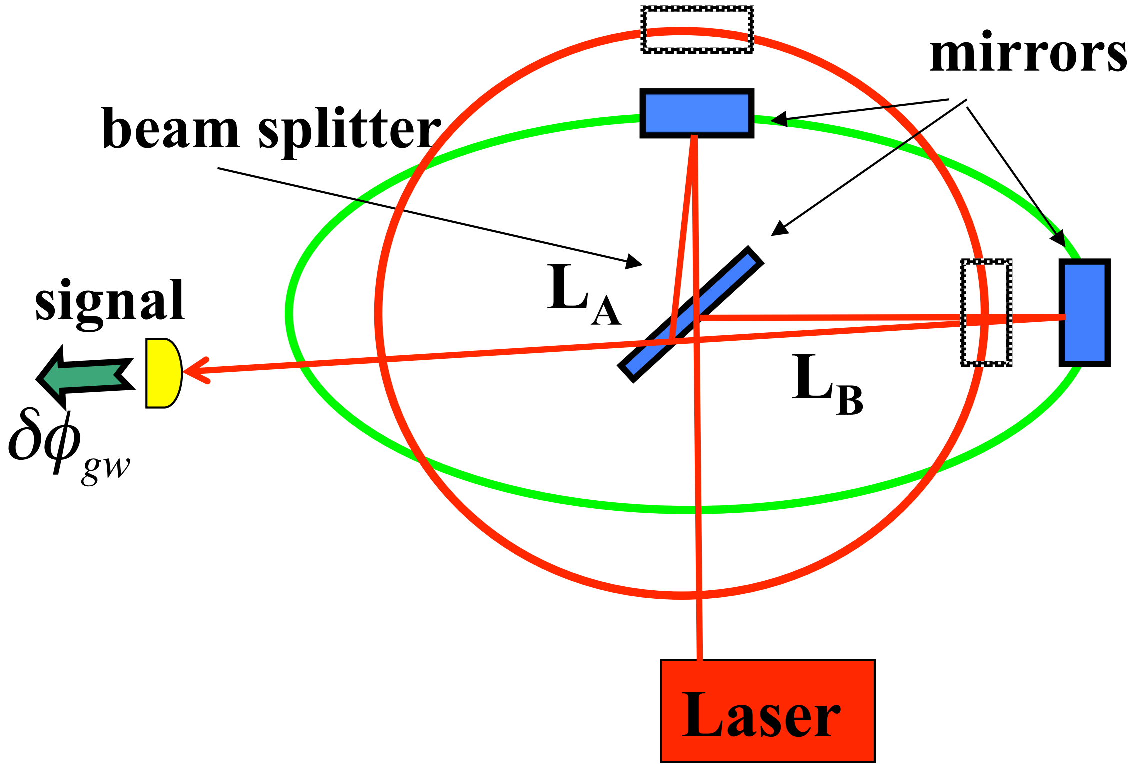

Michelson ITF, response to GW

$$ds^2 = -c^2dt^2 + (1+h_+(t))dx^2 + (1+h_+(t))dy^2 + dz^2 \;\Big|_{\text{along } x} \Rightarrow \frac{dx}{dt} = \pm\frac{c}{\sqrt{1+h_+(t)}}$$

$$\int_{t_1}^{t} \frac{dt'}{\sqrt{1+h(t')}} = \frac{1}{c}\left(\int_0^{l_1} dx - \int_{l_1}^{0} dx\right) = \frac{2l_1}{c}$$

$$\int_{t_1}^{t}\left(1-\frac{1}{2}h(t')\right)dt' = (t-t_1) - \frac{1}{2}\int_{t-\frac{2l_1}{c}}^{t} h(t')dt' \approx \frac{2l_1}{c}$$

$$\varphi_x(t) = \omega t_1 \approx \omega\cdot\left(t - \frac{2l_1}{c} - \frac{1}{2}\int_{t-\frac{2l_1}{c}}^{t} h(t')dt'\right)$$

in the same way

$$\varphi_y(t) = \omega t_2 \approx \omega\cdot\left(t - \frac{2l_2}{c} + \frac{1}{2}\int_{t-\frac{2l_2}{c}}^{t} h(t')dt'\right)$$

if $l_1=l_2=l$ $$\Delta\varphi(t) \approx \omega\int_{t-\frac{2l}{c}}^{t} h(t')dt' = \Delta\varphi_{GW}(t)$$

Antenna Pattern for free-mass detectors

$$\frac{\Delta L}{L} = \frac{\Delta L_1 + \Delta L_2}{L} = \frac{1+\cos^2\theta}{2}\cos(2\varphi)h^{+} + \cos\theta\,\sin(2\varphi)h^{x}$$

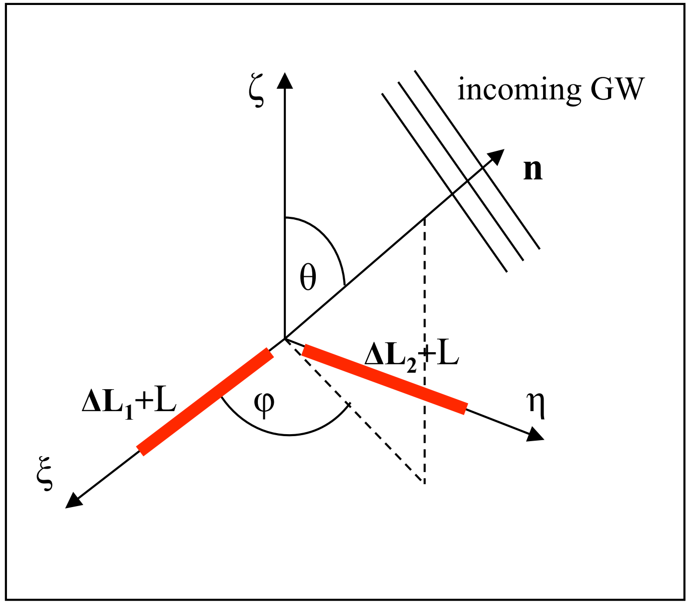

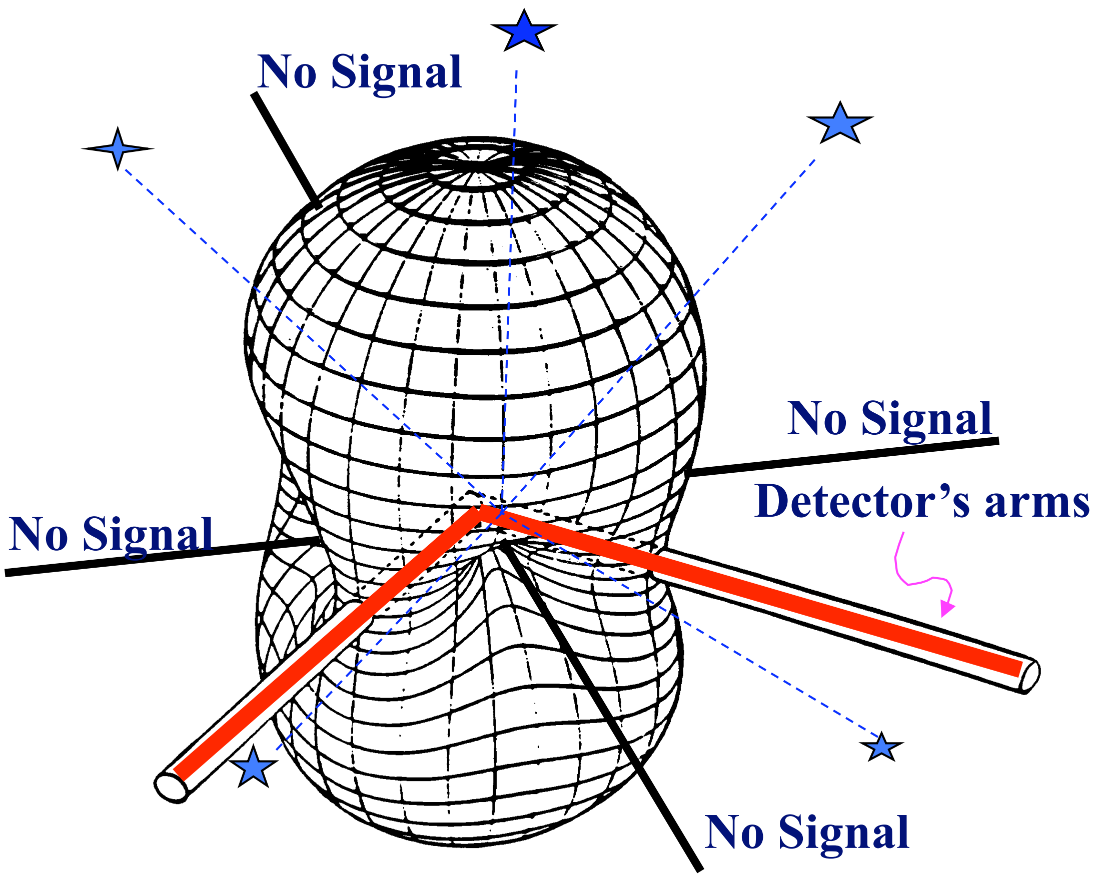

EMVESF270710

Antenna Pattern for free-mass detectors

$$\frac{\Delta L}{L} = \frac{\Delta L_1 + \Delta L_2}{L} = \frac{1+\cos^2\theta}{2}\cos(2\varphi)h^{+} + \cos\theta\,\sin(2\varphi)h^{x}$$

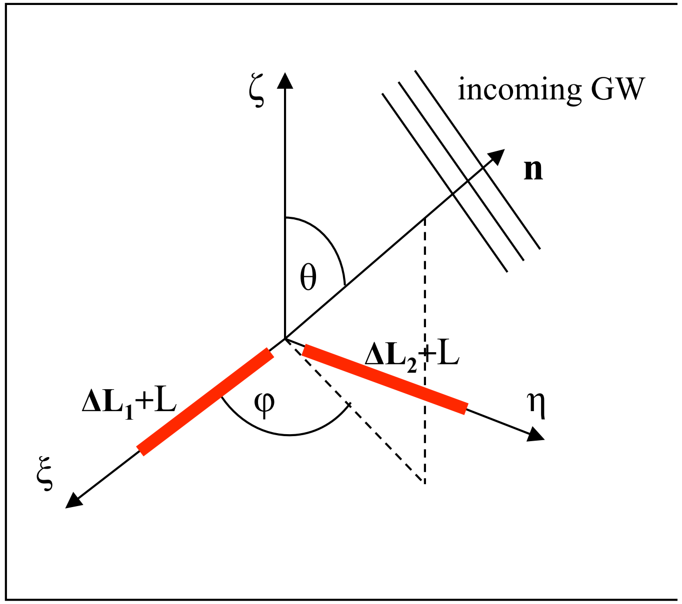

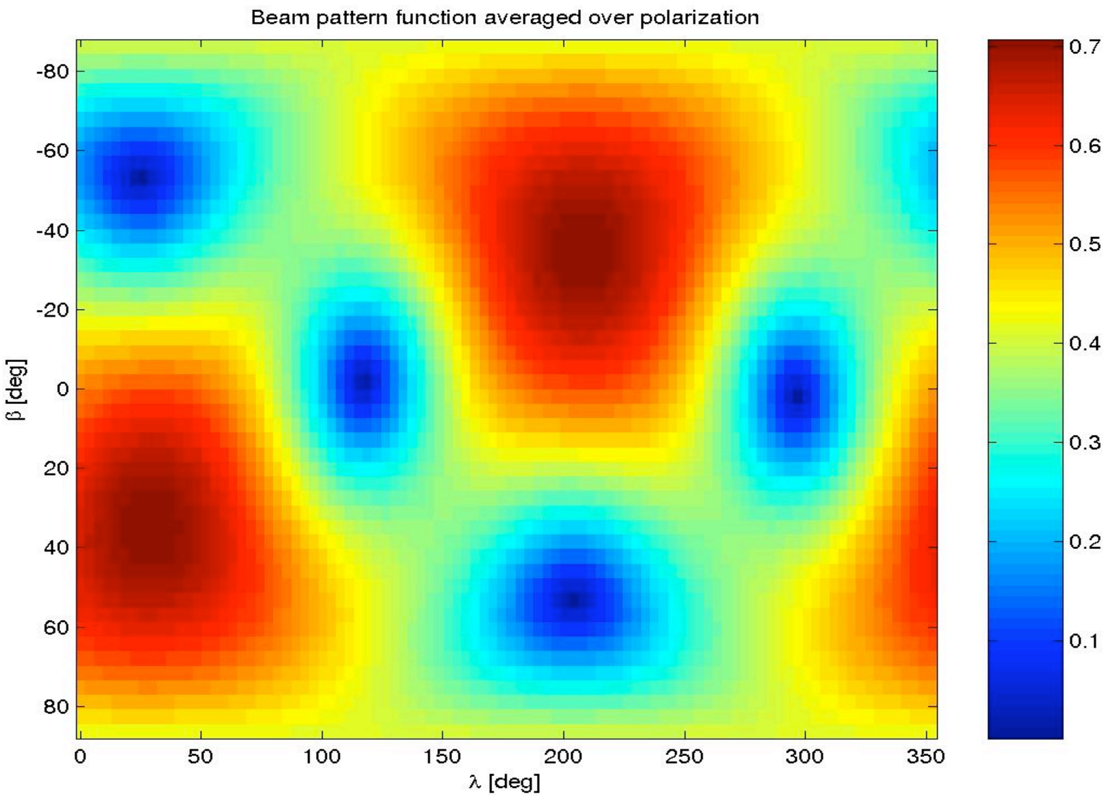

EMVESF270710

(ecliptic coords)

Network of gravitational wave detectors as a global instrument

Coherent analysis with several detectors:
crucial to detect the signal and to reconstruct the 5 parameters of the wave

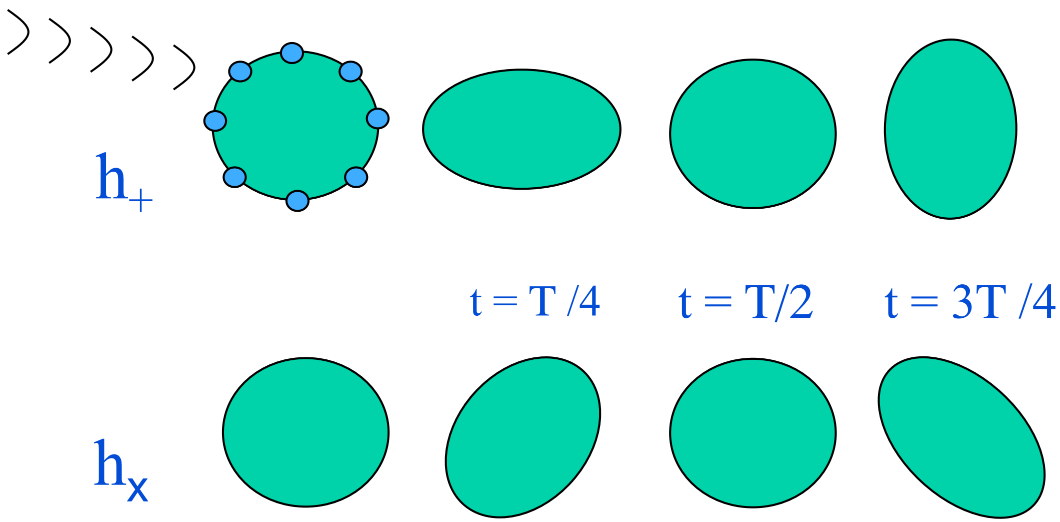

2 polarization states and initial phase
(h_+, h_x, ϕ_0)

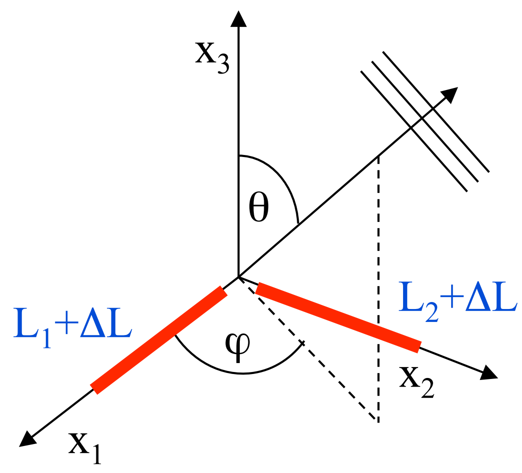

incidence direction
(φ, θ)

Network patterns

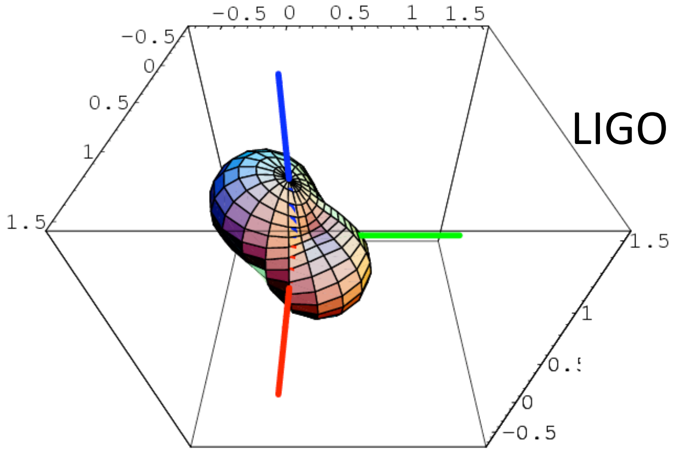

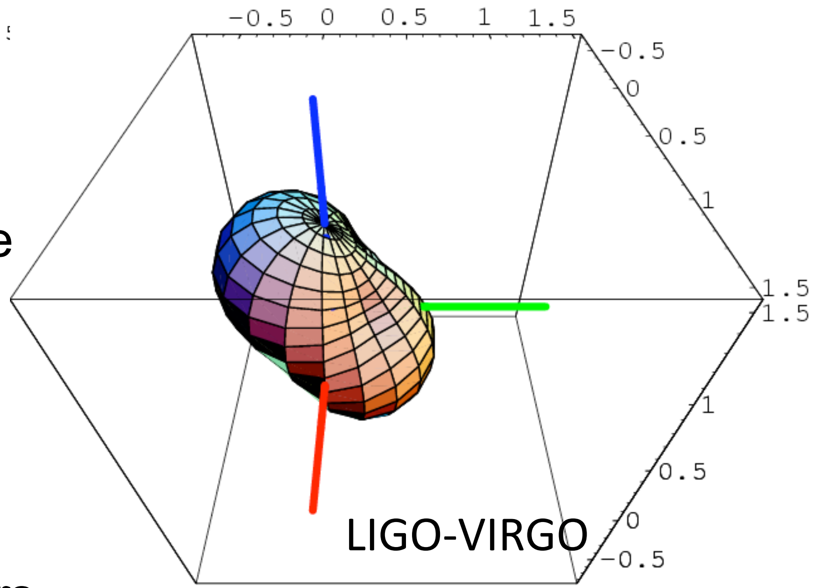

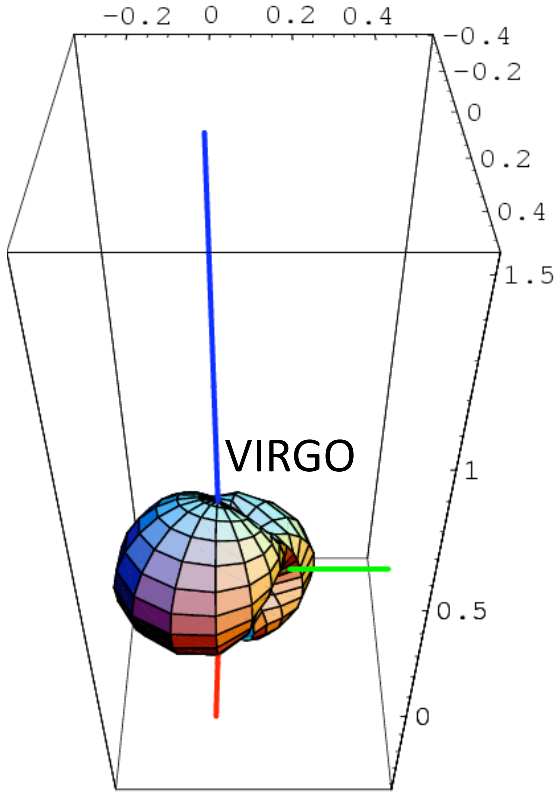

(A. Viceré)

Environmental monitoring and engineering signals are used to discard big local disturbances. Coincidence analysis is essential to discard false alarms at the level of the residual noise affecting the single detectors.

For example, coherent combination advanced LIGO-H/LIGO-L/Virgo (SNR=8, eff. 90%), enlarges the BNS detection distance at which BNS from 150-170 Mpc of the single antennas ➔ 270 Mpc

Michelson ITF, basic formalism (I)

$$\psi_{in} = Ke^{i\chi}$$

$$\psi_1 = t_{BS}\psi_{in} \qquad \psi_5 = ir_{BS}\psi_{in}$$

$$\psi_2 = e^{-ikl_1}\psi_1 \qquad \psi_6 = e^{-ikl_2}\psi_5$$

$$\psi_3 = ir_1\psi_2 \qquad \psi_7 = ir_2\psi_6$$

$$\psi_4 = e^{-ikl_1}\psi_3 \qquad \psi_8 = e^{-ikl_2}\psi_7$$

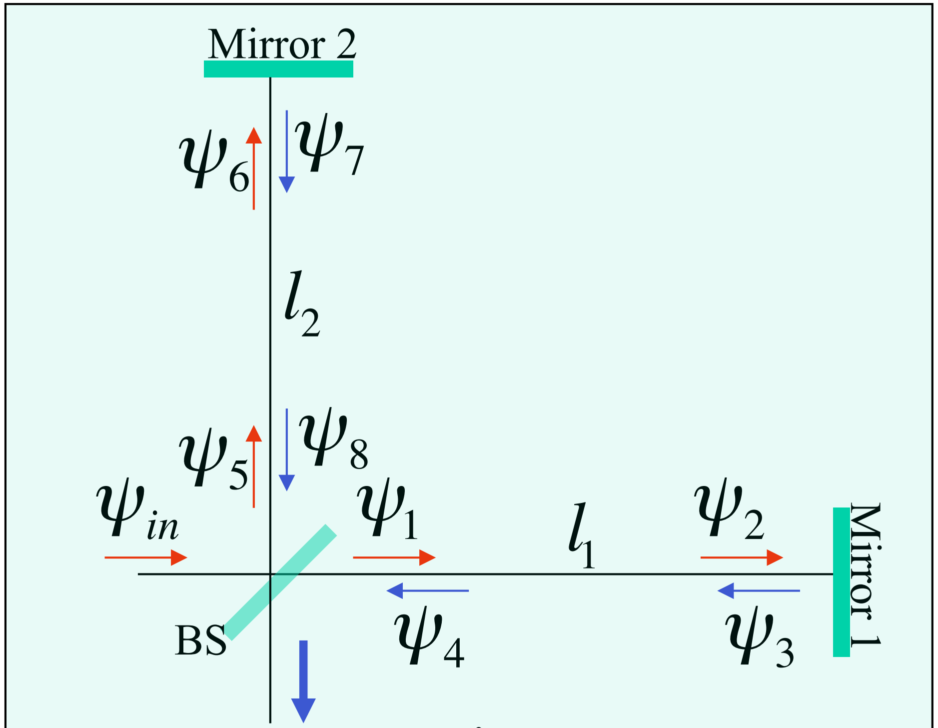

$$\psi_{out} = ir_{BS}\psi_4 + t_{BS}\psi_8$$

$$|\psi_{out}|^2 = P_{in} r_{BS}^2 t_{BS}^2 (r_1^2 + r_2^2)\left(1 + \frac{2r_1 r_2}{r_1^2 + r_2^2}\cos(2k \cdot \delta l)\right)$$

$$C = contrast = \frac{2r_1 r_2}{r_1^2 + r_2^2} = \frac{P_{out}^{\max} - P_{out}^{\min}}{P_{out}^{\max} + P_{out}^{\min}}$$

$$l_1 - l_2$$

Michelson ITF, basic formalism (II)

Given a GW source at distance r the effect due to optimal coupling of polarization "+" is:

$$l_1 \to l_1\left(1+\frac{1}{2}h_+\right)$$

$$l_2 \to l_2\left(1-\frac{1}{2}h_+\right)$$

$$P_{out} = \frac{P_{in}}{2}\left(1 + C\cos(2k\cdot\delta l) + Ck(l_1+l_2)\cdot h_+\sin(2k\cdot\delta l)\right)$$

$$= P_{Mich.} + \delta P_{GW}$$

$$\boxed{\delta P_{GW} \propto Amplitude_{GW}}$$

ITF **power** signal is sensitive to the **amplitude** of gravitational waves (and not to their **power**, as in e.m. wave detection).

ITF GW signal fades as 1/r (and not as 1/r^2 as in e.m. telescopes): the number detectable sources increases as **ΔSensitivity^3**

Sensitivity intrinsically limited by the noise source affecting the power at the detection port: **shot noise**. Dark-fringe ($P_{out}^{\min}=0$) ensures the best SNR

A very important parameter: the contrast

$$\boxed{C = \frac{P_{out}^{Max} - P_{out}^{\min}}{P_{out}^{Max} + P_{out}^{\min}} = \frac{2r_1 r_2}{r_1^2 + r_2^2}}$$

Shot noise, the intrinsic readout noise (Vinet's lesson)

In **absence** of GW signal, during Δt :

$$N\frac{h\nu}{\Delta t} = P_{Mich}\eta \qquad \sqrt{N}\frac{h\nu}{\Delta t} = \delta P_{shot}\eta$$

quantum eff.

that leads to

$$\delta P_{shot} = \sqrt{P_{in}\frac{hc}{\lambda\eta\Delta t}}\sqrt{1 + C\cos(2k\delta l)}$$

contrast

In **presence** of GW signal :

$$SNR = \frac{\delta P_{GW}}{\delta P_{shot}}$$

Max for: $\cos(2k\delta l) = -1$

i.e. dark fringe detection : $C = 1$

In terms of linear spectral density :

$$Sh_{shot}^{1/2}\Big|_{C=1} = \frac{\lambda}{4\pi L}\sqrt{\frac{2\hbar\omega}{\eta P}} \quad [1/\sqrt{Hz}]$$

Conceptual best table-top

$$Sh_{shot}^{1/2} \approx 10^{-17} [1/\sqrt{Hz}]$$

EMVESF270710

Actual cases tuning, shot noise*

In terms of power spectral density the SNR is

$$\frac{S_{GW}(f)}{S_{shot}(f)} = \frac{P}{\hbar\omega}(r_1^2 + r_2^2)\cdot C \cdot F(2k\delta l, r_1, r_2)\cdot S_x(f)$$

Sharp function of δl around the dark fringe

when $C < 1$

$$1 - C = 1 - \frac{2r_1 r_2}{r_1^2 + r_2^2}$$

$r_1 = r_2 = 0.99$

$R_1 = 0.99$, $r_2 = 0.98$
1-C=5 10^{-5}

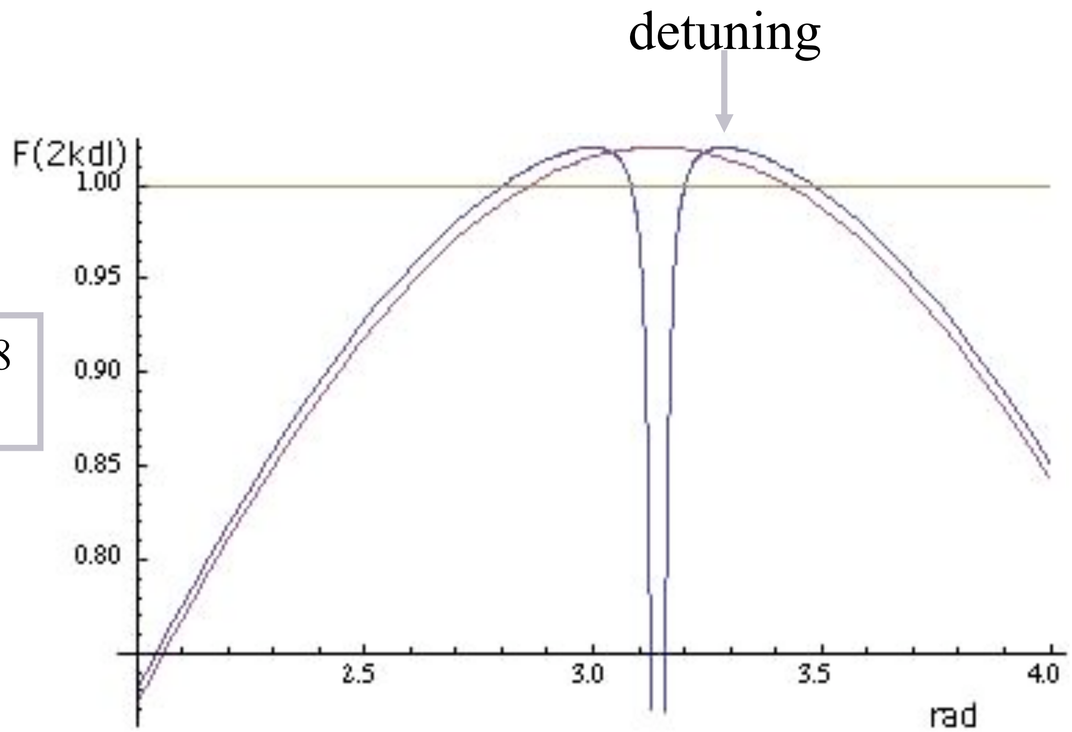

Read-out: Simple Michelson low noise detection concept

Contrast < 1 (e.g. 1-C~10^{-4}) → Leakage of laser source power flucutations

$$\frac{\Delta P}{P} < \sqrt{\frac{\hbar\omega}{\eta P_C}} \approx 10^{-10} / \sqrt{Hz}$$

→ Laser power and $1/f$ noise

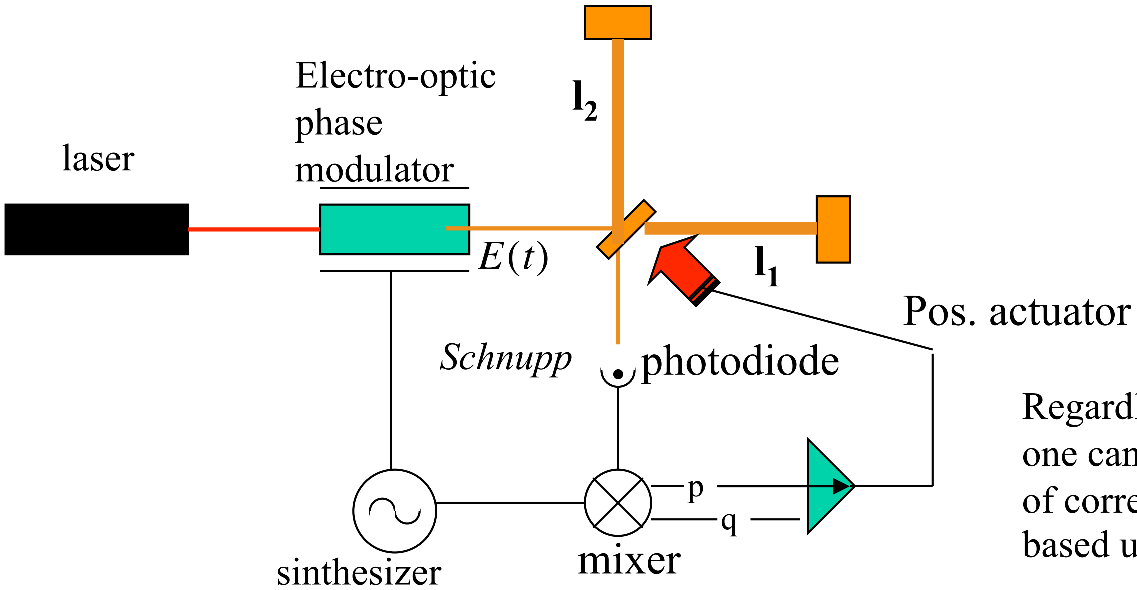

Regardless of actuation methods one can introduce at this level the concept of correcting the position of optical elements based upon the demodulated output signal

$$\Psi_{in}(t) = A_0 e^{i\omega_0 t}$$

$$\Psi_{in}^{m}(t) = E_0 \cdot e^{i(\omega_0 t + m \sin \Omega t)} \approx E_0 (J_0(m) e^{i\omega_0 t} + J_1(m) e^{i(\omega_0 + \Omega)t} - J_1(m) e^{-i(\omega_0 - \Omega)t})$$

At the detection port we have: $\Psi^{m}_{out}(t) = \Psi_0 + \Psi_+ e^{i\Omega t} + \Psi_- e^{-i\Omega t}$

$$\Psi_0 = -J_0\left(e^{i\delta l\omega_0/c} + e^{-i\delta l\omega_0/c}\right)$$

$$\Psi_\pm = \pm J_1\left(e^{i\delta l(\omega_0 \pm\Omega)/c} + e^{-i\delta l(\omega_0 \pm\Omega)/c}\right)e^{\pm i(l_1 + l_1)\Omega/c}$$

- global phase neglected.
- $\delta l \equiv \Delta l + \delta l_{gw}$

arm-length asymmetry

\+

GW

Detected power: $\left|\Psi_D\right|^2 \approx \left|\Psi_0\right|^2 + \left|\Psi_-\right|^2 + \left|\Psi_+\right|^2 + \left|\Psi_+\Psi_0^* - \Psi_0\Psi_-^*\right|e^{i\Omega t} + \left|\Psi_-\Psi_0^* - \Psi_0\Psi_+^*\right|e^{-i\Omega t}$

$$= DC + A\cdot\sin\frac{\Omega}{c}\Delta l \sin 2\frac{\omega_0}{c}\delta l_{gw}\cdot(A_1\sin\Omega t + A_2\cos\Omega t)$$

A, A_1 e A_2 constants

A small ITF arm-asymmetry is necessary

in order to detect the strain signal (in-fase at Ω)

EMVESF270710

II) Designing ITF configuration in real cases

By exploiting edge-technology solutions it is possible in principle to reach 10^{-21}-10^{-23} $Hz^{-1/2}$ strain sensitivity over a quite large bandwidth.

Expected rate of coalescences:

3/yr within 40 ÷ 200 Mpc

[Grishchuk et al. Astro-ph/0008481]

Coalescence event rate

at ~ 20 Mpc

[Kalogera et al. ApJ. 601, L 179, 2004]

- 0.3/yr for NS/NS
- 0.6/yr for BH/BH

INITIAL VIRGO !!!!

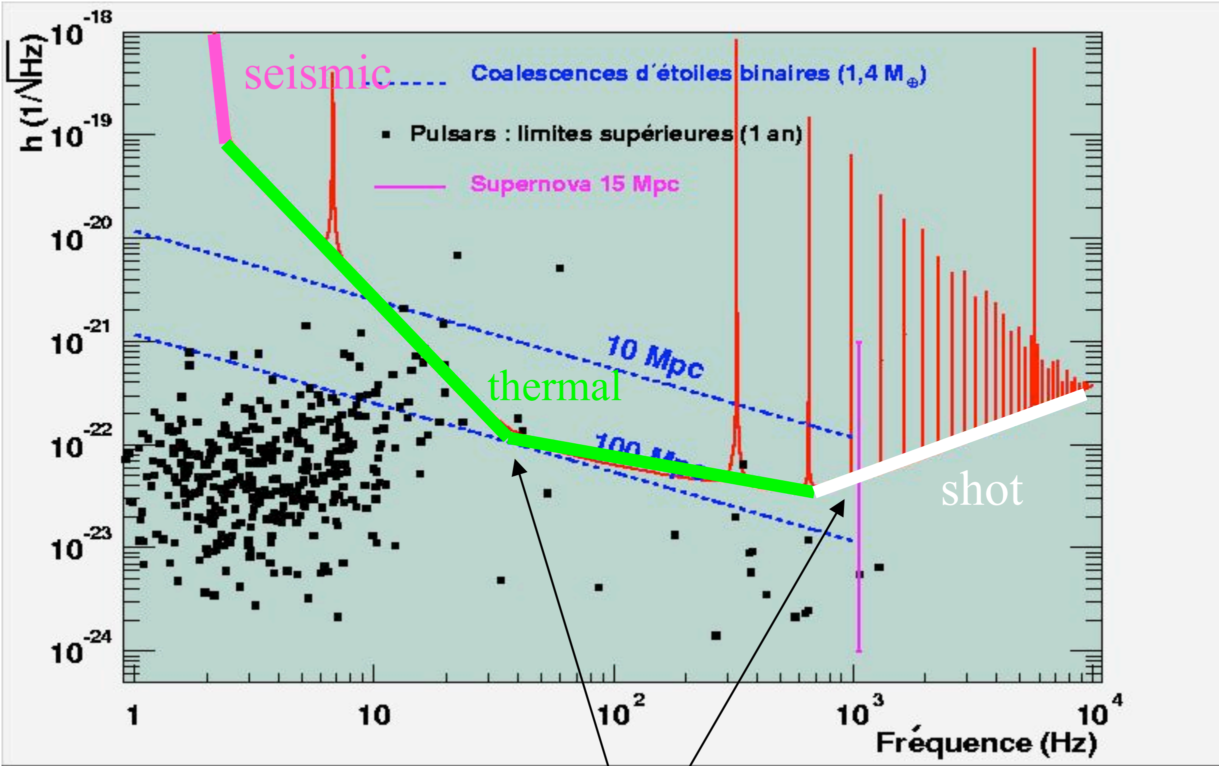

Intrinsic test-mass and readout noise sources

Estimated rate of SNe:

several /yr in the Virgo cluster (20 Mpc).

II) Designing ITF configuration in real cases

By exploiting edge-technology solutions it is possible in principle to reach 10^{-21}-10^{-23} $Hz^{-1/2}$ strain sensitivity over a quite large bandwidth.

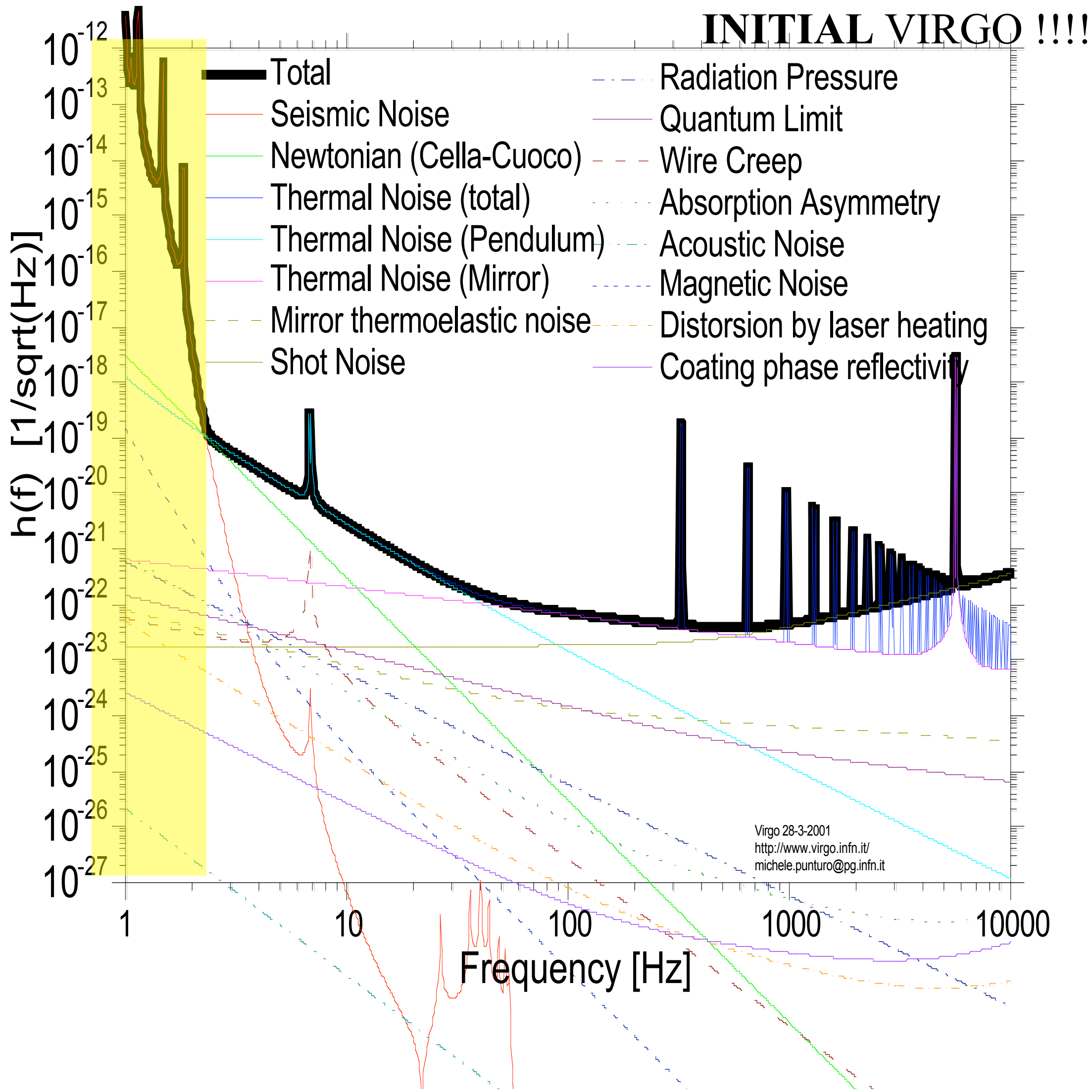

Virgo

Final Design 1998

An ambitious project

• **Ground-based** detector of **extragalactic GW** whose bandwidth starts from low frequency (**few Hz - few kHz**).

• Noise due to **external disturbance** must be reduced to the level of **core intrinsic noise** (test-mass and optical probe).

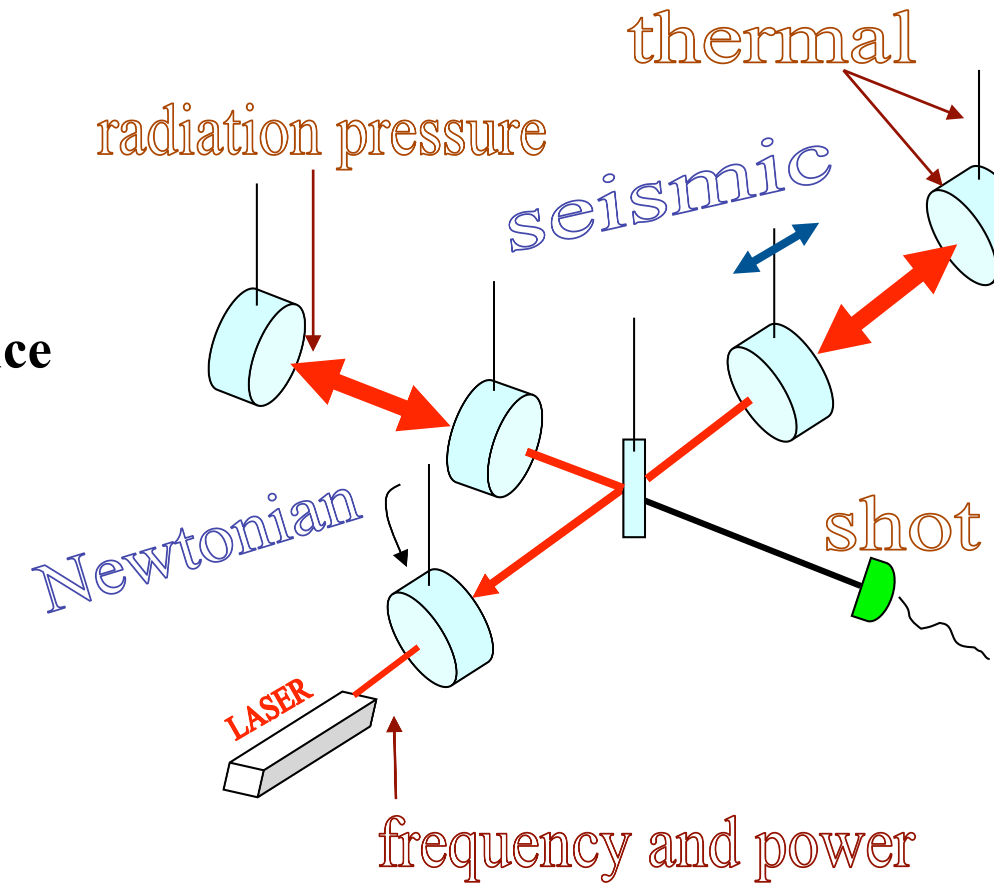

Designing path

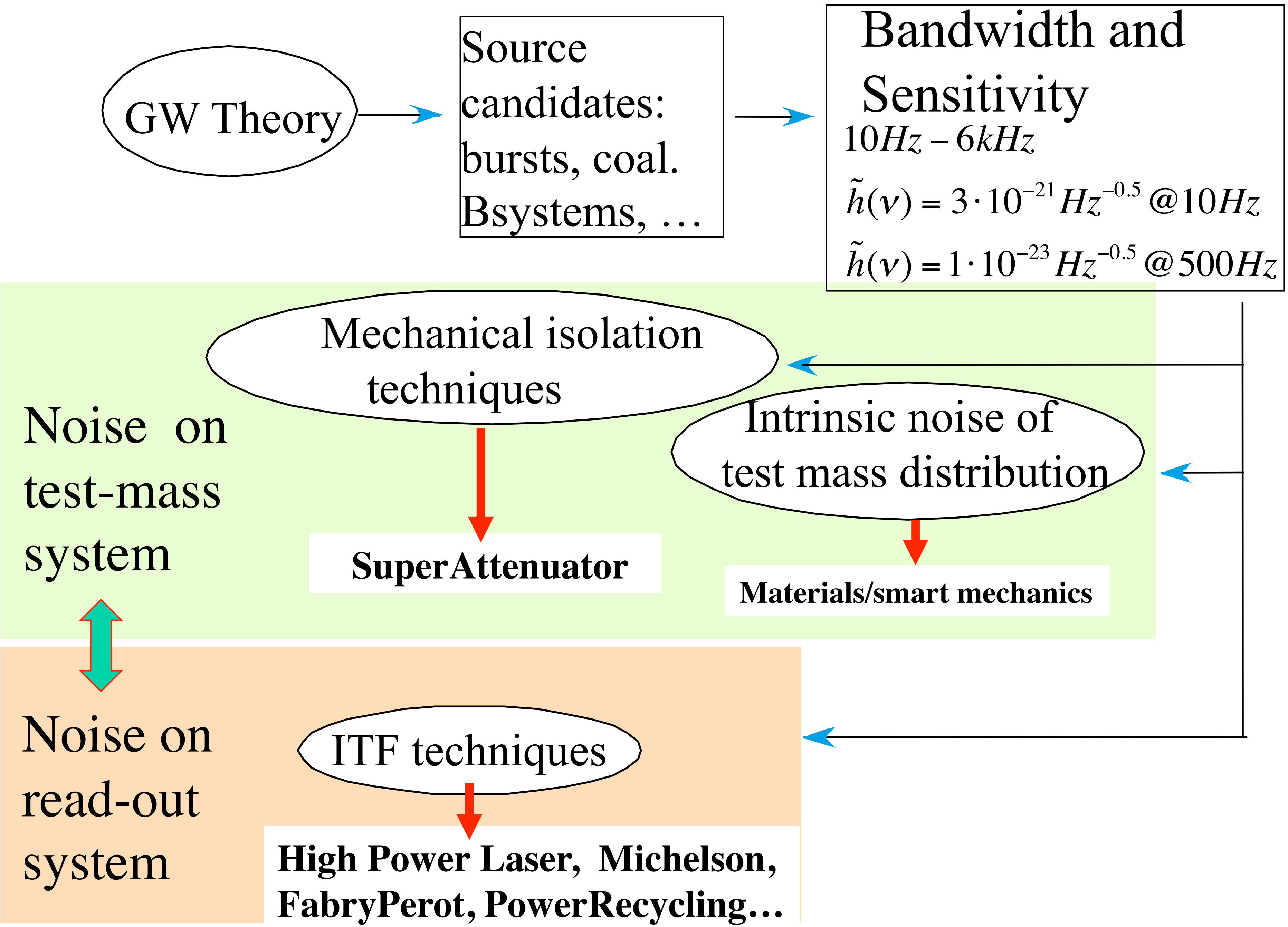

Further reduction of intrinsic read-out noise sources

I) Given dark-fringe operation, higher SNR: $\cos(2k\delta l) = -1$

II) Shot noise target (L=optical path, P=power)

$$Sh_{shot}^{1/2} \cong 3 \cdot 10^{-23} / \sqrt{Hz}$$

$$S\phi_{shot}^{1/2} = \sqrt{\frac{2\hbar\nu}{P}} \Rightarrow Sh_{shot}^{1/2} = \frac{\lambda}{4\pi L}\sqrt{\frac{2\hbar\omega}{\eta \cdot P}}$$

III) Technical solutions:

=> Fabry-Perot cavities on the ITF arms: $L = L_{FP}\frac{2F}{\pi}; F = 50, L_{FP} = 3\text{km}$

Finesse

=> ITF reflected light recycled: $P = G_{\mathrm{Rec}} \cdot P_{in}; G_{\mathrm{Rec}} = 50, P_{in} = 20W$

Recycling factor

=> Basics: see next slides..

Laser beam/cavity basics (I)

$$\nabla^2 U(x,y,z) + k^2(x,y,z) = 0$$ Coherent monocromatic wave emitted by the source

Along *z,* Hermite-Gauss complete set:

$$U(x,y,z) = \frac{A_{mn}}{w(z)} H_m(\sqrt{2}\frac{x}{w(z)})\ H_n(\sqrt{2}\frac{y}{w(z)}) + \exp\left[-\frac{x^2+y^2}{w^2(z)} - i\frac{k(x^2+y^2)}{2R(z)} - i(kz-\phi_{mn})\right]$$

$$w^2(z) = w_0^2\left[1+\left(\boxed{\frac{\lambda z}{\pi w_0^2}}\right)^2\right]$$

beam divergence θ_∞

$$R(z) = z\left[1+\left(\frac{\pi w_0^2}{\lambda z}\right)^2\right]$$

$$\phi = (m+n+1)\ \arctan(\theta_\infty \frac{z}{w_0})$$

Laser beam/cavity basics (II)

In a mode-matched cavity, if the cavity is stable and R(z) and w(z) are the same after an arbitrary number of reflections,

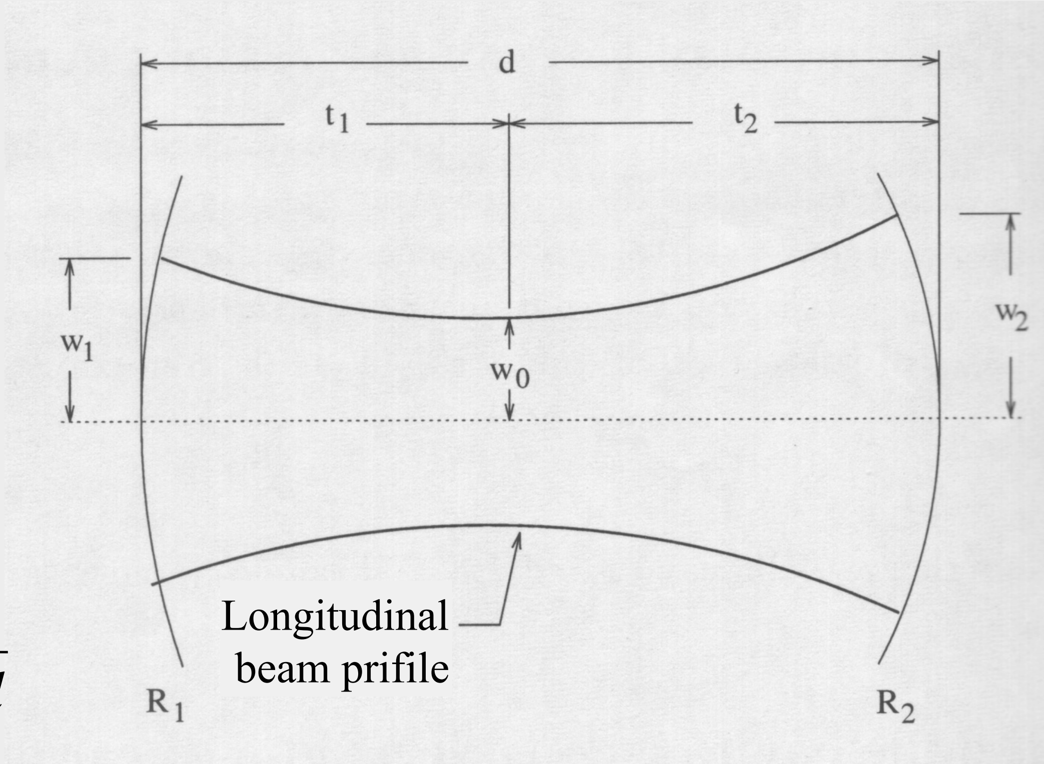

being $$\nu_0 = \frac{c}{2d}$$

TEM$_{mn}$ resonant condition is :

$$\nu = \nu_0 \left[(q+1) + \frac{1}{\pi}(m+n+1)\ \arccos\sqrt{(1-\frac{d}{R_1})(1-\frac{d}{R_2})} \right]$$

arb.integer   mode order   Cavity stability

EMVESF270710

FP basics (I) (plane waves)

$$\psi_{in} = Ke^{i\chi}$$

$$\psi_1 = unknown$$

$$\psi_2 = e^{-ikl}\psi_1$$

$$\psi_3 = ir_2\psi_2$$

$$\psi_4 = e^{-ikl}\psi_3$$

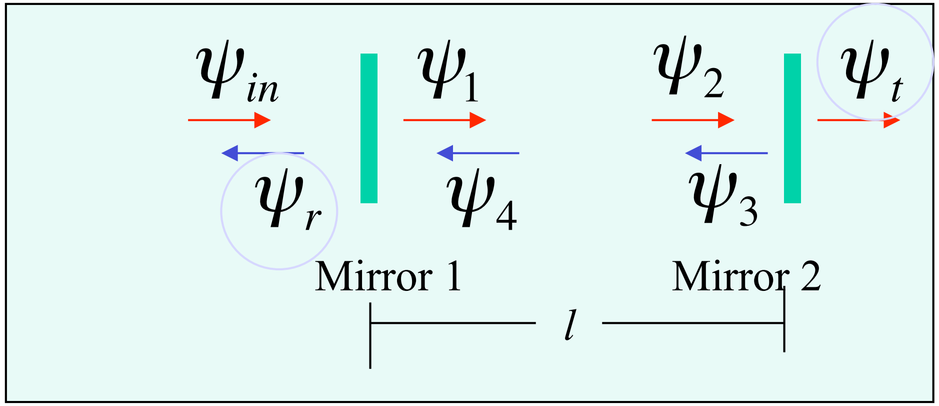

steady state: $\psi_1 = t_1\psi_{in} + ir_1\psi_4 \Longrightarrow$

$$\psi_1 = \frac{t_1}{1 + r_1 r_2 e^{-2ikl}}\psi_{in}$$

$$\psi_4 = \frac{ir_2 t_1}{1 + r_1 r_2 e^{-2ikl}}\psi_{in}$$

Reflected wave: $\psi_r = ir_1\psi_{in} + t_1\psi_4 = i\dfrac{r_1 + r_2 e^{-2ikl}}{1 + r_1 r_2 e^{-2ikl}}\psi_{in}$

Transmitted wave: $\psi_t = t_2\psi_2 = \dfrac{t_1 t_2 e^{-ikl}}{1 + r_1 r_2 e^{-2ikl}}\psi_{in}$

stored wave

FP basics (II)

$$|\psi_r|^2 = |A_r|^2 \qquad A_r = \sqrt{\frac{r_1^{\,2} r_2^{\,2} + 2 r_1 r_2 \cos 2kl}{1 + r_1^{\,2} r_2^{\,2} + 2 r_1 r_2 \cos 2kl}}$$

$$|\psi_t|^2 = |A_t|^2 \qquad A_t = \sqrt{\frac{1}{1 + r_1^{\,2} r_2^{\,2} + 2 r_1 r_2 \cos 2kl}}\, t_1 t_2$$

if :

$$L = (2m+1)\frac{\lambda}{4} \Longrightarrow A_r = \min = \frac{r_2 - r_1}{1 - r_1 r_2}; A_t = MAX = \boxed{\frac{t_1 t_2}{1 - r_1 r_2}} \quad \boxed{A_{max}}$$

$$L = m\lambda \Longrightarrow A_r = MAX = \frac{r_2 + r_1}{1 + r_1 r_2}; A_t = \min = \frac{t_1 t_2}{1 + r_1 r_2}$$

FP basics (III)

The stored wave amplitude ratio is $\dfrac{\psi_1}{\psi_{in}} = \dfrac{t_1}{1 + r_1 r_2 e^{-2ikl}}$

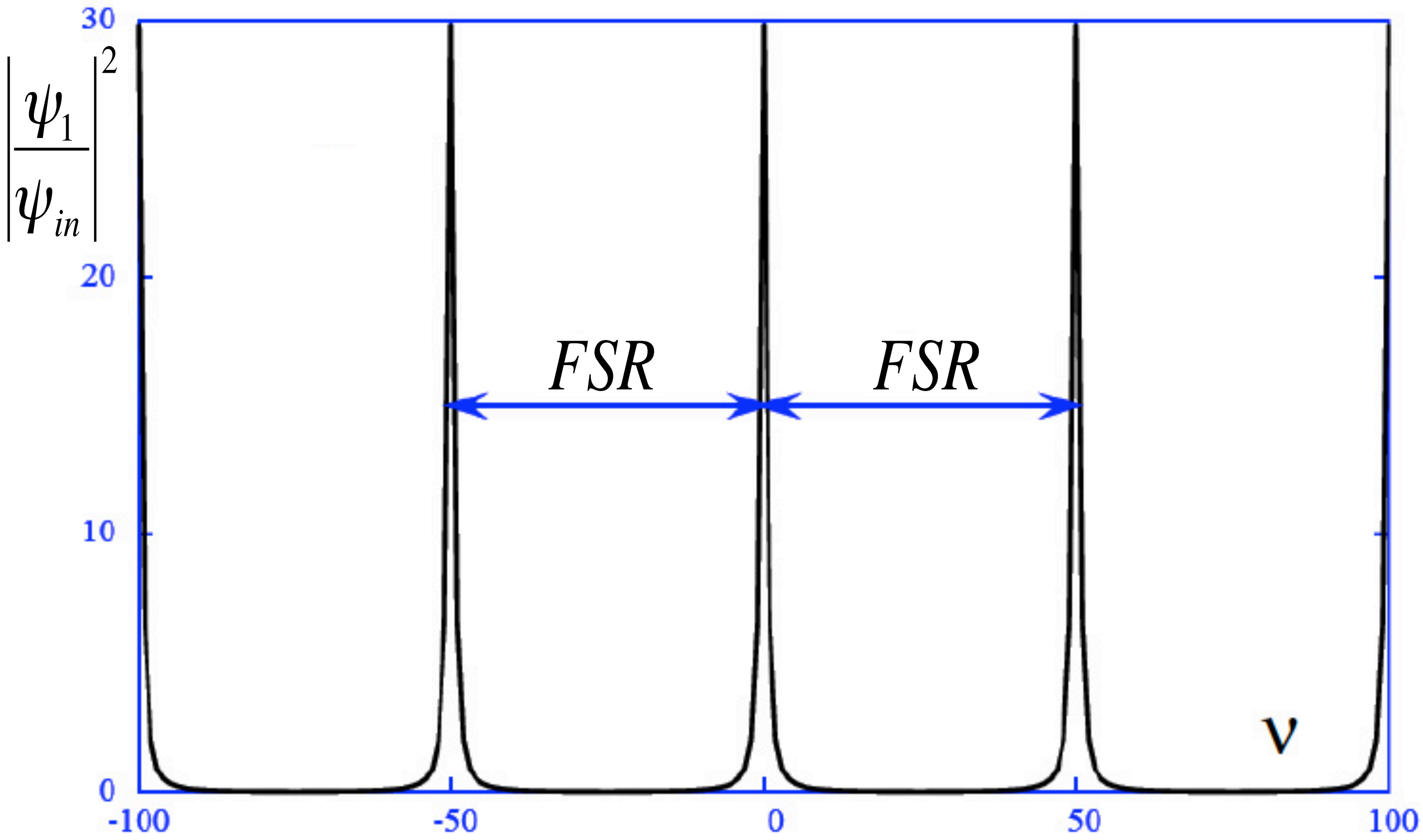

EMVESF270710

FP basics (IV)

Given a resonance condition for λ_0 $\quad L = (2m+1)\dfrac{\lambda_0}{4} \Rightarrow 2k_0 l = (2m+1)\pi$

=> Frequency separation between peaks (FSR)

$$2kl = (2m+1)\pi + 4\pi l\frac{\nu-\nu_0}{c} = (2m+1)\pi + 2\pi\frac{\delta\nu}{FSR} \qquad \boxed{\frac{c}{2l}}$$

$$\frac{\psi_1}{\psi_{in}} = \frac{t_1}{1+r_1r_2e^{-i2kl}} = \frac{t_1}{1-r_1r_2e^{i2\pi\frac{\delta\nu}{FSR}}}$$

Power gain

Full Width @ Half Max

$$\left|\frac{\psi_1}{\psi_{in}}\right|^2 = A_{Max}^2\frac{1}{1+\left(\dfrac{2\sqrt{r_1r_2}}{1-r_1r_2}\sin\left(\pi\dfrac{\delta\nu}{FSR}\right)\right)^2} \Bigg|_{\frac{\delta\nu}{FSR}<<1} = A_{Max}^2\frac{1}{1+\left(2F\dfrac{\delta\nu}{FSR}\right)^2}$$

$$FWHM = \frac{FSR}{F}$$

$$\mathit{Finesse} = \frac{\pi\sqrt{r_1r_2}}{1-r_1r_2}$$

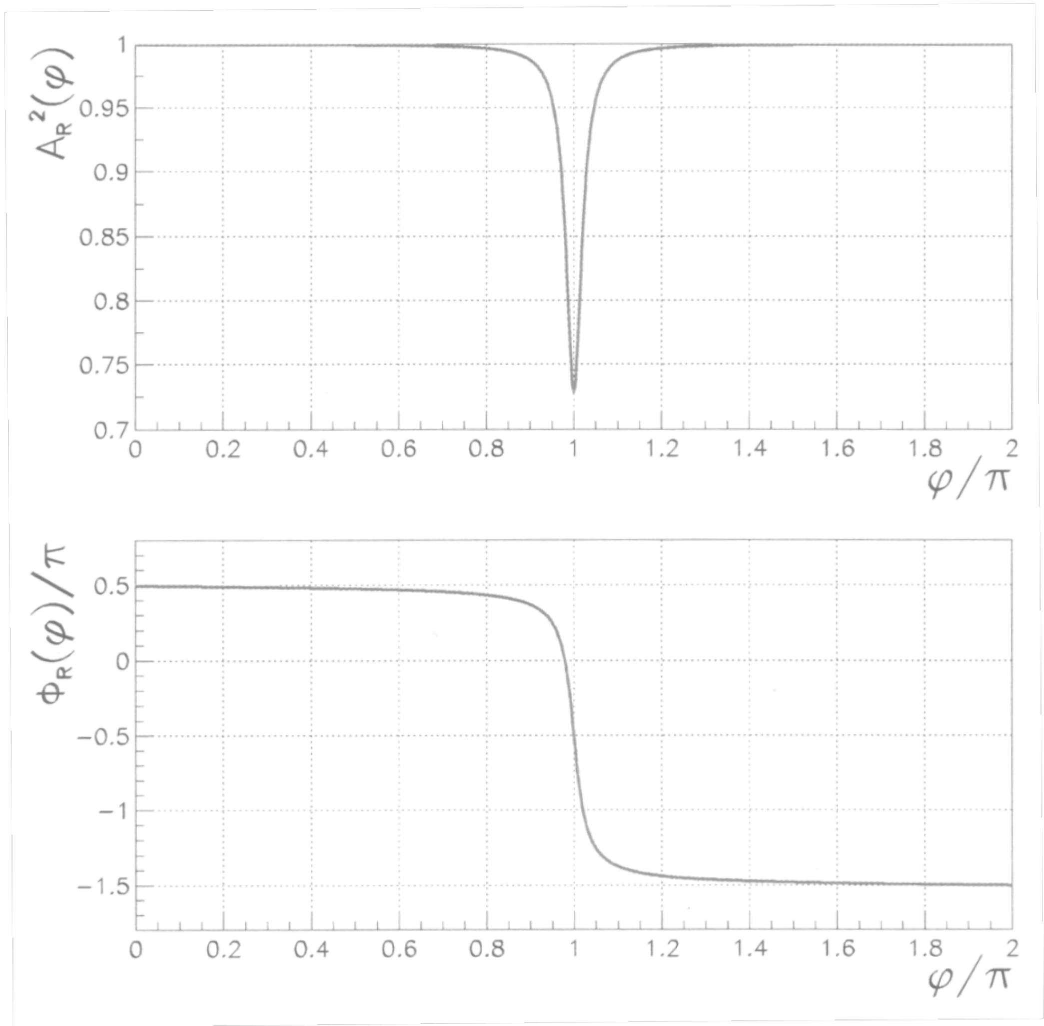

Absorption peak (reflected)

EMVESF270710

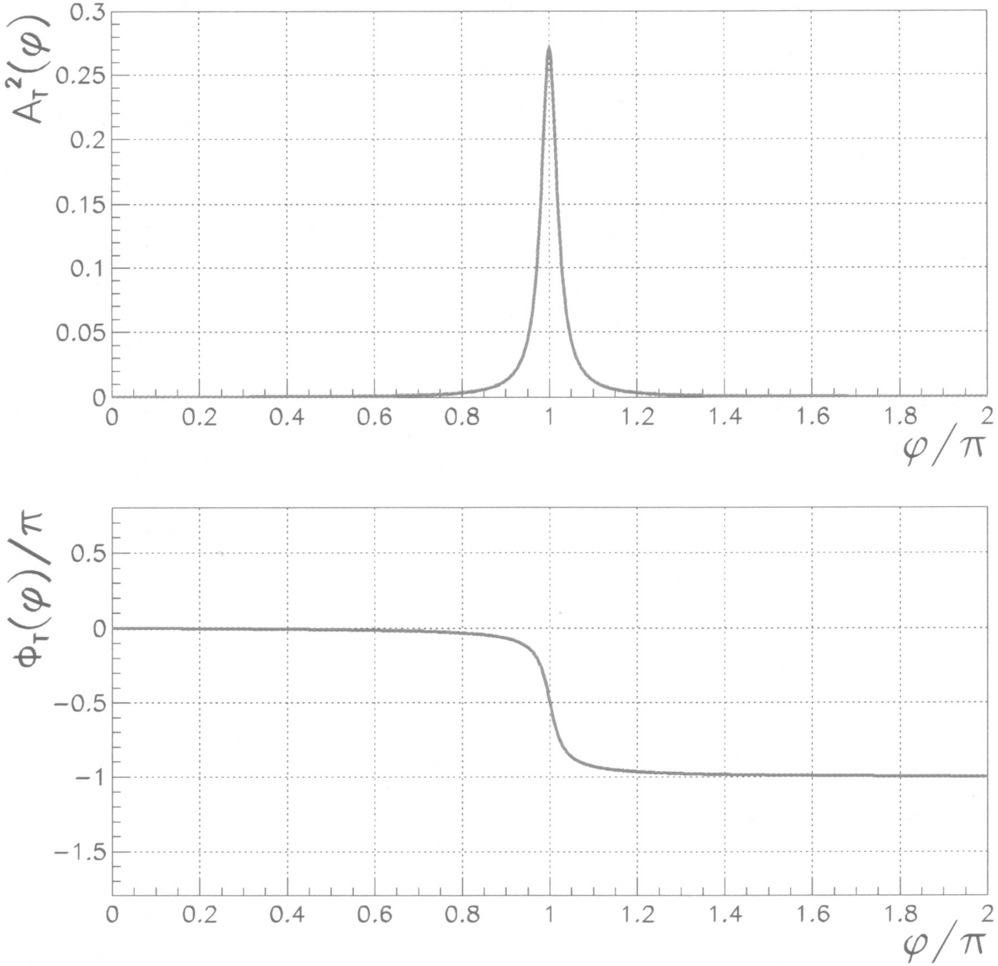

Absorption peak (transmitted)

FP basics (V) (optical length…towards Michelson intererometer)

$$\psi_r = i\frac{r_1 + r_2 e^{-2ikl}}{1 + r_1 r_2 e^{-2ikl}}\psi_{in} \qquad \varphi_r(l) = \arctan\left(\frac{r_1(1+r_2^2) + r_1(1+r_2^2)\cos(2kl)}{r_2(1-r_1^2)\sin(2kl)}\right)$$

$$\varphi_r(l_{res} + \delta l) = \varphi_r(l_{res}) + \left.\frac{d\varphi_r}{dl}\right|_{l=l_{res}}\delta l = \varphi_r(l_{res}) - 2k\left(\frac{2F}{\pi}\right)\delta l$$

The response of phase of FP reflecion to length variations is enhanced by its Finesse

Finite light speed to be taken into account

$$\omega_c = 2\pi\frac{FWHM}{2} = \frac{\pi c}{2Fl} = \frac{1}{\tau_s} \quad \text{cavity storage t}$$

Frequency cut-off in the response to GW

FP basics (VI) (optical length…towards Michelson intererometer)

$$|\psi_{out}|^2 = \frac{|\psi_{in}|^2}{2}(1 + C\cos(2kl))$$

$$|\psi_{out}|^2 = \frac{|\psi_{in}|^2}{2}(1 + C\cos(2kl + \varphi_{r-FP2} - \varphi_{r-FP1}))$$

For a given optimal polarization:

$$|\varphi_{r-FP2} - \varphi_{r-FP1}| = 2k \underbrace{\frac{\frac{2F}{\pi}L_0}{\sqrt{1 + \left(\frac{\omega_{GW}}{\omega_c}\right)^2}}}_{L_{opt}} \cdot h$$

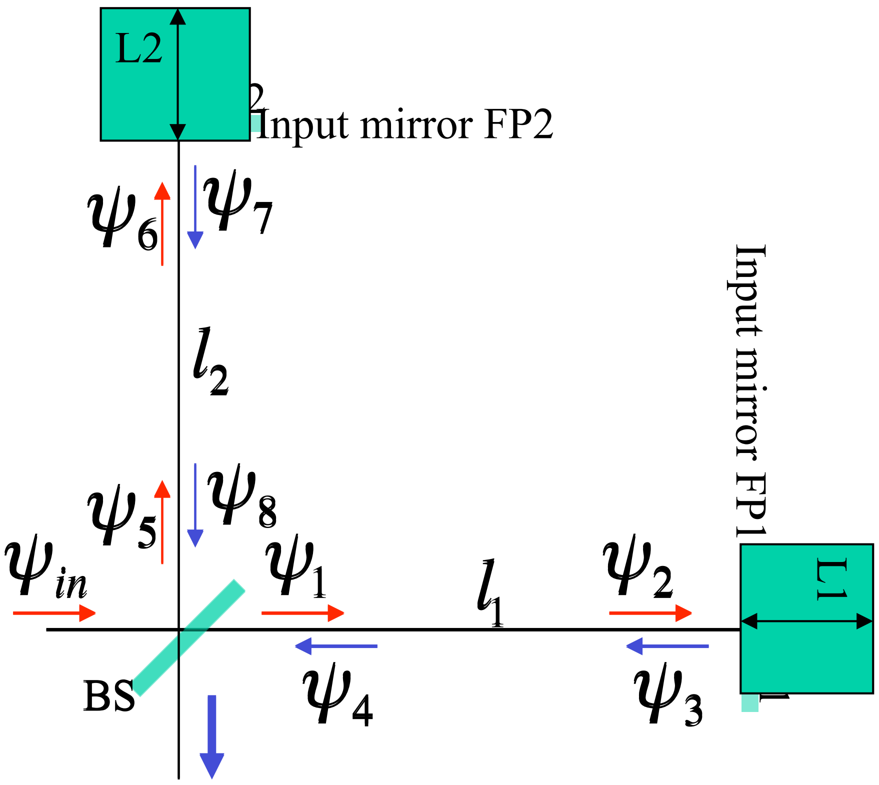

Optical length of cavities depends on the frequency!

FP-Michelson ITF-power recycling I

$$\psi_1 = \frac{t_1}{1 + r_1 r_2 e^{-2ikl}} \psi_{in}$$

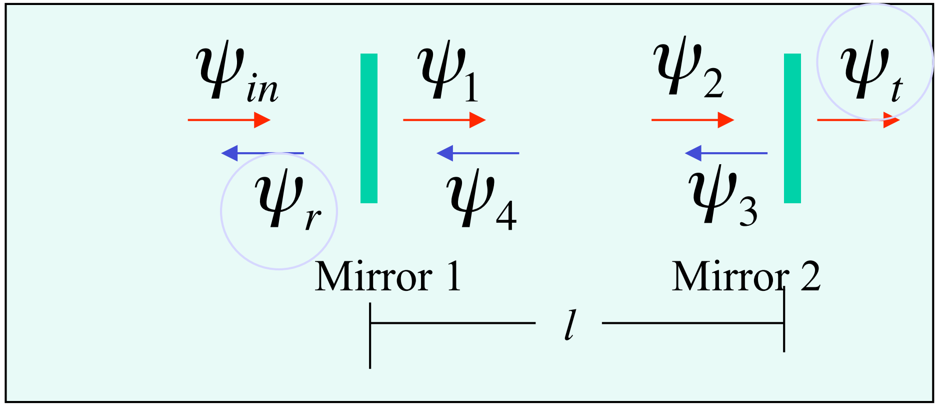

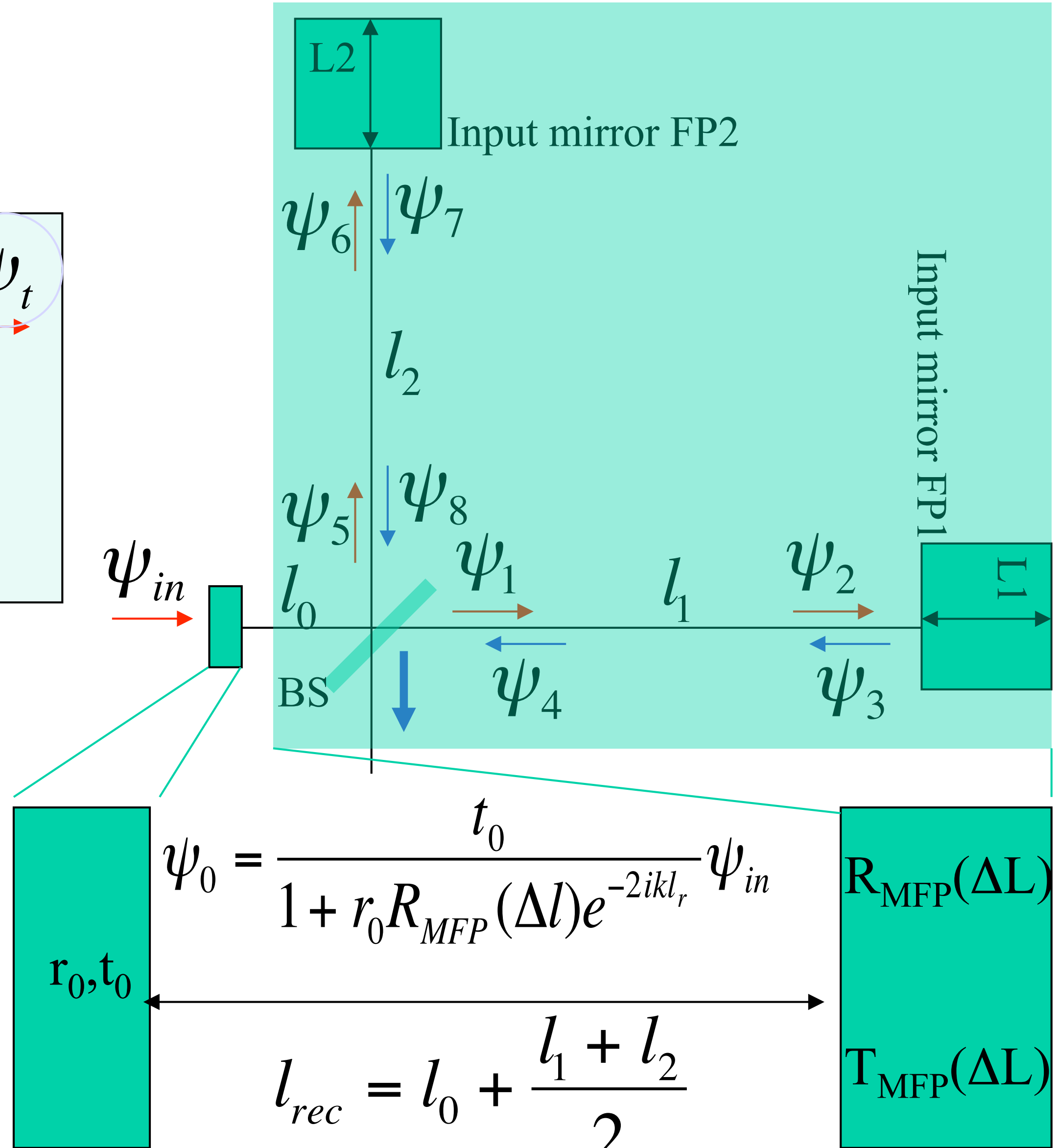

$$\psi_0 = \frac{t_0}{1 + r_0 R_{MFP}(\Delta l) e^{-2ikl_r}} \psi_{in}$$

$$l_{rec} = l_0 + \frac{l_1 + l_2}{2}$$

Resonance depends on:

$\Rightarrow$ l_{rec}

$\Rightarrow$ complex refrectivity $R_{MFP}(\Delta L)$

$$\boxed{|\psi_{out}|^2 = |T(\Delta L)|^2 |\psi_0|^2}$$

FP-Michelson ITF-power recycling II (power built-up and losses)

$\phi_{Mic}/2$ = Michelson phase/2
$(\delta l = l_1 - l_2)$

$$|\psi_{out}|^2 = |T(\Delta L)|^2 |\psi_0|^2 = |\psi_0|^2 \cos^2(k\delta l)$$

Recycled power $|\psi_0|^2$ implicitly depends on

⇒Recycling cavity length l_r
⇒Michelson recombination phase ϕ_{Mic}

At symmetric resonance and dark fringe
(no losses)

$$\varphi_{r-FP1} = \varphi_{r-FP2} = -\frac{\pi}{2},$$

$$|\psi_{r-FP1}| = |\psi_{r-FP2}| = 1$$

$$\longrightarrow \boxed{|\psi_0|^2 = \frac{t_0^2}{(1-r_0)^2} |\psi_{in}|^2}$$

G_{rec} (power recycling gain)

Power rec. mirror reflectivity choice depends on ITF and Recycling cavity losses:

$$\boxed{|\psi_0|^2 = \frac{1}{p_{Rec}^2 + p_{ITF}^2} |\psi_{in}|^2}$$

EMVESF270710

noise

Intrinsic optical noise sources: power and frequency noise sources

- To get rid of the power fluctuation effects:
  - *Interferometer (cavity, fringe and recycling) locked with the Pound-Drever-Hall technique (heterodyne at about 10 Mhz);*
  - *Signal extracted through partial sidebands transmission (Schnupp technique);*

To have sidebands partially transmitted an asymmetry of the Michelson is necessary (about 0.8 m in Virgo);

The arm asymmetry produces laser frequency noise;

- The frequency fluctuations requirements are about 10^{-4} Hz/sqrt(Hz) at 1 Hz. A complex frequency stabilization is necessary:
  - Input mode cleaner filtering fluctuations
  - Rigid frequency cavity reference
  - Laser frequency locking on the interferometer common mode

a very small part of the story

Standard layout used in ground-based detectors (i.e. framework upon Advanced detectors are being based)

I) The optical path where the GW-induced phase shift is accummulated can be enhanced by means of Fabry-Perot resonant cavities.

II) Dark fringe detection to reduce read-out noise.

III) Recycling of ITF reflection.

Effective path =120 km

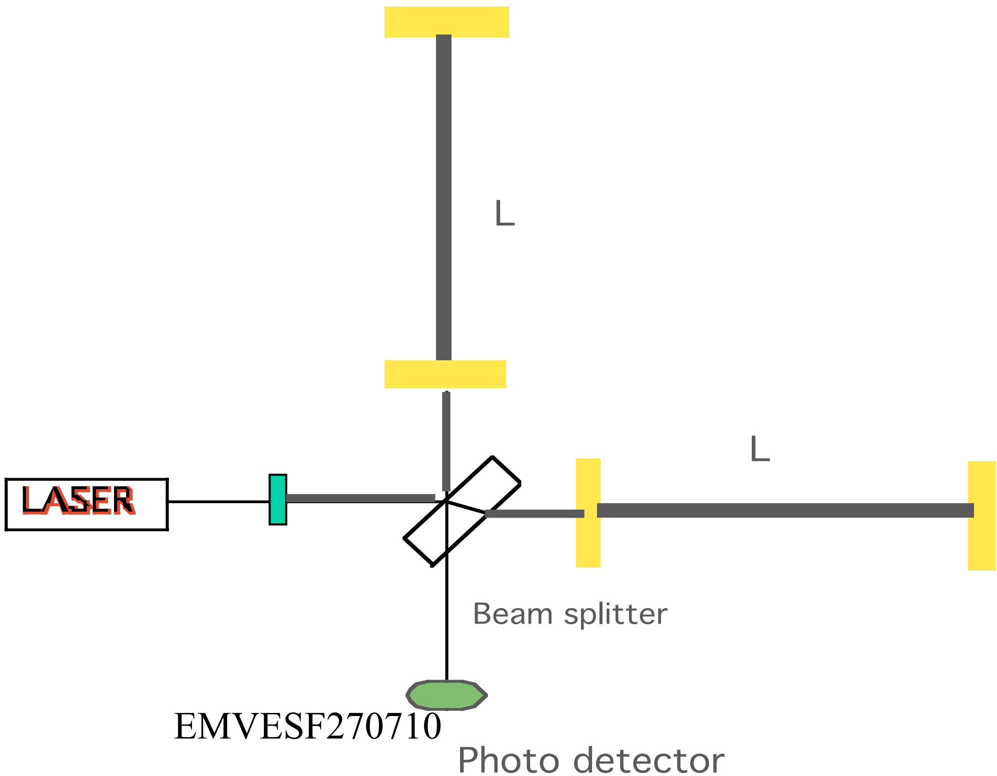

EMVESF270710

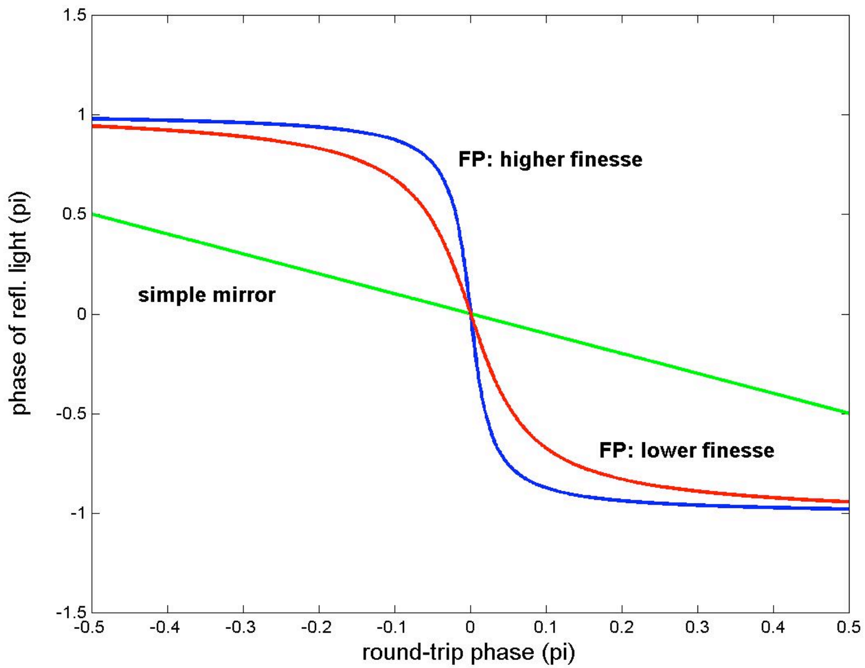

The response of the ITF is much steeper => control system needed

FP lock concept

Widely used in radiophysics (R.Pound 1946), and later on adopted in GW detector optics (R. Drever), nowadays it is the standard method for cavity lock and laser stabilization.

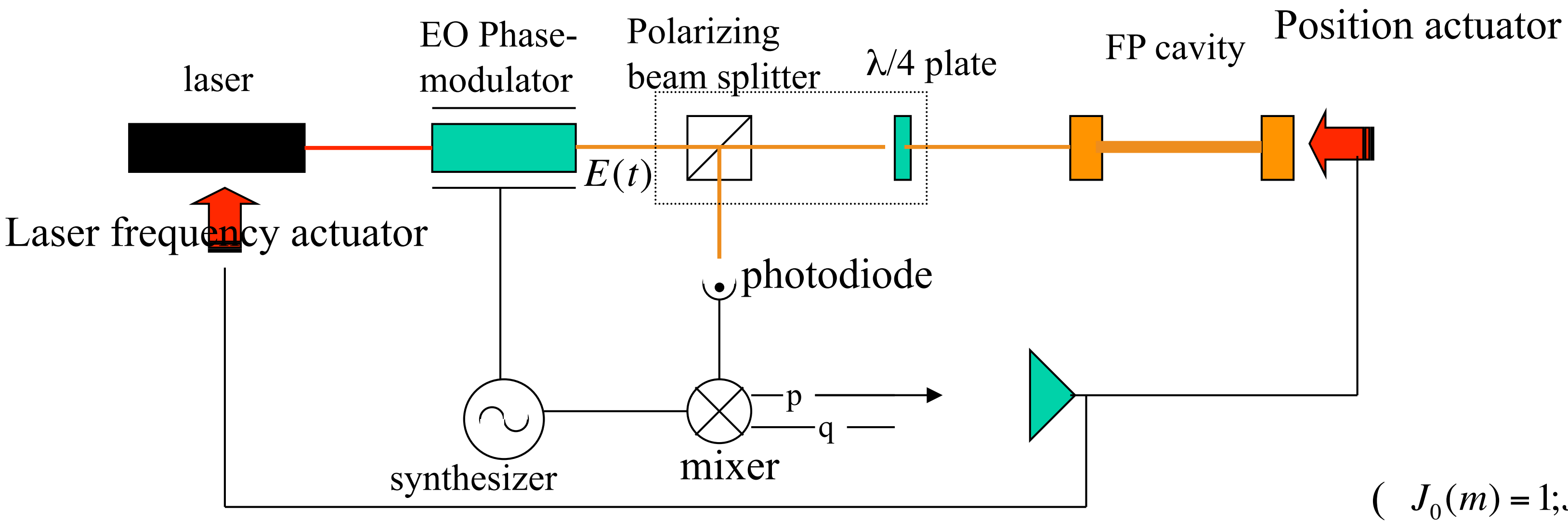

$$\left(\; J_0(m) = 1; J_1(m) = m/2 \; \right)$$

$$E(t) = E_0 \cdot e^{i(\omega_0 t + m\cos\Omega t)}\Big|_{m<<1} \approx E_0\left(J_0(m)e^{i\omega_0 t} + J_1(m)e^{i(\omega_0+\Omega)t} - J_1(m)e^{i(\omega_0-\Omega)t}\right)$$

$$\mathrm{Re}\{E(t)\} = E_0\cos(\omega_0 t + m\cos\Omega t)\Big|_{m<<1} \approx E_0 \cdot \cos\omega_0 t - E_0 \sin\omega_0 t \cdot (m\cos\Omega t) \qquad (15)$$

EMVESF: $$= E_0 \cdot \cos(\omega_0 t) - m\frac{E_0}{2}\sin(\omega_0 + \Omega)t - m\frac{E_0}{2}\sin(\omega_0 - \Omega)t$$

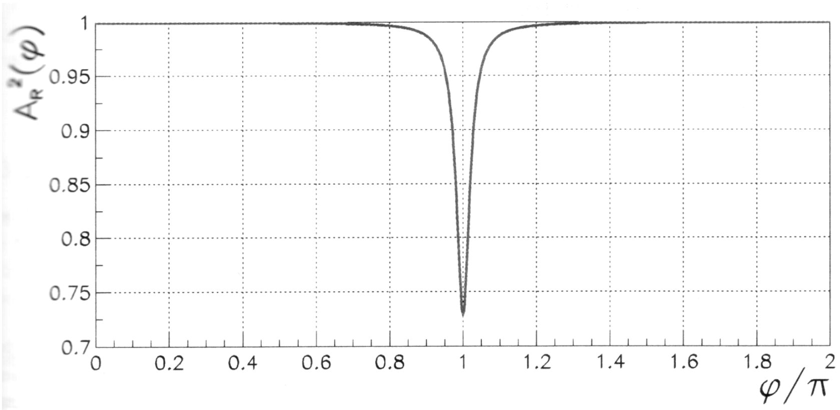

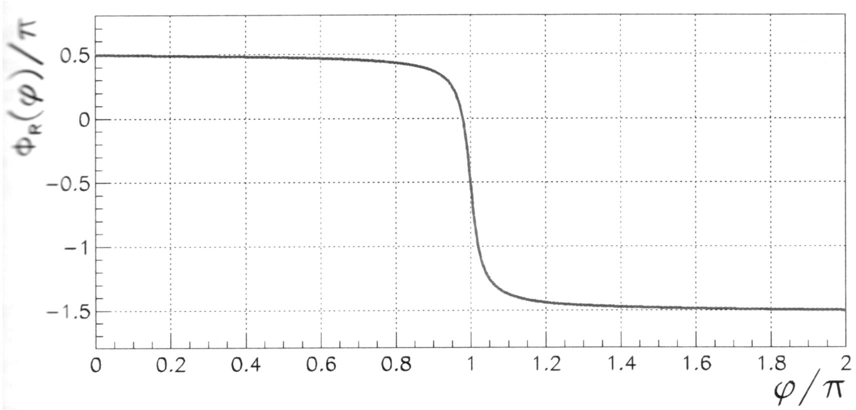

$\arctan(\mathrm{Im}\psi_r / \mathrm{Re}\psi_r)$

At resonance length incident light is reflected with -π/2 phase at carrier frequency and with π/2 at sidebands.

$$E_r(t) = -E_0 \cdot \cos(\omega_0 t) - mE_0 \cos(\Omega t) \cdot \sin(\omega_0 t)$$

A small change in cavity length :

$$E_r(t) = -E_0 \cdot \cos(\omega_0 t + \phi_d) - mE_0 \cos(\Omega t) \cdot \sin(\omega_0 t + \phi_d)$$

$$|E_r(t)|^2 \propto m \cdot \sin\phi_d \cos\Omega t$$

$\boxed{\text{In-phase demodulated signal at } \Omega \text{ is driven by length variations}}$

DC reflected light

Demodulated
Pound-Drever
signals

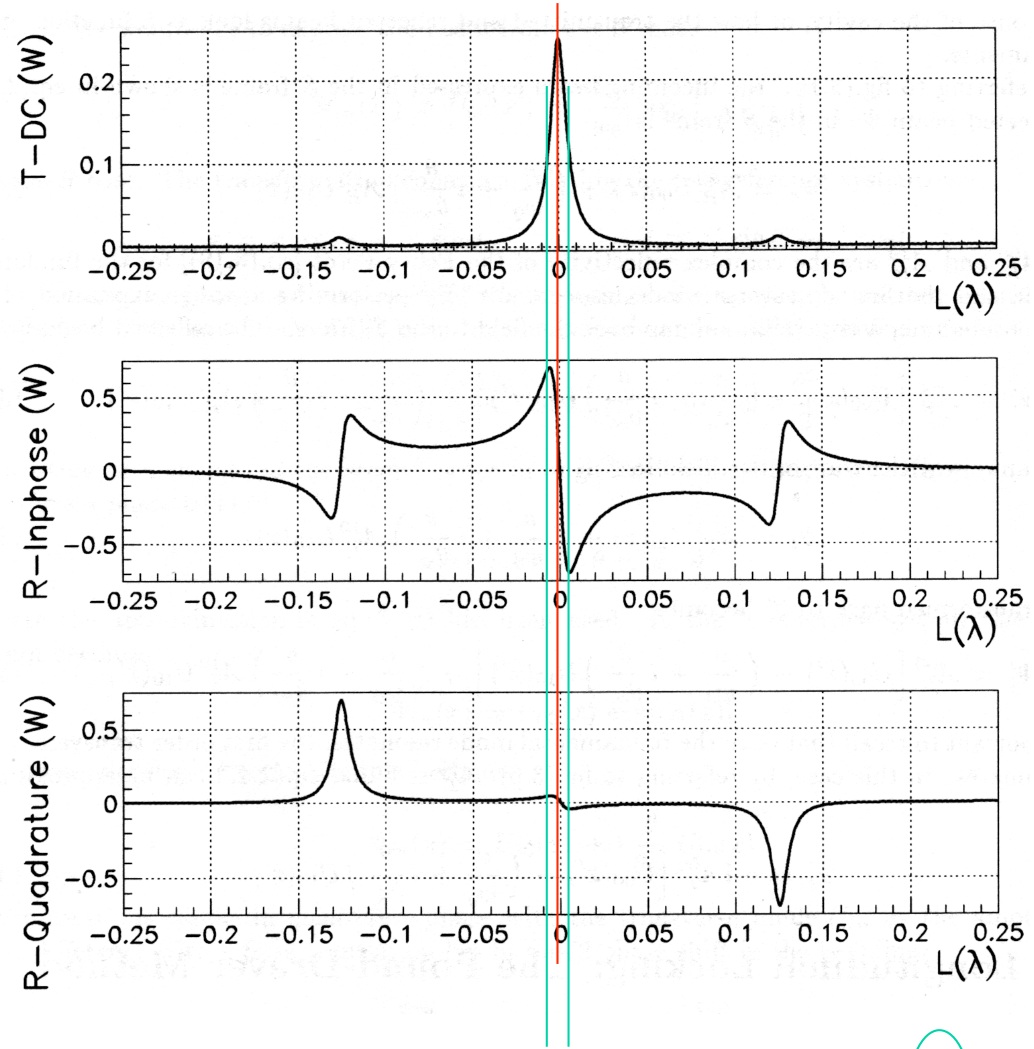

Linear range $$FWHM = \frac{\lambda}{2F}$$

FSR

Control $$\delta l = \frac{1}{100}\frac{FWHM}{2} = \frac{\lambda/2}{100 \cdot 2 \cdot F}$$

safety factor

EMVESF270710

Summarizing shot noise

Simple Michelson

$$Sh_{shot}^{1/2}(t) = \frac{1}{2\pi}\frac{1}{2L}\sqrt{\frac{\hbar c\lambda}{\eta P_{in}}}$$

Michelson +Fabry-Perot

$$Sh_{shot}^{1/2}(t) = \frac{1}{2\pi}\frac{1}{2L_{opt}}\sqrt{\frac{\hbar c\lambda}{\eta P_{in}}}\sqrt{1+\frac{\omega^2}{\omega_c^2}}$$

Michelson +Fabry-Perot
+Power recycling

$$Sh_{shot}^{1/2}(t) = \frac{1}{8FL}\sqrt{\frac{hc\lambda}{\eta G_{\mathrm{Re}\,c}P_{in}}}\sqrt{1+\frac{\omega^2}{\omega_c^2}}$$

back-action noise

$$Sx_{RP} = \frac{1}{m \cdot 2\pi\nu_0^2} \frac{SP_{shot}^{1/2}}{c}$$

displacement power spectrum due
to radiation pressure on suspended mirrors

$$Sh_{overall}^{1/2} = \frac{1}{L_{FP}} \sqrt{\frac{c_{shot}}{F^2 P} + \frac{c_{RP}}{(m\nu_0^2)^2} F^2 P}$$

m = suspended mirror mass; $c_{shot} = c_{shot}(const_{shot}); c_{RP} = c_{RP}(const_{RP})$

F and P cannot be increased without mechanical reaction

m can be used to reduce the suspended mirror reaction

$$3 \cdot 10^{-21} / \sqrt{Hz} \, @10Hz \geq Sh_{TN}^{1/2} \geq Sh_{overall}^{1/2}$$

tuning $\longrightarrow$ F,P,L,m

SQL is far…

thermal noise

Intrinsic test mass noise source: thermal

• The test masses are a part of a large ground-based digitally controlled mechanical system meant to keep them in quasi-inertial state.
• The spatial coordinate *x* of such a mechanical chain is probed by the ITF at the mirror.
• Each test-mass is not point-like and then at thermal equilibrium *x* fluctuates due to thermal impulse fluctuation within its body.

$$SF_{xx} = 4kT \cdot \Re\{Z_{xx}\}$$

$$\boxed{SX_{xx}{}^{2} = \frac{4kT}{\omega^{2}} \cdot \Re\{Z^{-1}{}_{xx}\}}$$

Z is the mechanical impedance of the system; it has to be known (theory or measurement) in order to be inverted. Close to a mechanical resonance $\tilde{x}_{TN}$ is a Lorentian. Phenomenological models are often used (…) for internal friction noise predictions.

$$Sh_{TN}^{1/2} = \frac{\sqrt{SX_{TN}}}{L} = \frac{1}{L}\sqrt{\frac{4kT}{m\omega} \frac{\phi\omega_o{}^2}{(\omega^2 - \omega_o{}^2)^2 - (\phi\omega_o{}^2)^2}}$$

EMVESF270710

distance

Mass Temperature,dissipation

II) External mechanical disturbance: Suspended Optics (14)

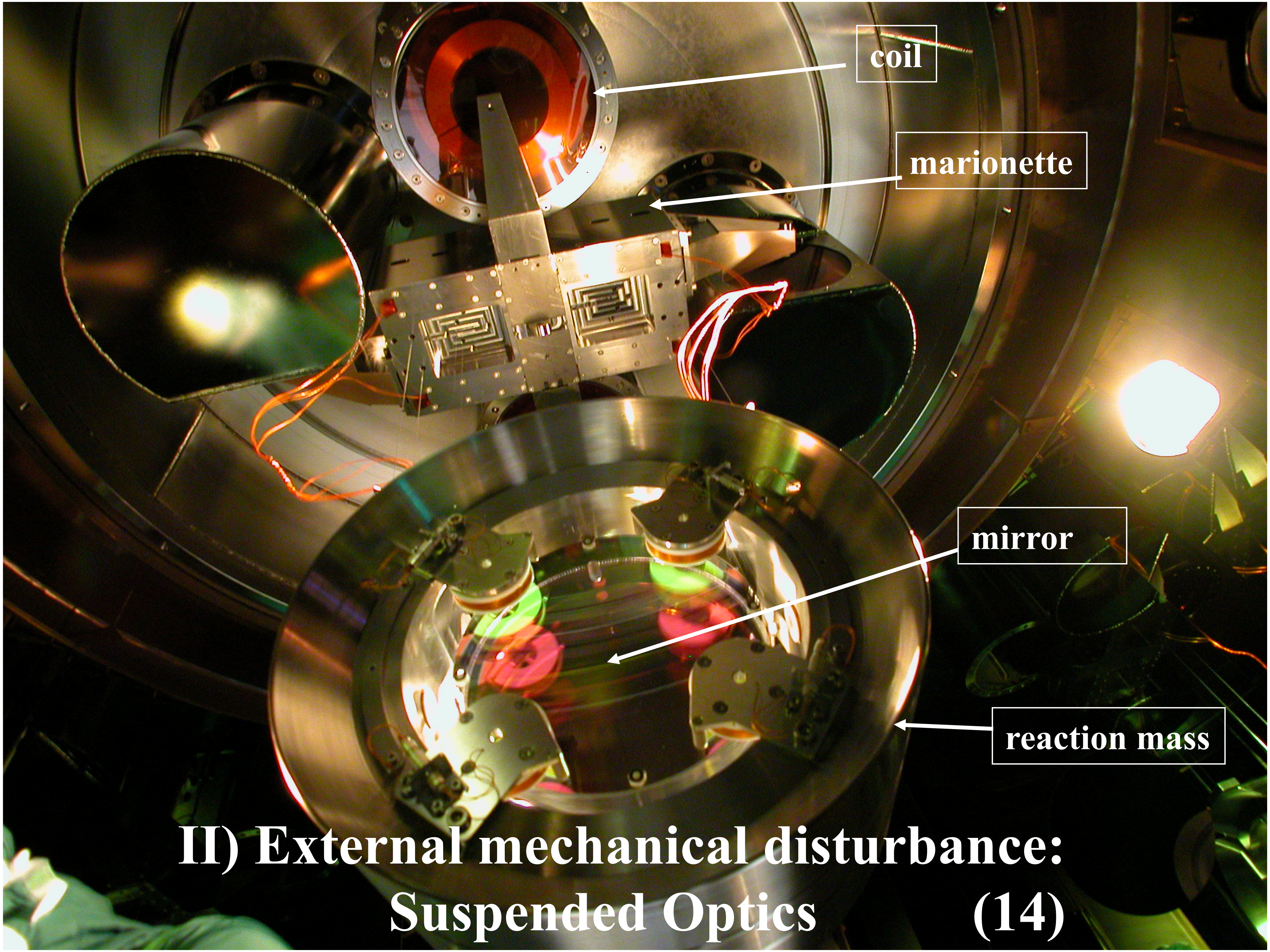

Virgo-like approach in TAMA and GEO

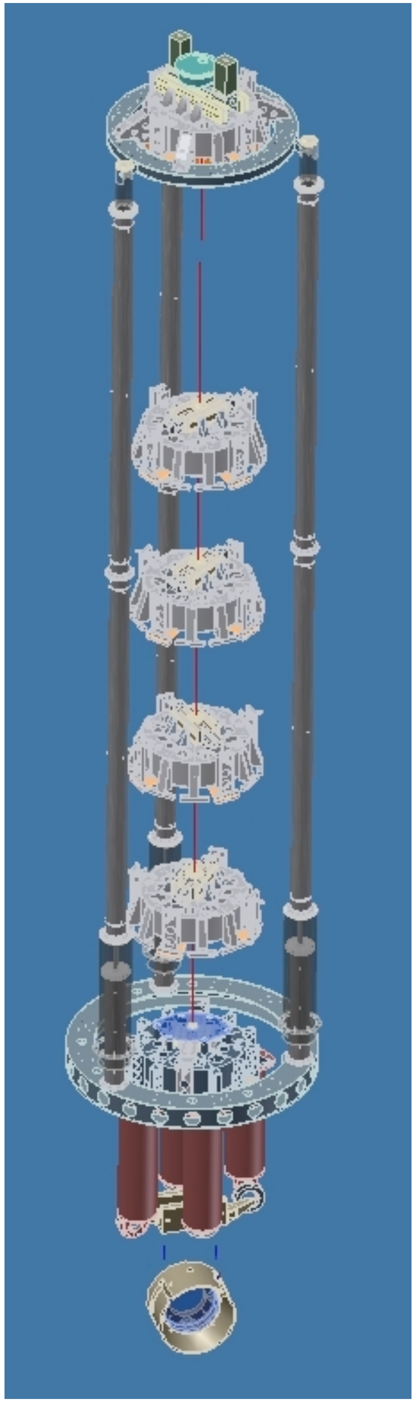

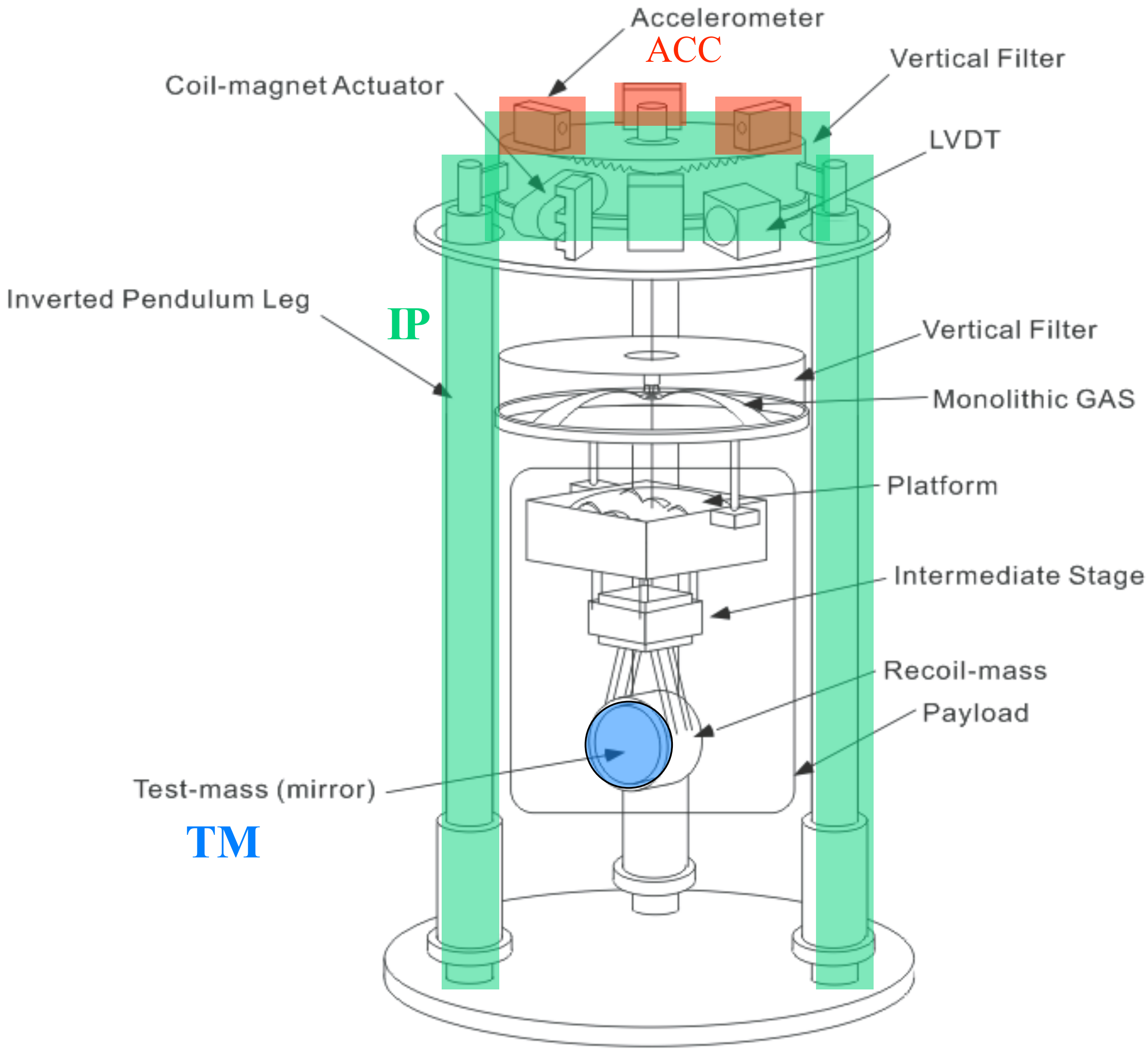

LIGO

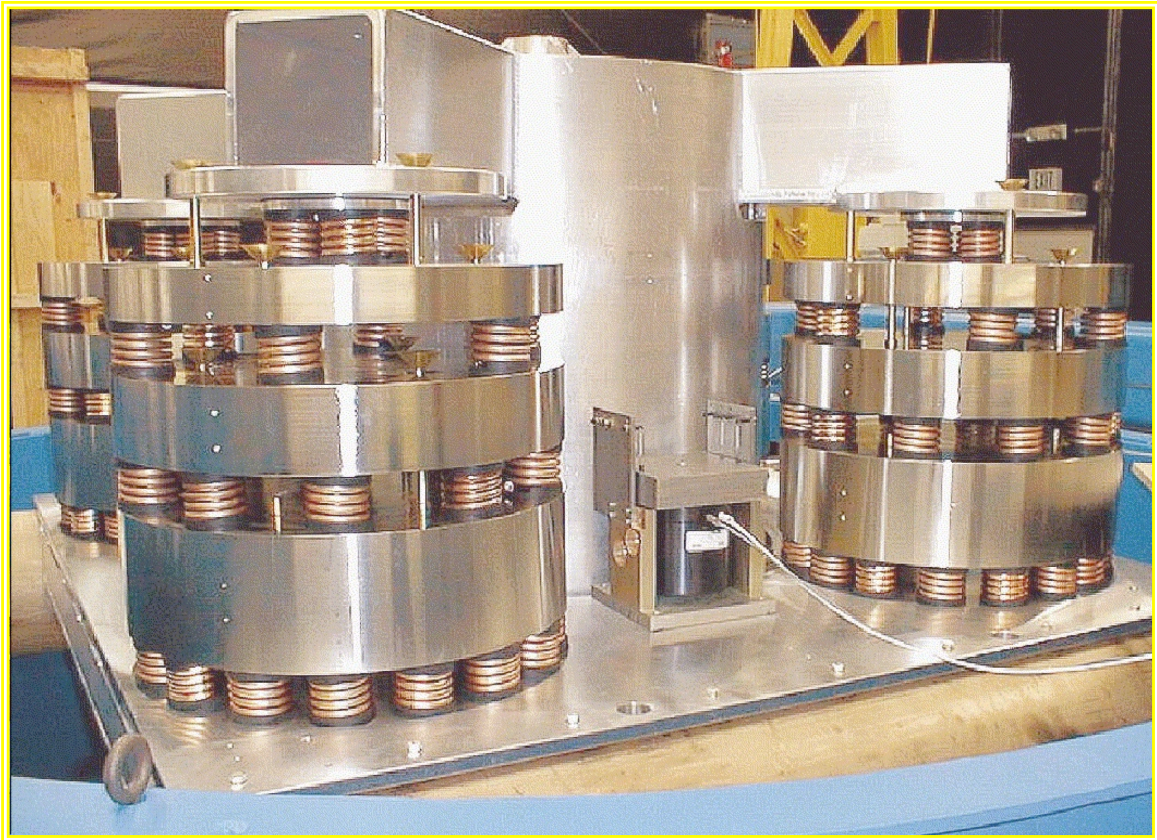

Passive (to reduce noise in sensitive freq. band)

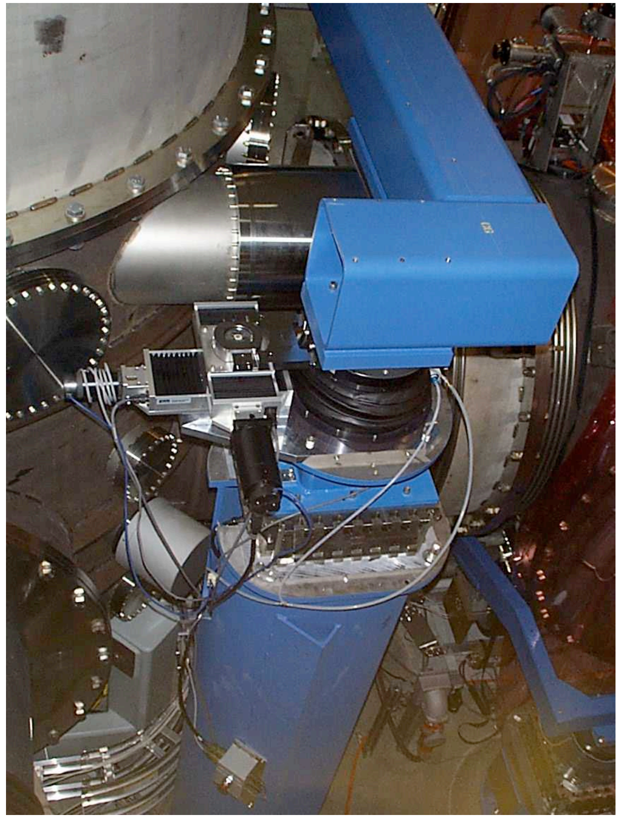

Active (to improve lock acquisition/maintenance)

Remark: AdV-LIGO active seismic isolation (very different, but still aimed to LF detection)

- One new approach is 'active' suppression, used in Advanced LIGO
  - Low-noise seismometers on payload detect motion in all six degrees-of-freedom
  - Actuators push on payload to eliminated perceived motion
  - Multiple 6-DOF stages to achieve desired suppression, allocation of control
- Challenges in structural resonances, sensor performance
- Nice to have a quiet table to mount lots of stuff on
- Enhanced LIGO using this approach for one chamber per interferometer
  - Meets requirements, will remain in place for AdvLIGO

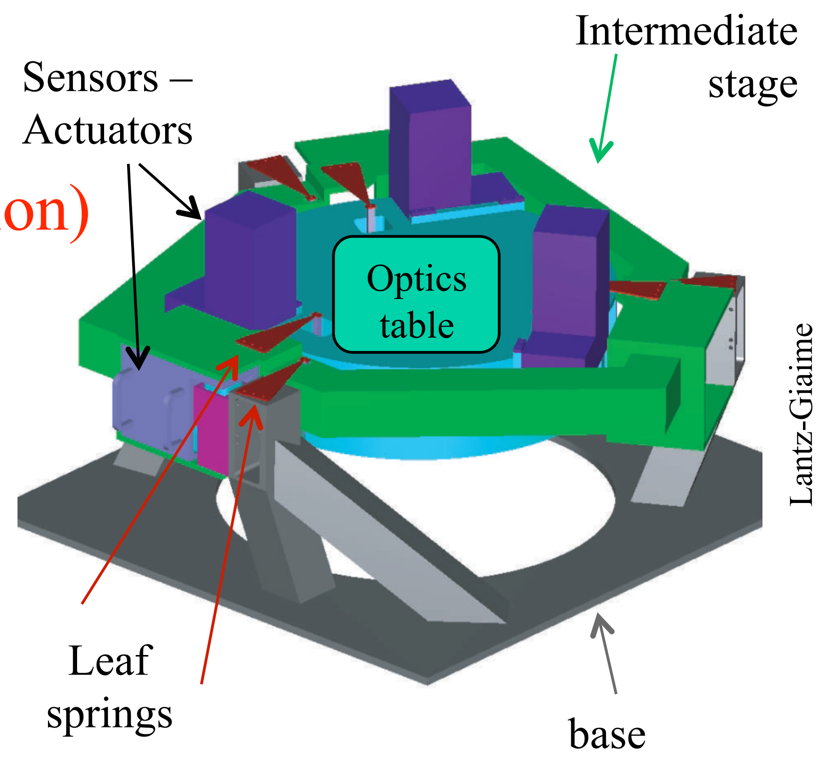

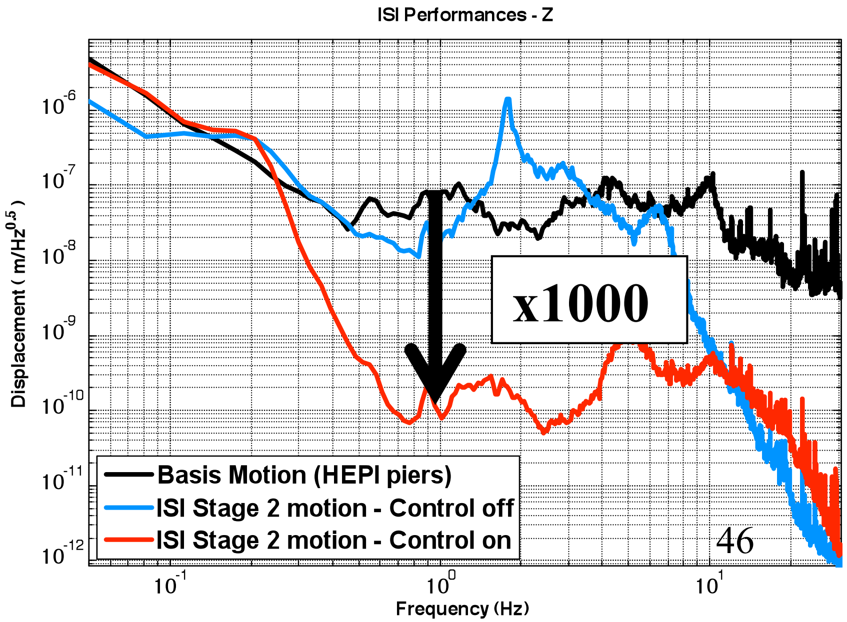

EMVESF270710

credits D. Shoemaker

Suspended mirror speed, orders of magnitude

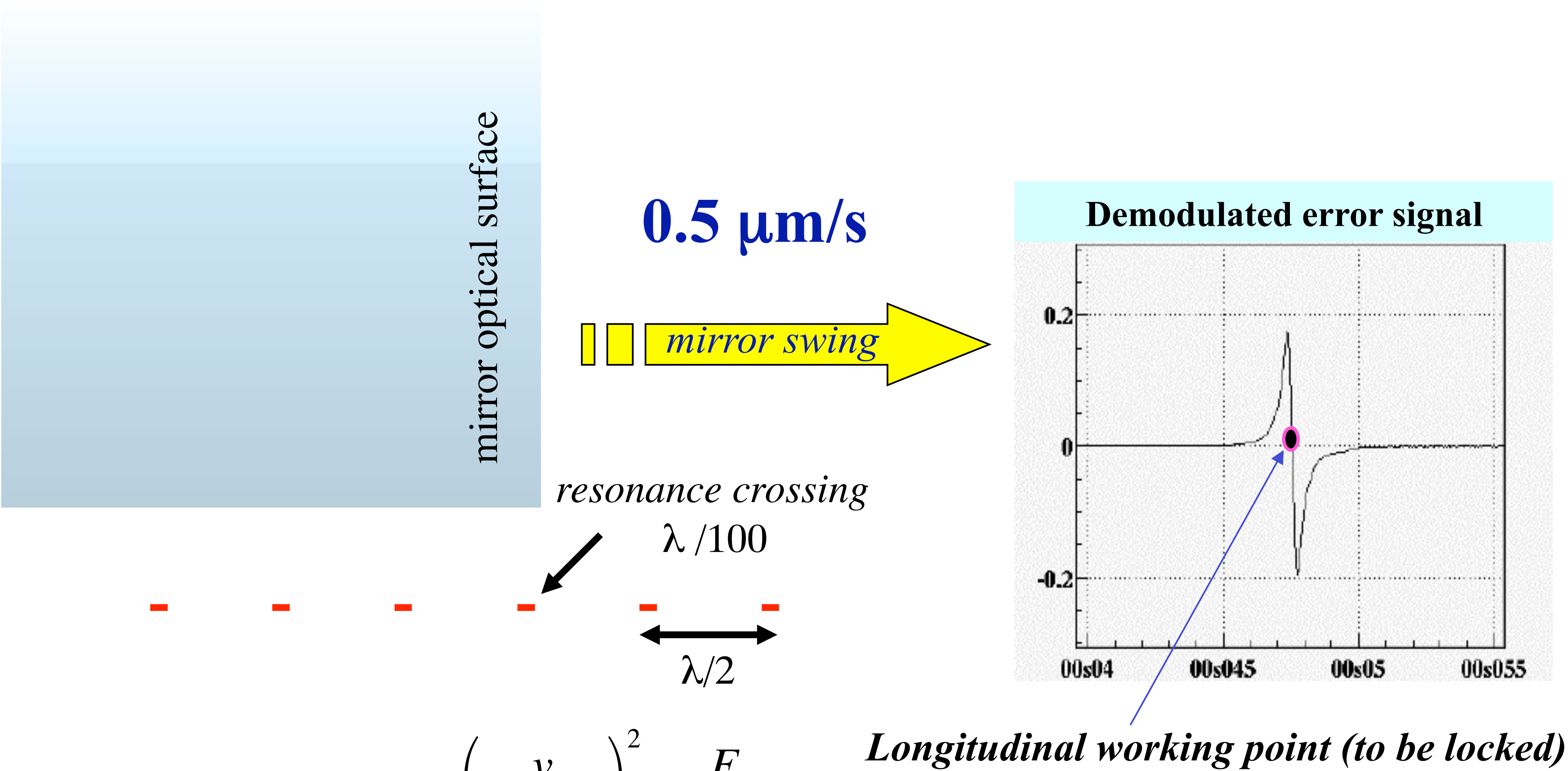

$$f = 10mN \times \left(\frac{v}{1\mu m/s}\right)^2 \times \frac{F}{250}$$

$$\Delta t = 2 \cdot 10^{-3} s \times \left(\frac{1\mu m/s}{v}\right) \times \frac{F}{250}$$

Few mN, few ms range
For actual detectors

M. Barsuglia

Suspended mirror position fluctuation

The mechanics of SA suspension is designed to reach 10^{-18} m/Hz$^{1/2}$ at 10 Hz (thermal noise)

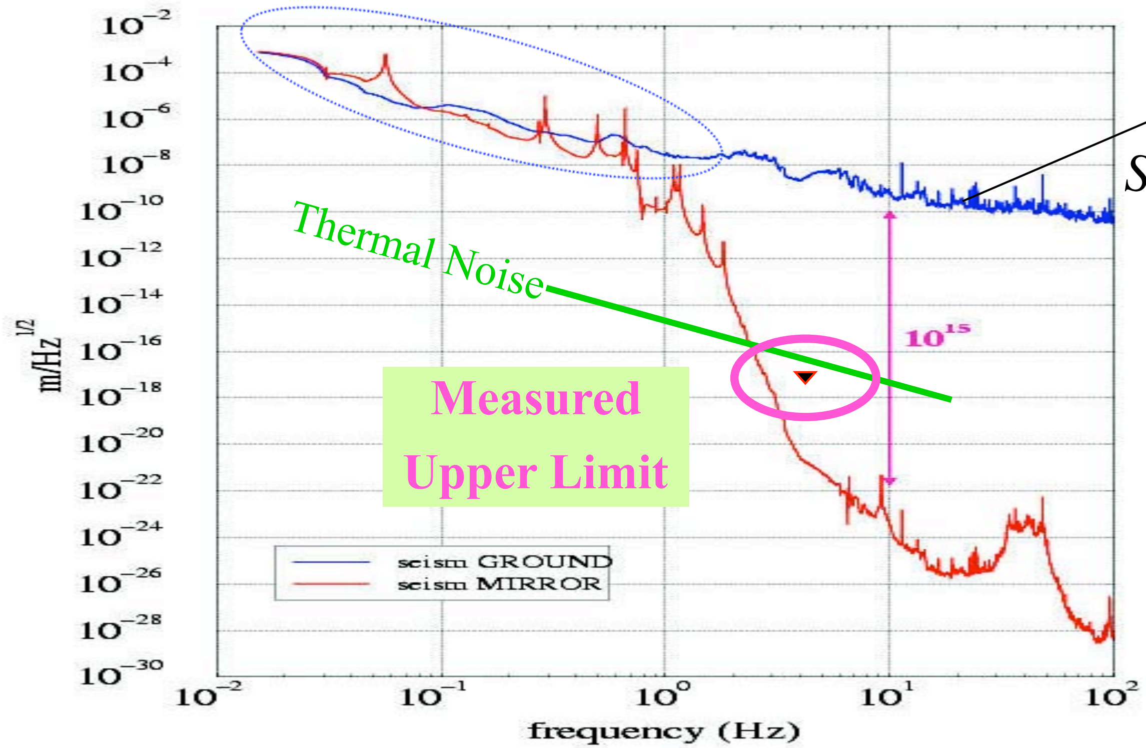

seism at the ground

$$S^{1/2}(f) \approx \frac{10^{-7}}{f^2} m/\sqrt{Hz} \quad (f > 1\ Hz)$$

- The SA filters off the seismic noise above 4 Hz
- Below 4 Hz the mirror moves at the SA resonances few tens of μm
- ITF locking requires resonance damping

TOP: Sophisticated control system for the suspension chain

BOTTOM: Efficient and noiseless payload control

SA

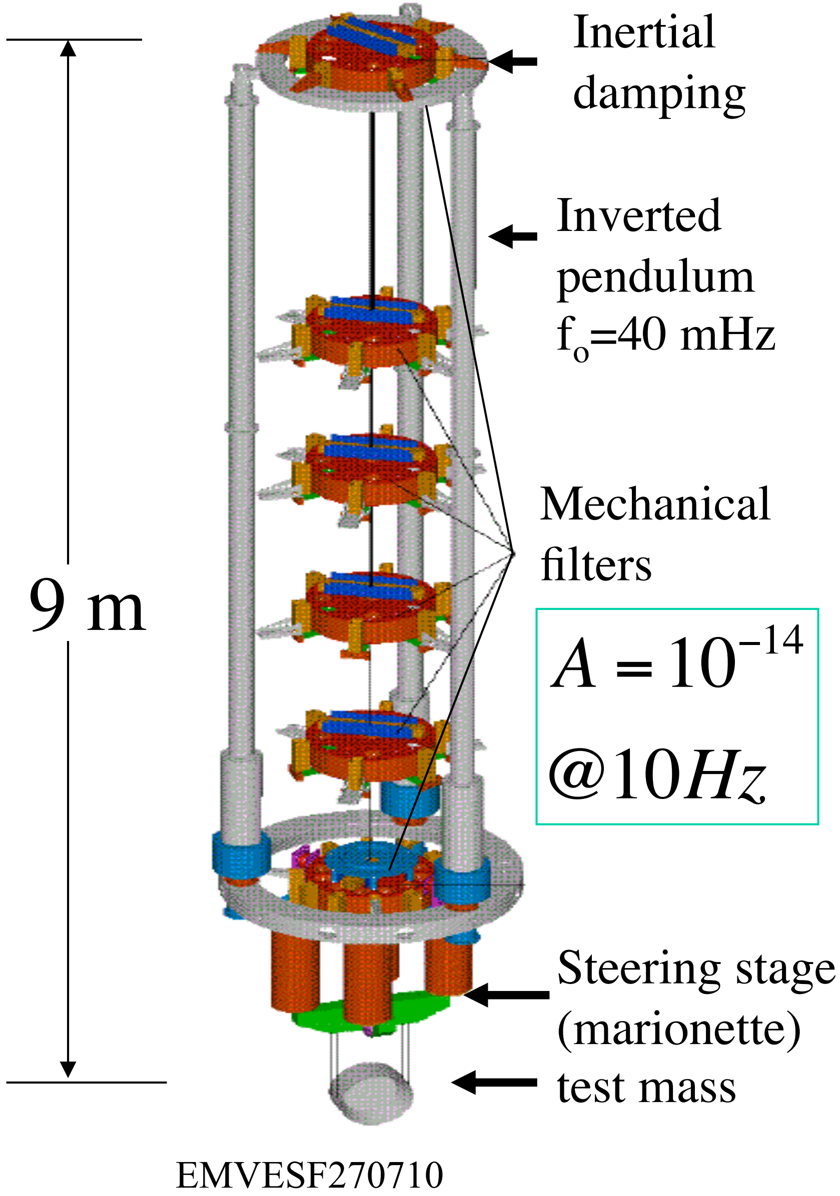

meter

The test masses are optical parts of the ITF !!

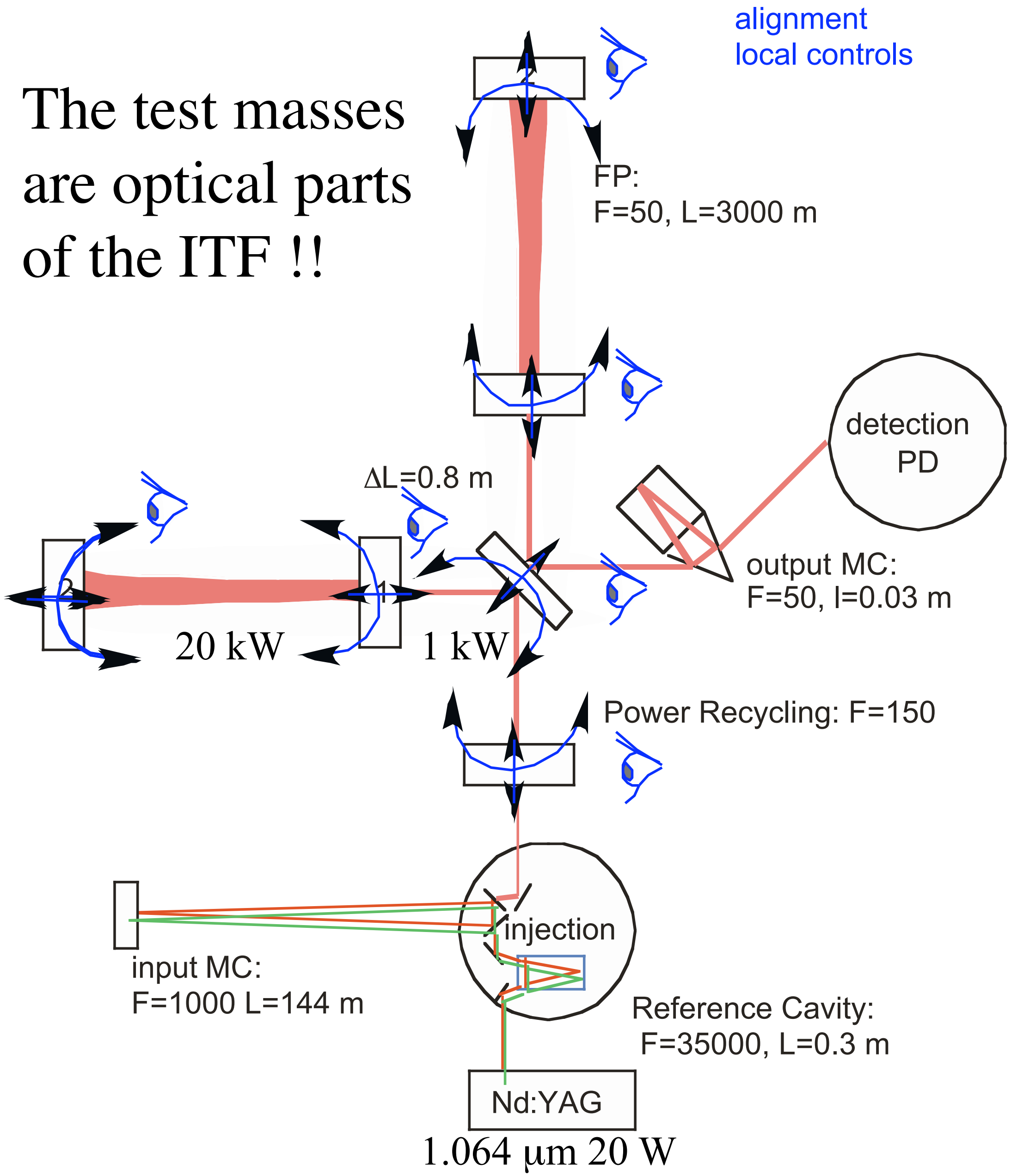

Susp-gallery

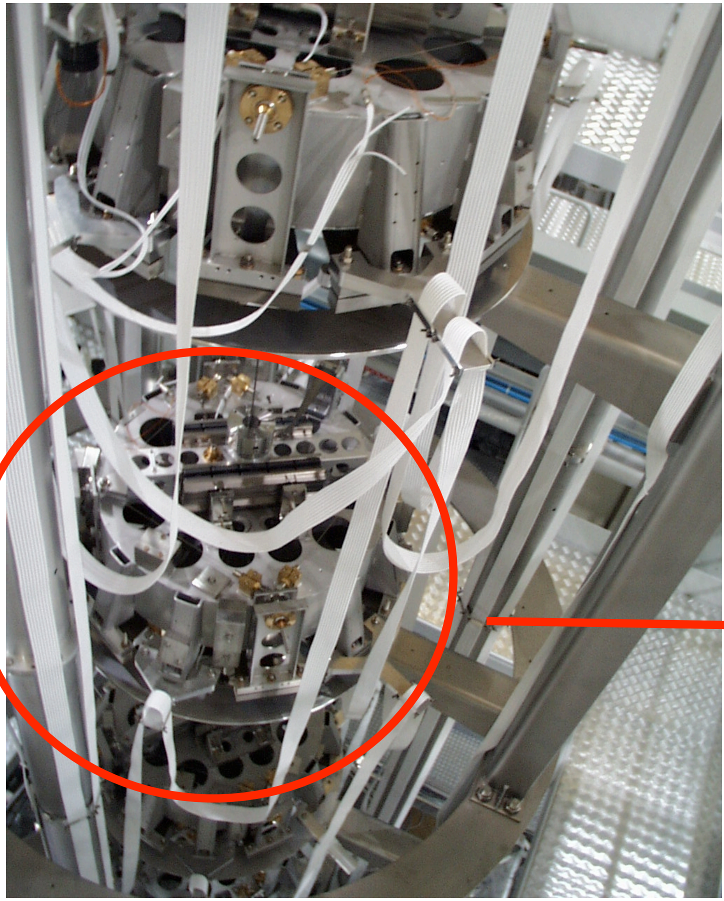

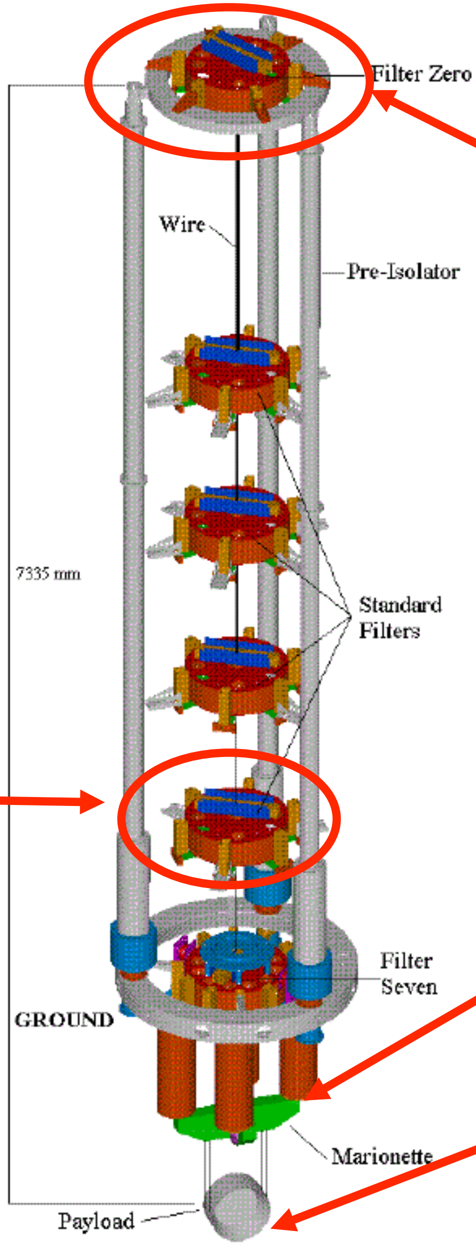

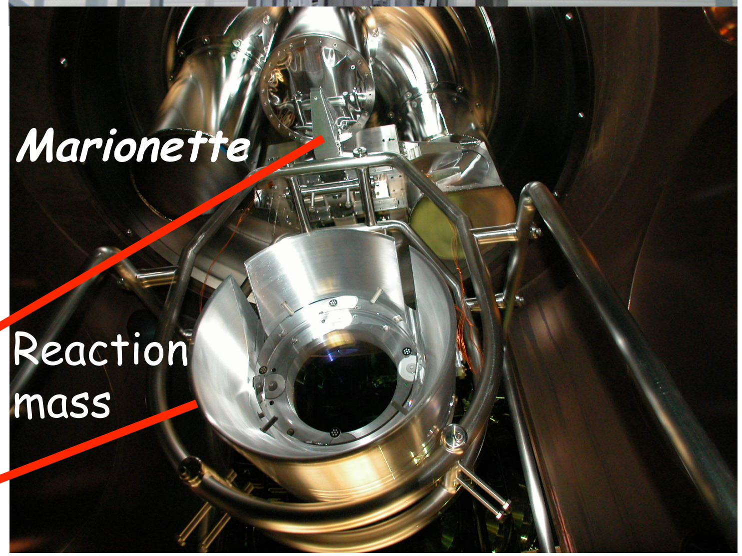

At 10 Hz seismic displacement is 10^{12} times larger than expected GW

EMVESF270710

Local Controls: Inertial Damping

- Inertial sensors (accelerometers):
  - DC-100 Hz bandwidth
  - Equivalent displacement sensitivity: 10^{-11} m/sqrt(Hz)
- Displacement sensors LVDT-like:
  - Used for DC-0.1 Hz control
  - Sensitivity: 10^{-8} m/sqrt(Hz)
  - Linear range: ± 2 cm
- Coil magnet actuators:
  - Linear range: ± 2 cm
  - 0.5 N for 1 cm displacement
- Loop unity gain frequency:
  - 5 Hz
- Sampling rate:
  - 10 kHz

Virgo "standard-super-attenuator" to allow LF sensitivity

Soft isolator concept:

1. very efficient passive attenuation
2. active controls for suspension mode damping

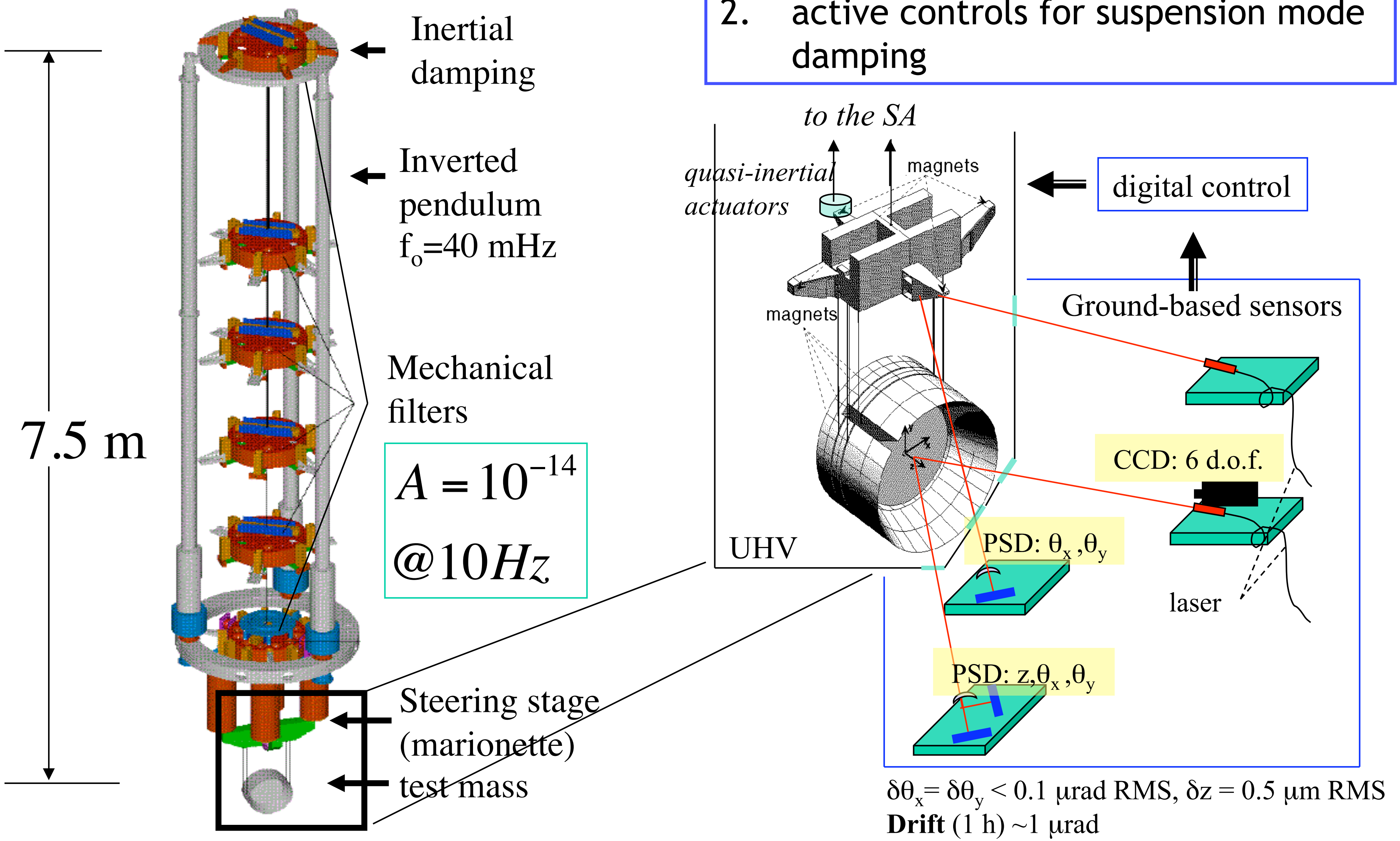

$\delta\theta_x = \delta\theta_y < 0.1$ μrad RMS, $\delta z = 0.5$ μm RMS

Drift (1 h) ~1 μrad

Range: 5×10^{4}-5×10^{-2} μrad, 10^{4}-0.1 μm

Suspension digital control (9 stations): ~all controls are operated using suspended actuators

I) Local controls apply corrections to mirror position using local sensors: swinging interference

II) Local controls receive error signals from global sensors. ITF Locked, resonant light

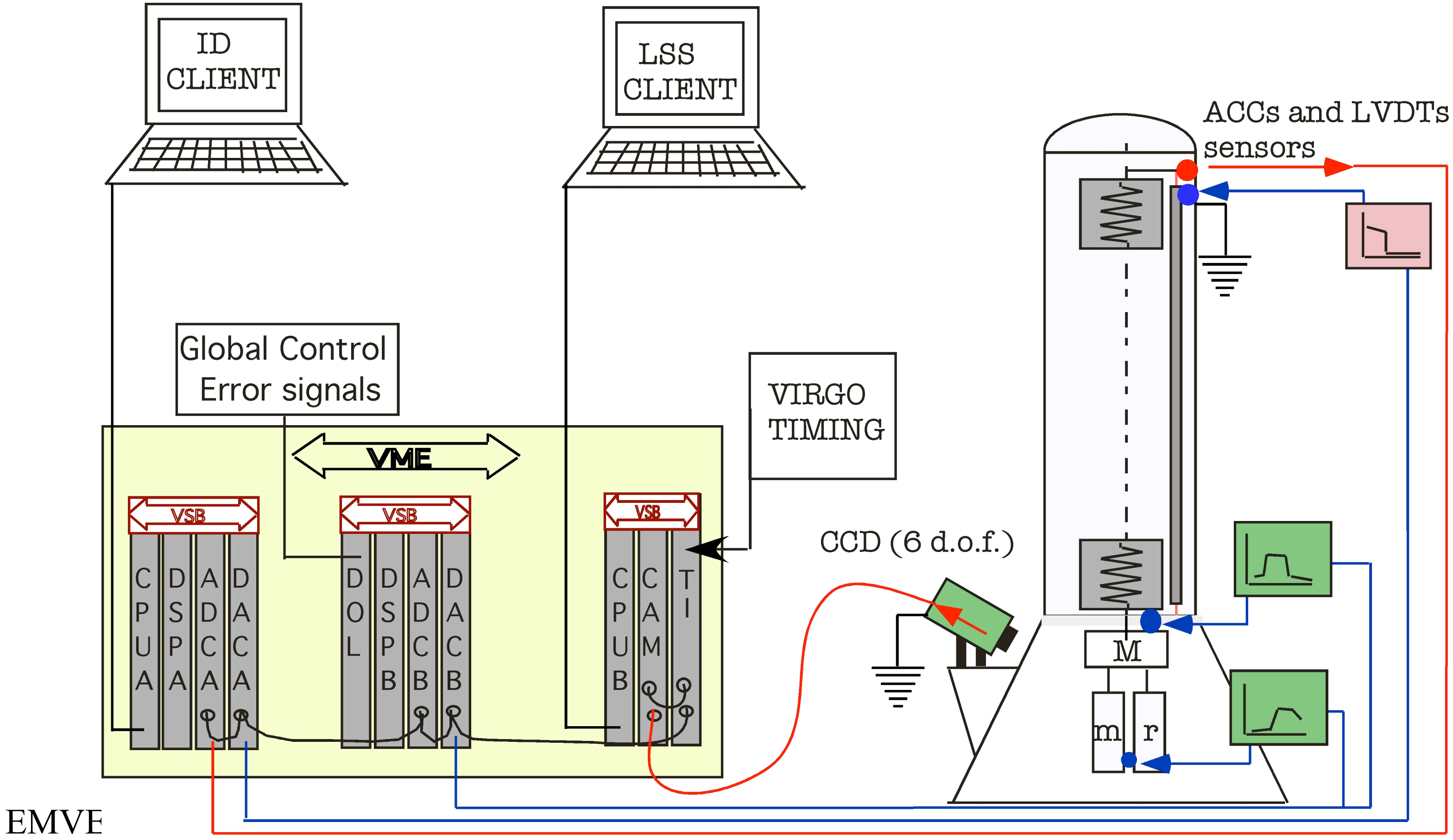

Orientate suspended optics with respect to local ground reference

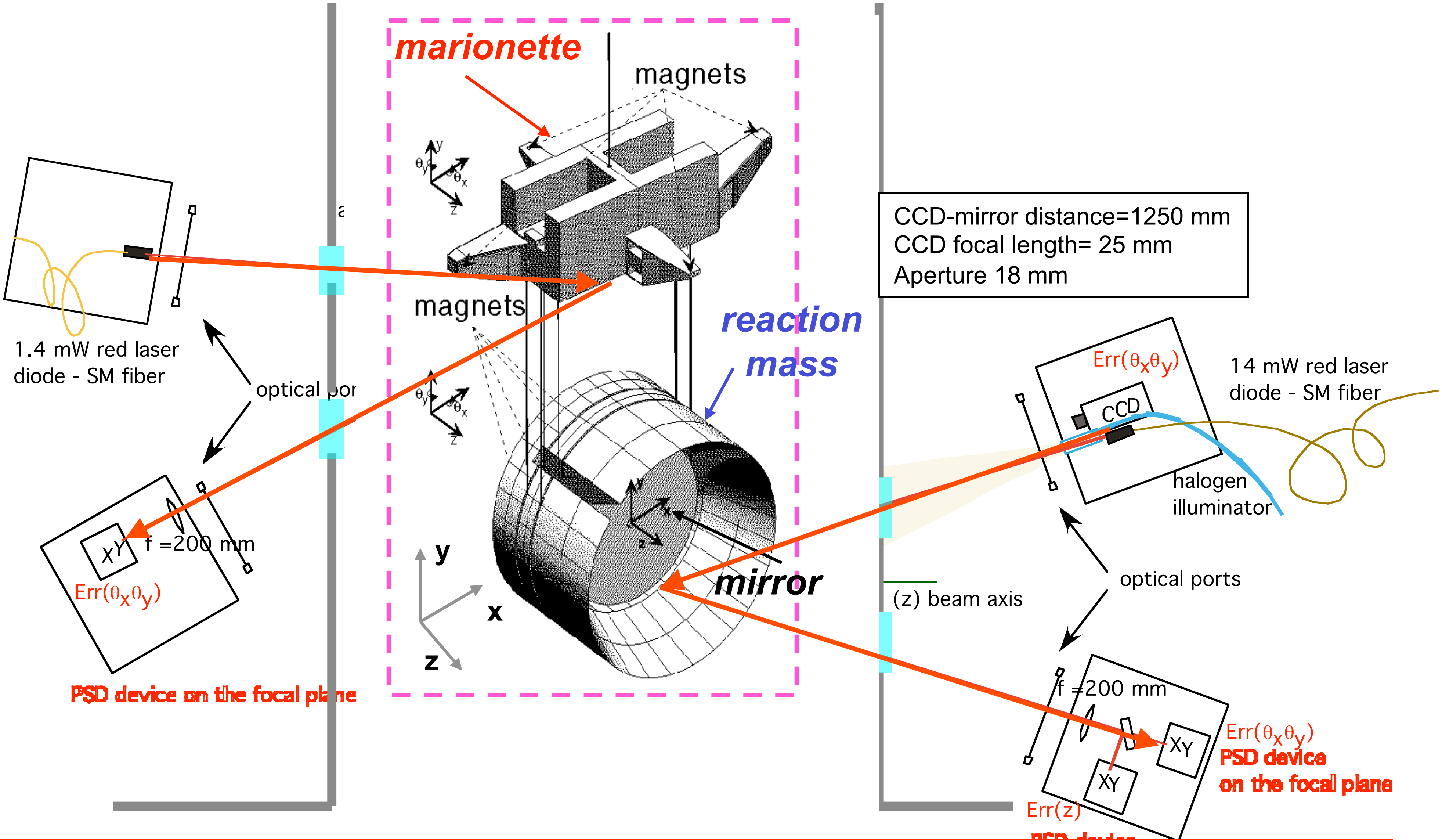

Optical diagonalization of optical levers allow to reduce the coupling among mirror d.o.f. to <1% => Large dynamics: 50 mrad < 80 nrad thanks to hybrid sensor syetem

Two states of operation of mirror suspension control

I) **Incoherent** (Local Control) : the mirrors are controlled by means of independent ground-based sensors and quasi-inertial actuators.

➔ relative position of mirrors is correlated by the ground

II) **Coherent** (Global Control): the operation point has to be locked by using ITF light. Angular control performed coherenty with respect to the light into the ITF by means of beam wavefront sensing (i.e. detection of $TEM_{01,10}$ modes due to misalignment.

➔ relative position of mirrors is correlated by light

Functions of suspension stages and control configuration: the Virgo case (TAMA, LCGT similar): 1) single point suspension, 2) DOF separation, 3) inertial damping, 4) hierarchical control ➔ small forces close to the test mass.

	stage	variable	actuator ref
SA: meant to prevent external disturbance	SA TOP	**Pos/Accel** 3D+yaw	Ground(~)/stars
	SA BOTTOM	**Position** 2D+yaw	Ground
Payload: meant to use test masses as optical elements	MARIONETTE	**Position** 2D+pitch/yaw	SA BOTTOM
	REACT. MASS	**Position** 1D+pitch/yaw	REACT. MASS

Basic requirements: sensing and actuation diagonalization

+

hiearchical control

Divide et impera!

III) Feed-back control basics

(12)

negative feedback basics (I)*

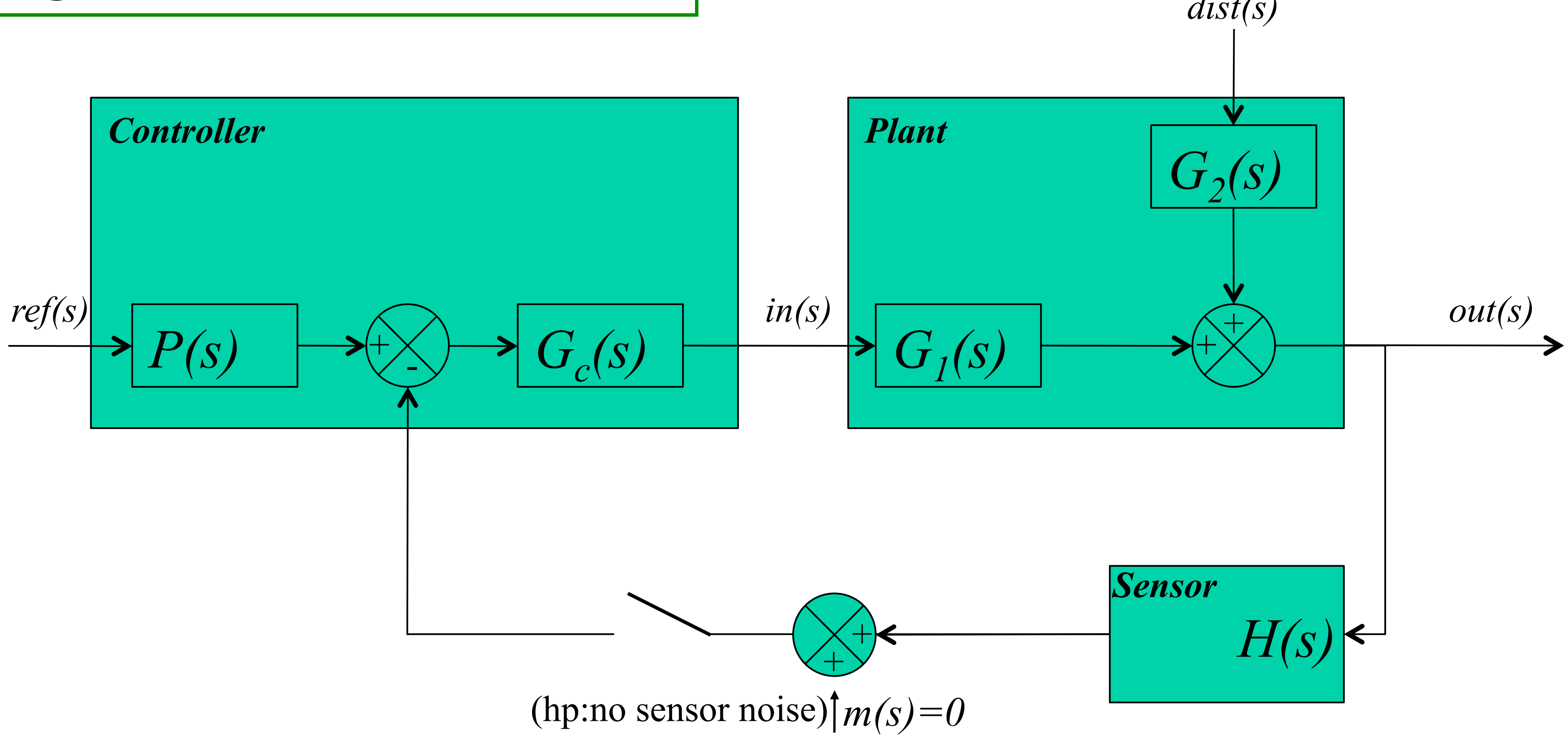

In open-loop we have:

$$out(s) = in(s)G_1(s) + dist(s)G_2(s)$$

In order to deduce the effect of the feedback switch block schematization can be used.

*feed-forward is also used in several subsystems ITFs, but is not mentioned here

negative feedback basics (II)

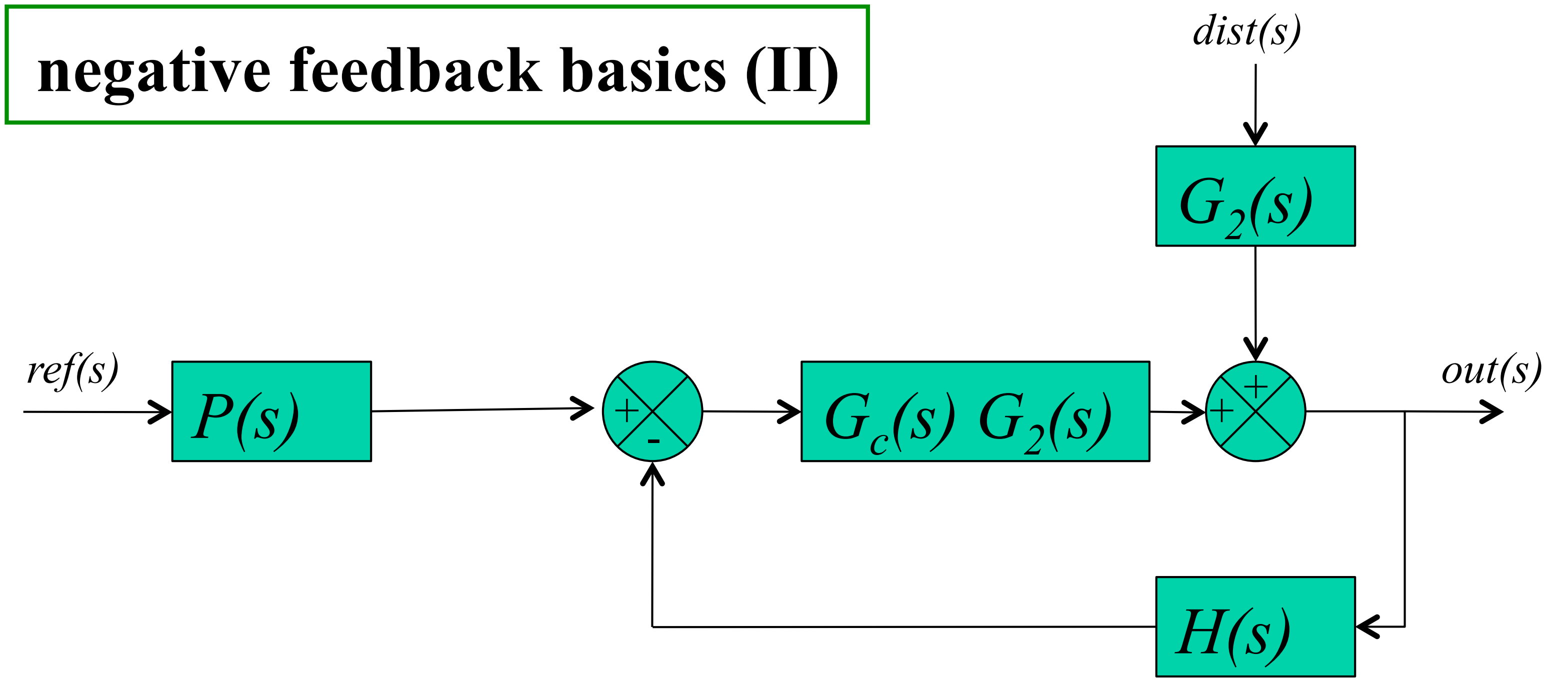

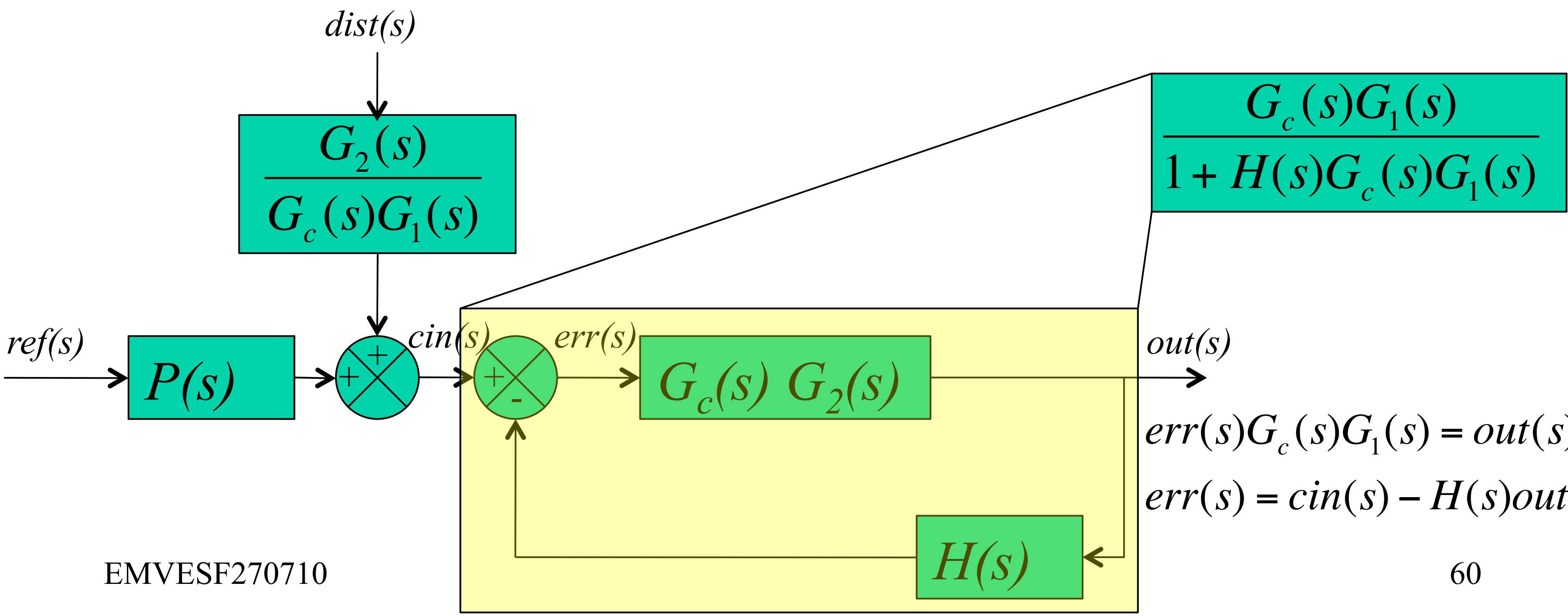

$$err(s)G_c(s)G_1(s) = out(s)$$

$$err(s) = cin(s) - H(s)out(s)$$

negative feedback basics (III)

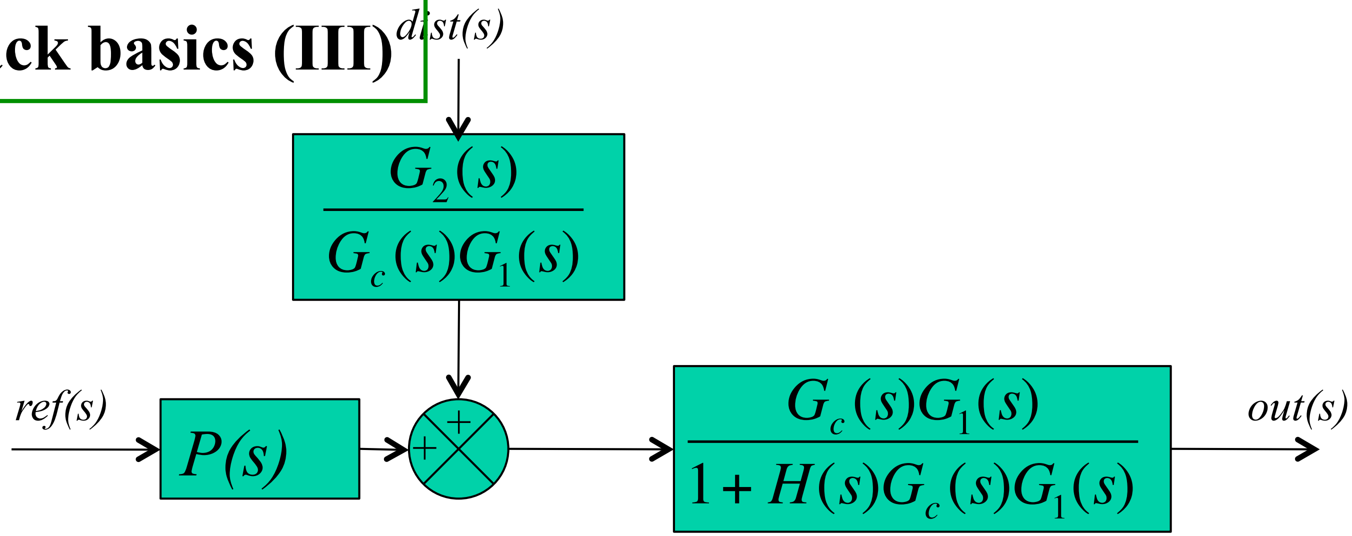

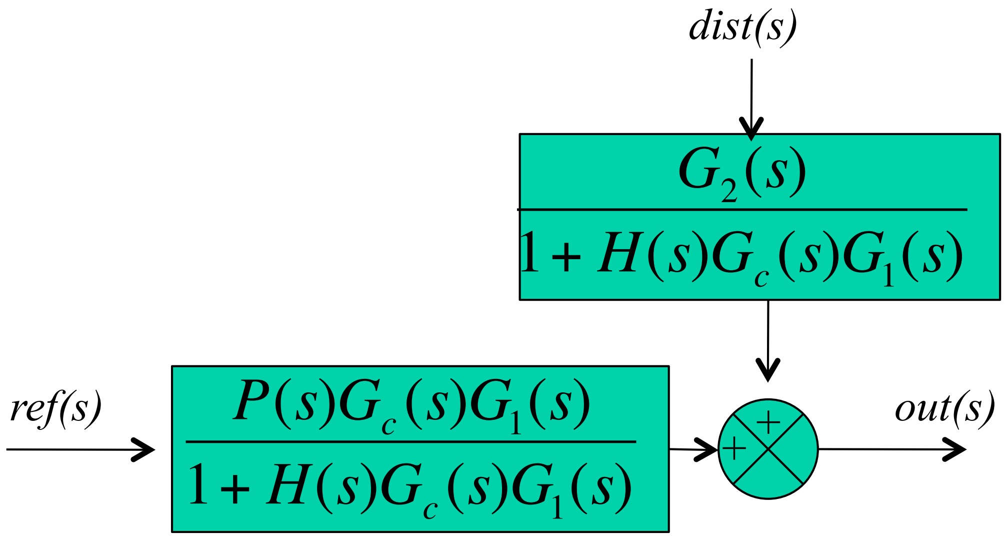

$$out(s) = ref(s)P(s)\frac{G_c(s)G_1(s)}{1+H(s)G_c(s)G_1(s)} + dist(s)G_2(s)\frac{1}{1+H(s)G_c(s)G_1(s)}$$

$$out(s) = ref(s)\frac{P(s)}{H(s)}\frac{T(s)}{1+T(s)} + dist(s)G_2(s)\frac{1}{1+T(s)}$$

$$T(s) = G_c(s)G_1(s)H(s)$$ Loop gain

$$\left.\frac{out(s)}{dist(s)}\right|_{in(s)=0} = \frac{G_2(s)}{1+T(s)}$$

In absence of input driving the disturbance transfer function is reduced by increasing the loop gain *T(s)*

$$\left.\frac{out(s)}{ref(s)}\right|_{dist(s)=0} = \frac{P(s)}{H(s)}\frac{T(s)}{1+T(s)}\left.\right|_{T(s)>>1} \approx \frac{P(s)}{H(s)}$$

The capability to follow the reference with high-gain loops makes the system stuck by *H(s)*

Considering a noise on *H(s)*

$$out(s) = \frac{ref(s)P(s) - m(s)}{H(s)}\frac{T(s)}{1+T(s)} + dist(s)G_2(s)\frac{1}{1+T(s)}$$

Useful definitions and relations

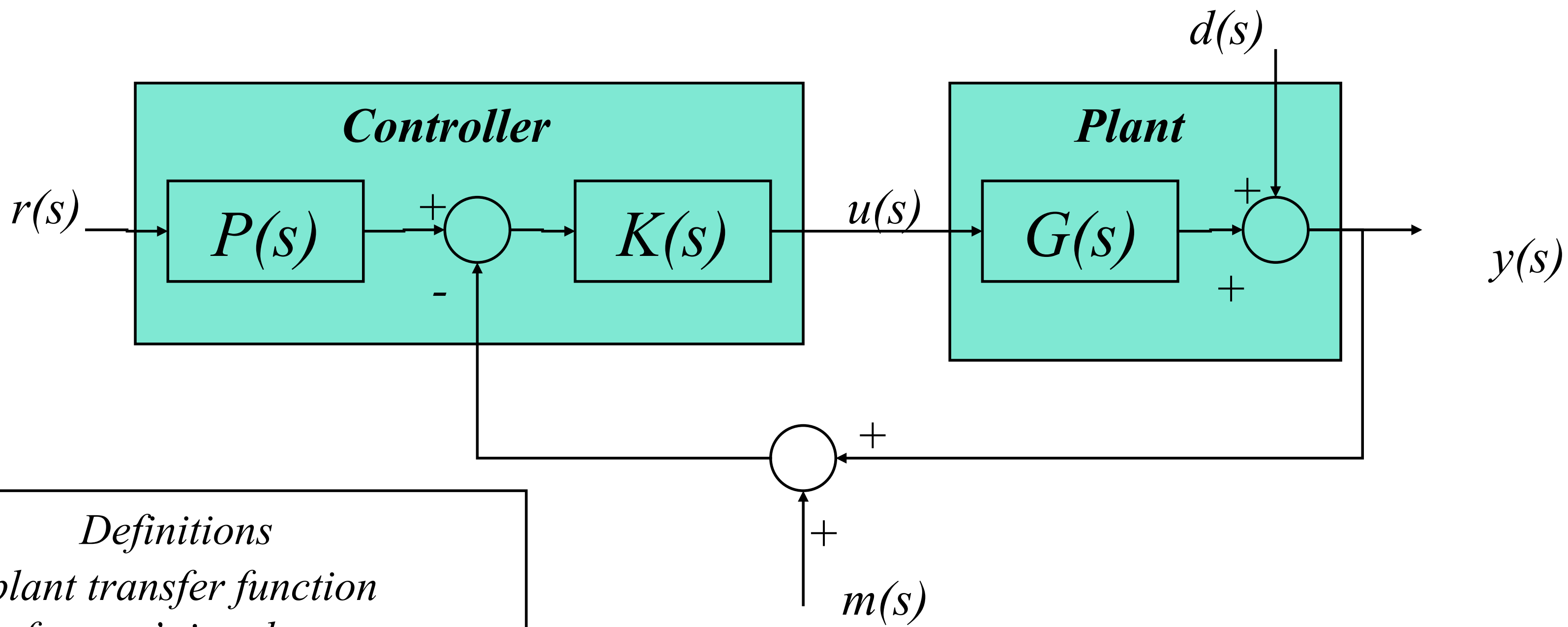

Definitions

$G(s) \rightarrow$ *plant transfer function*
$r(s) \rightarrow$ *'reference' signal*
$u(s) \rightarrow$ *'input' signal*
$y(s) \rightarrow$ *'output' signal*
$m(s) \rightarrow$ *measurement error*
$d(s) \rightarrow$ *disturbance signal*
$P(s) \rightarrow$ *Pre-filter*
$K(s) \rightarrow$ *Feedback compensator*
$G(s)\,K(s) \rightarrow$ *Open Loop Return Ratio*

Fundamental Relations

Return difference $\rightarrow F_o(s) = I + G(s)\,K(s)$
Sensitivity $\rightarrow S(s) = F_o^{-1} = [I + G(s)\,K(s)]^{-1}$
Complementary Sensitivity $\rightarrow T(s) = S(s)\,G(s)\,K(s) = I - S(s)$
Closed Loop Tr. F. $\rightarrow G_c(s) = T(s)\,P(s)$

$$y(s) = S(s)\,d(s) + G_c(s)\,r(s) - T(s)\,m(s)$$

EMVESF270710

credits A. Gennai

Feedback Specifications

- The most common approach to feedback design is to work directly on **open-loop return ratio G(s) K(s)**. Usual specification are the following:

  – $\mathrm{Abs}(G(s)\,K(s)) > L >> 1$, for $0 \leq f < f_l$
  – $\mathrm{Abs}(G(s)\,K(s)) < \varepsilon << 1$, for $f > f_h$
  – Gain margin > m , Phase margin > ϕ

- Above specifications are usually converted in the following one:

  – "Use high loop gain over some frequency range then decrease the gain as rapidly as possible" keeping into account that:
    - An Open-loop stable the roll-off rate in the unity gain region must not exeed 40 dB/dec; for a reasonable phase margin it should be smaller ...
    - Right half-plane zeros impose an upper limit to unity gain frequency
    - Right half-plane poles impose a lower limit to unity gain frequency

Stability

- Stability of a feedback system is determined by the roots of the closed loop *characteristic equation* (i.e. the poles of closed loop transfer function)

$$1+G(s)\,K(s)=0$$

- Nyquist Stability Theorem
  - The closed loop system is stable if and only if the graph of G(jω) K(jω) in the complex plane, for $-\infty < \omega < \infty$, encircles the point -1+j0 as many times anticlockwise as G(s) K(s) has right half-plane poles

Digital Controllers

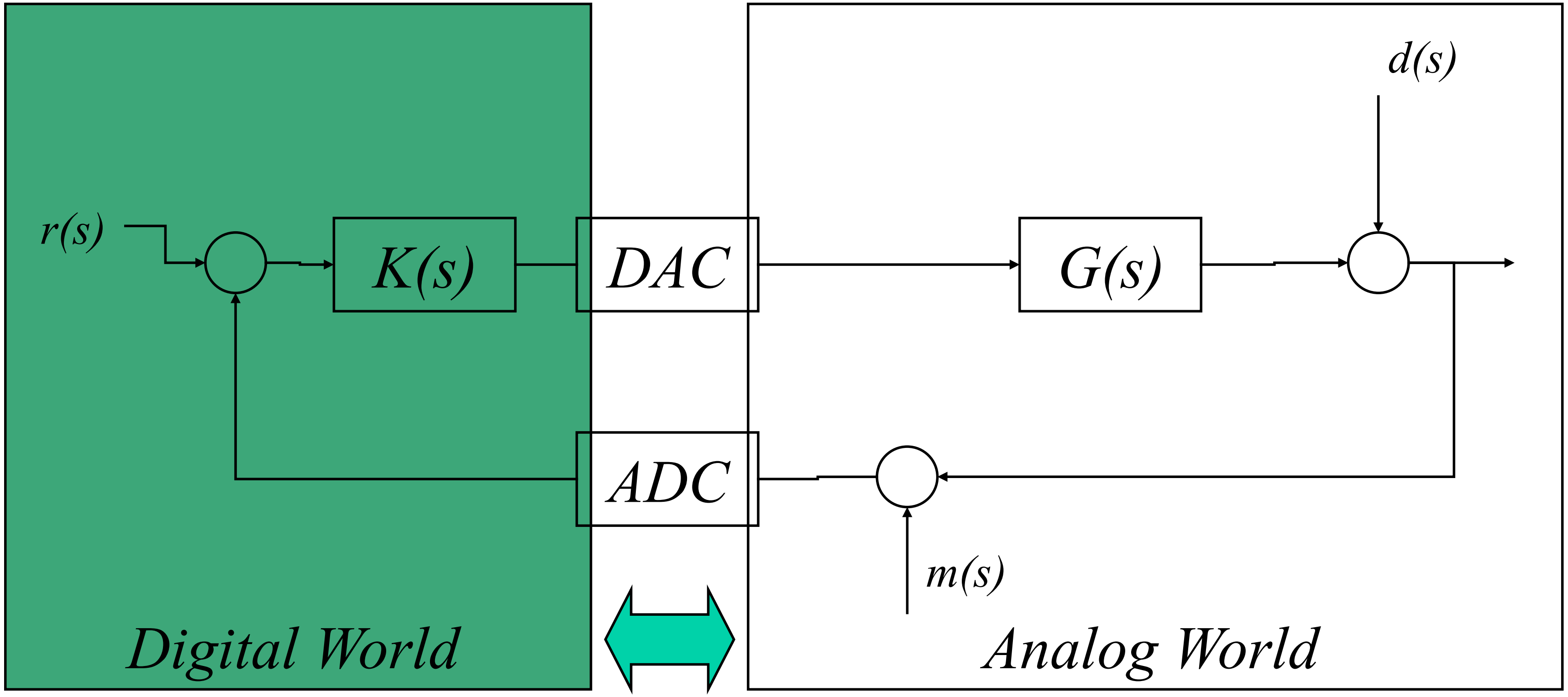

- Analog to Digital (ADC) and Digital to Analog Converters (DAC) are the interface between the 'Analog' and the 'Digital' world.

Time-continuous vs time-discrete controllers

- Why digital controllers?
  - Programmability and Flexibility
  - Stability and Repeatability
  - Performances

- Why analogue controllers?
  - Bandwidth
  - Dynamics

The Z-Transform

- The Z-transform of a discrete-time function *f(kT)* is designated by F(z) and is defined as follows:

$$F(z) = \sum_{k=-\infty}^{\infty} f(kT)\, z^{-kT}$$

T = Sampling Period

- Bilinear Transformation

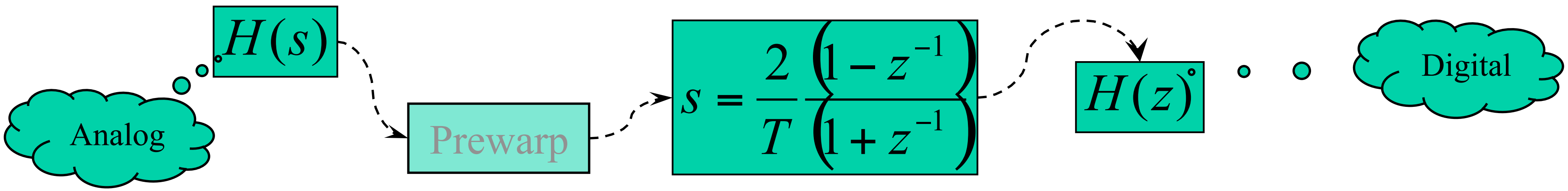

Timing And Time Delay

- Timing has a key role in any digital control system.
- The sampling period shall be constant since poles and zeros position are a function of sampling period. Varying the period means varying poles and zeros locations
- ADC and DAC must be synchronized not to introduce phase noise.

Sensing & Driving (implemented in DSP controllers)

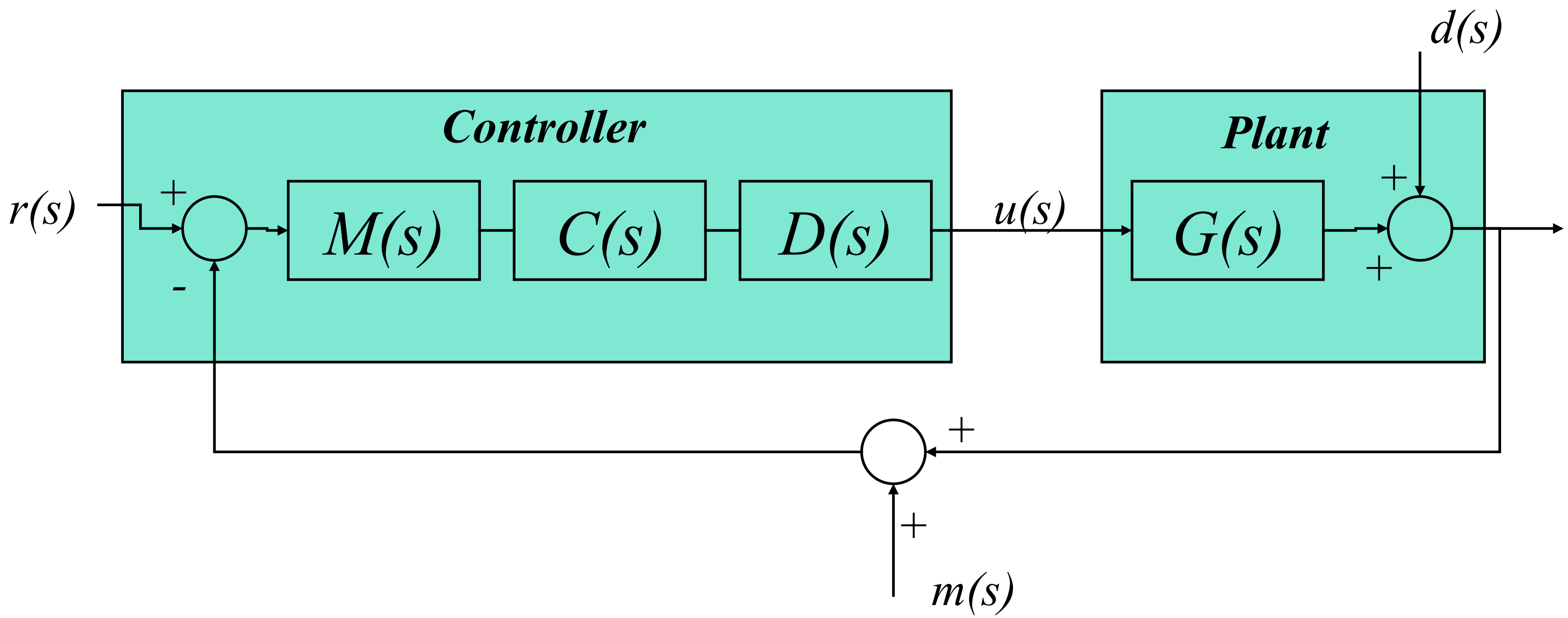

M(s) => 'Sensing' : projection of sensors output along given (preferred) directions
D(s) => 'Driving' : projection of correction signal along actuators directions
C(s) => Compensator

D and M implemented in Virgo are 'static' matrixes (constant) such that C(s) is diagonal, hence:
Multiple Input / Multiple Output (MIMO)
converted to a set of Single Input /Single Output (SISO)

IV) Locking

The operation point

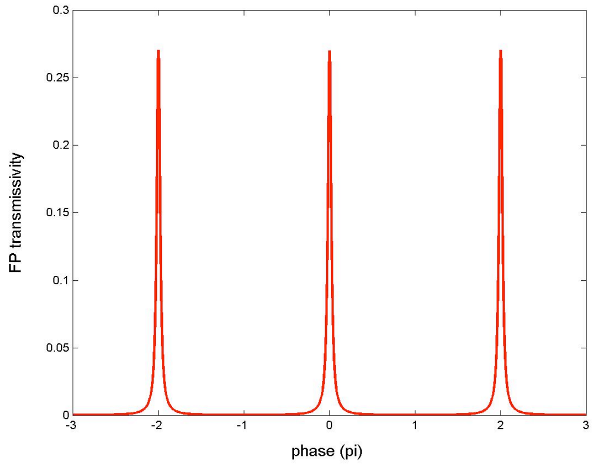

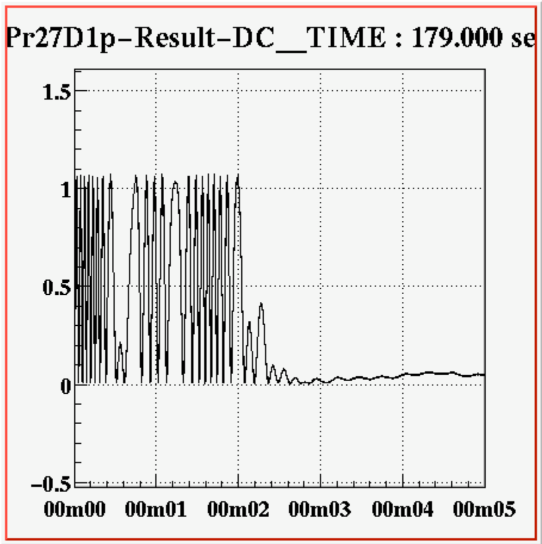

- Keep the FP cavities in resonance
  - Maximize the phase response
- Keep the PR cavity in resonance
  - Minimize the shot noise
- Keep the output on the “dark fringe”
  - Reduce the dependence on power fluctuations

LOCKING

Keep the armlength constant within 10^{-12} m !

Alignment configuration for Virgo (VSR1)

Note: Automatic alignment, based on wavefront sensing and DC asymmetry is a aommon practice in all interferometers (a specific chapter should be dedicated to the topic)

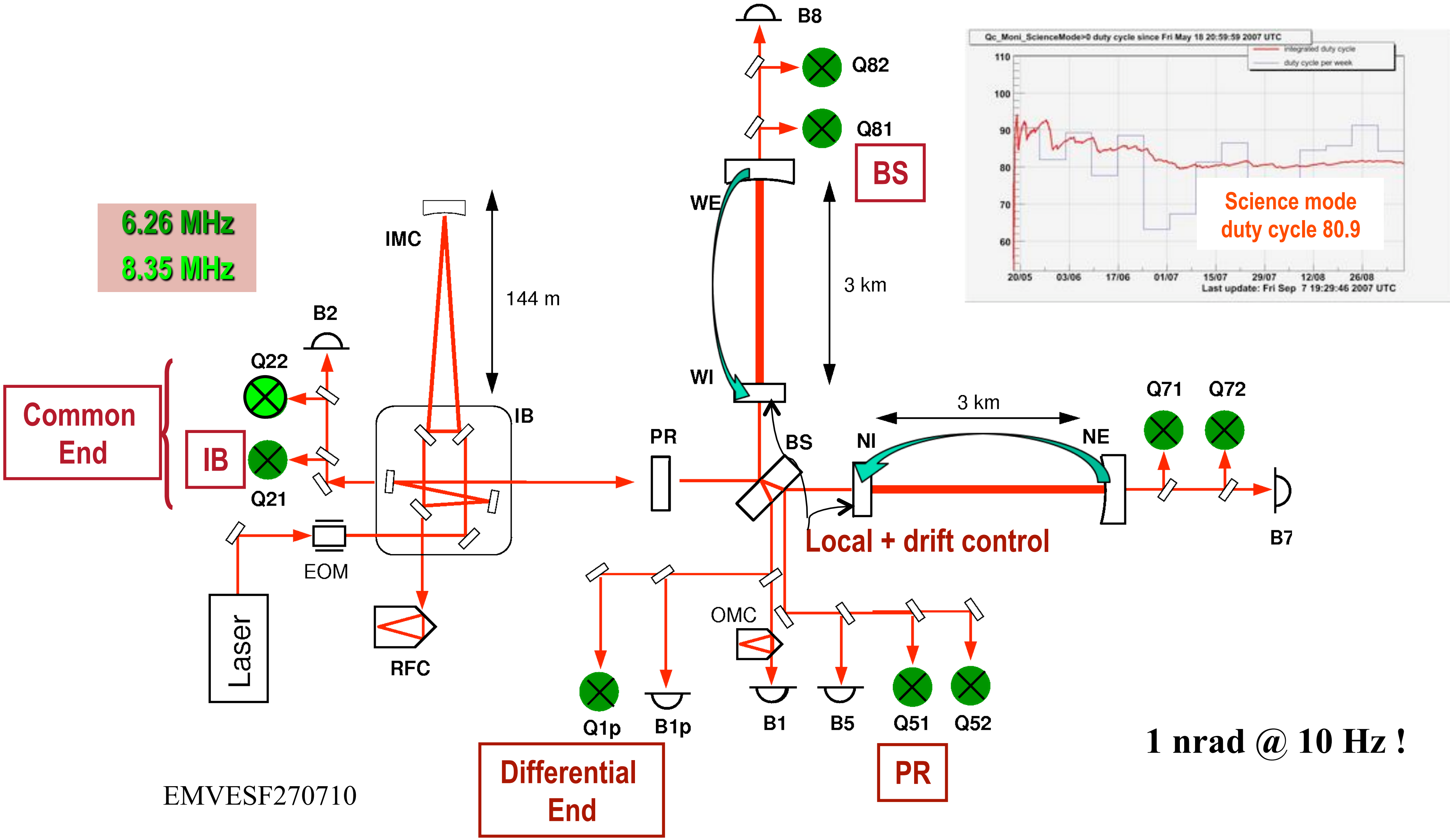

1 nrad @ 10 Hz !

EMVESF270710

Basic interference setup: two conditions

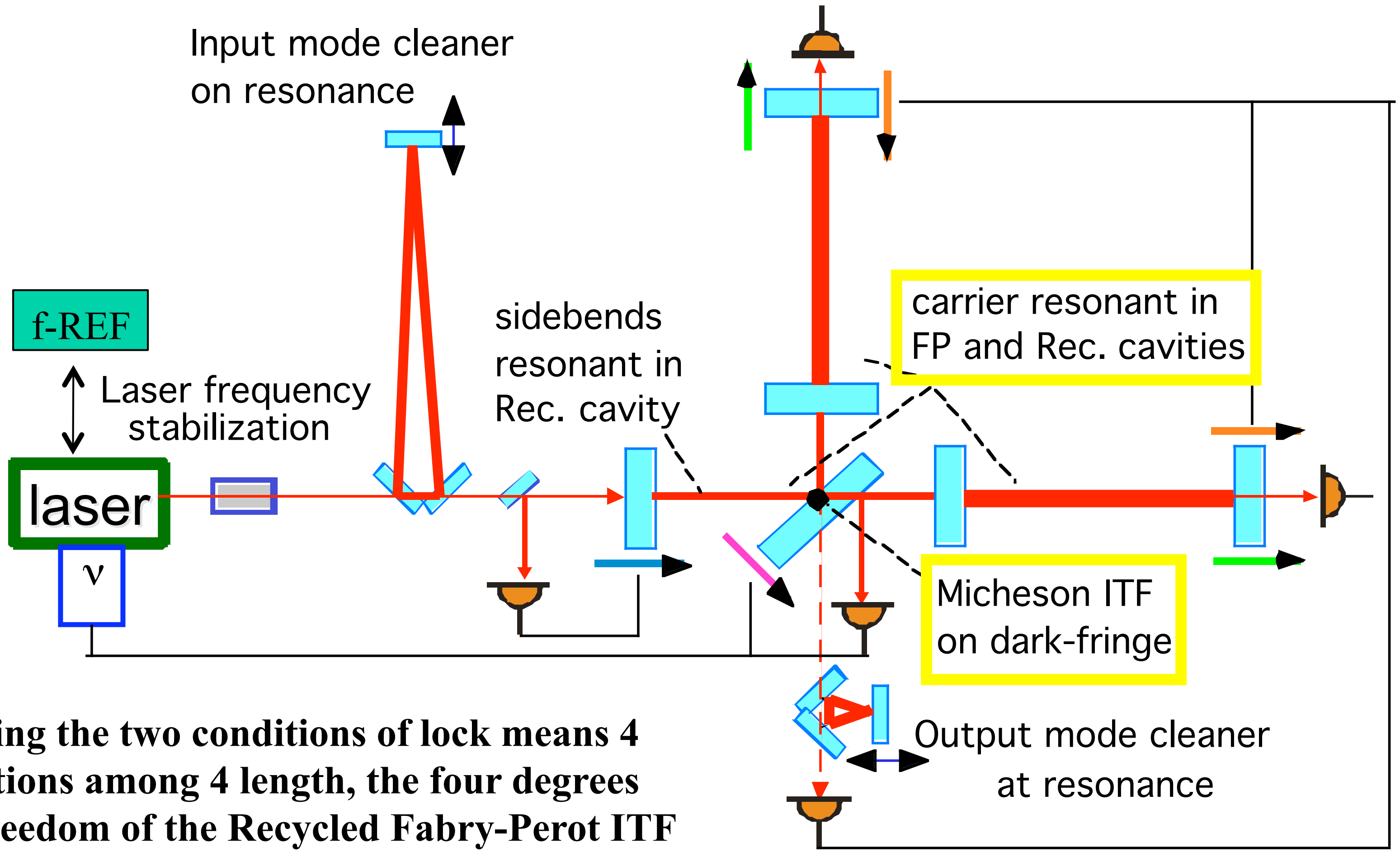

Setting the two conditions of lock means 4 relations among 4 length, the four degrees of freedom of the Recycled Fabry-Perot ITF

- Dark Fringe set point (MICH)
- Differential Arm length (DARM)
- Power Recycling Cavity Length (PRCL)
- Common Arm length (CARM)

EMVESF270710

Basic interference setup: two conditions

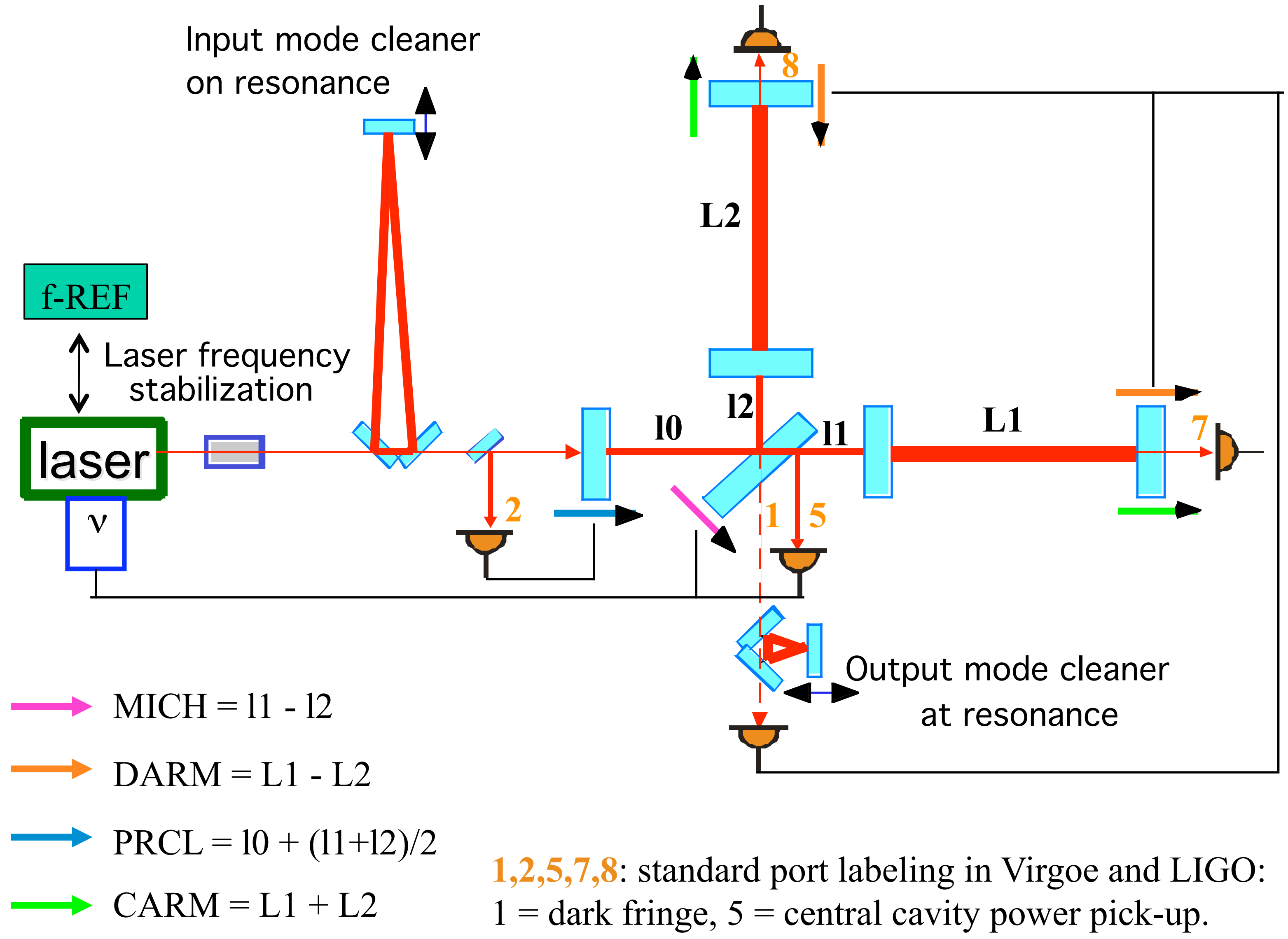

1,2,5,7,8: standard port labeling in Virgoe and LIGO:
1 = dark fringe, 5 = central cavity power pick-up.

2 stage Fstab concept:

ULE rigid REF. CAVITY➔ LASER@LF
CARM ➔ LASER@ HF

EMVESF270710

$$\begin{pmatrix} l_0 \\ l_1 \\ l_2 \\ L_1 \\ L_2 \end{pmatrix} = \begin{pmatrix} 1 & \sqrt{2} & 0 & 0 & 0 & 0 \\ 0 & -\sqrt{2} & 1 & 0 & 0 & 0 \\ 0 & 0 & 0 & 1 & 0 & 0 \\ 0 & 0 & -1 & 0 & 1 & 0 \\ 0 & 0 & 0 & -1 & 0 & 1 \end{pmatrix} \cdot \begin{pmatrix} x_{PR} \\ x_{BS} \\ x_{NI} \\ x_{WI} \\ x_{NE} \\ x_{WE} \end{pmatrix}$$

Physical displacement of mirrors

Error signals

$$\begin{pmatrix} PRCL \\ MICH \\ CARM \\ DARM \end{pmatrix} = \begin{pmatrix} 1 & 1/2 & 1/2 & 0 & 0 \\ 0 & 1 & -1 & 0 & 0 \\ 0 & 0 & 0 & 1/2 & 1/2 \\ 0 & 0 & 0 & 1 & -1 \end{pmatrix} \cdot \begin{pmatrix} l_0 \\ l_1 \\ l_2 \\ L_1 \\ L_2 \end{pmatrix}$$

E.g.: requirements for Virgo *G. Vajente 2010*

D.O.F.	Requirements [m]	Accuracy [m]	
		VSR1	May 2008
DARM	$3\cdot10^{-11}$	$3\cdot10^{-12}$	$1\cdot10^{-15}$
PRCL	$2\cdot10^{-10}$	$3\cdot10^{-11}$	$1\cdot10^{-12}$
MICH	$5\cdot10^{-10}$	$8\cdot10^{-11}$	$3\cdot10^{-11}$
CARM		$4\cdot10^{-8}$	$2\cdot10^{-8}$

Sensing

- How do we actually measure lengths?
  - Laser light is phase-modulated: we have a ‘carrier’ frequency and two sidebands
  - Carrier is resonant in the two long cavities
  - Sidebands are resonant in the recycling cavity
  - The demodulated photodiode output is a function of phase shift (i.e. a length variation) in the resonant field.
- Motion along the 4 degrees of freedom is detected using three photodiodes (for B5 we use both phase and quadrature components)

$$\begin{pmatrix} PRCL \\ MICH \\ CARM \\ DARM \end{pmatrix} = \begin{pmatrix} 0 & g_{PRCL} & 0 & 0 \\ g_{MICH} & g_X & 0 & 0 \\ 0 & 0 & 0 & g_{CARM} \\ 0 & 0 & g_{DARM} & 0 \end{pmatrix} \cdot \begin{pmatrix} B5\_Quad \\ B2\_Phase \\ B1\_Phase \\ B5\_Phase \end{pmatrix}$$

Driving

- MICH, PRCL and DARM are corrected applying forces on 4 mirrors
- CARM is corrected using a sort of trick
  - CARM error signal is used to change the laser frequency: in this way laser frequency swings following the common mode motion of the two long cavities
  - At low frequency laser frequency is ‘locked’ to a reference cavity length thus preventing CARM to drift away.

$$\begin{pmatrix} F_{BS} \\ F_{PR} \\ F_{NE} \\ F_{WE} \end{pmatrix} = \begin{pmatrix} 1/\sqrt{2} & 0 & 0 \\ -2 & -1 & 0 \\ 0.1 & 0 & 1 \\ -0.1 & 0 & -1 \end{pmatrix} \cdot \begin{pmatrix} F_{MICH} \\ F_{PRCL} \\ F_{DARM} \end{pmatrix}$$

Basic controller for Virgo

- A digital controller is used for MICH PRCL and DARM.
- An analog controller is used for CARM
- Dynamic compensators are quite complex. We have between 10 and 20 poles for each degree of freedom.
- Unity gain frequencies are in the 10 - 50 Hz range for MICH PRCL and DARM and in the 100-200 kHz range for CARM

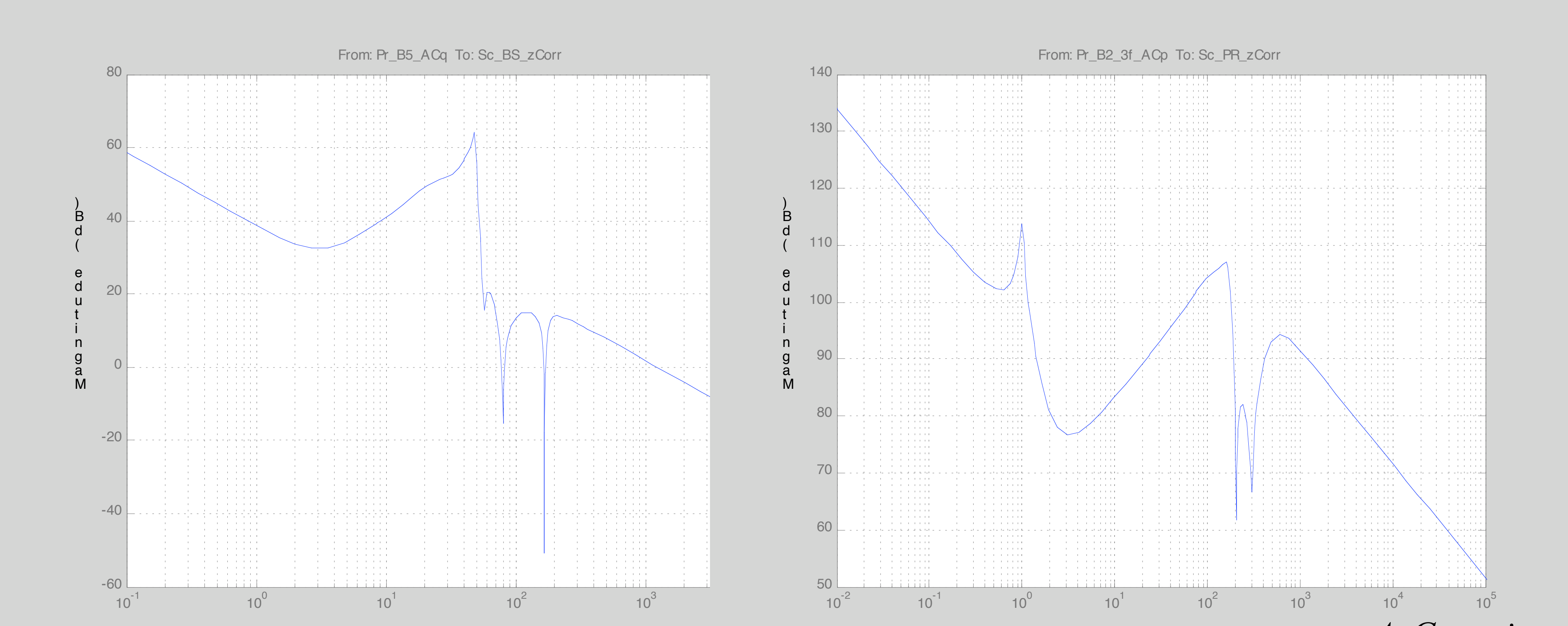

A Gennai

Locking strategies strongly depend on suspension systems: LIGO and Virgo
(strategies will be significantly different for Adv Detectors)

LIGO

sidebands
carrier

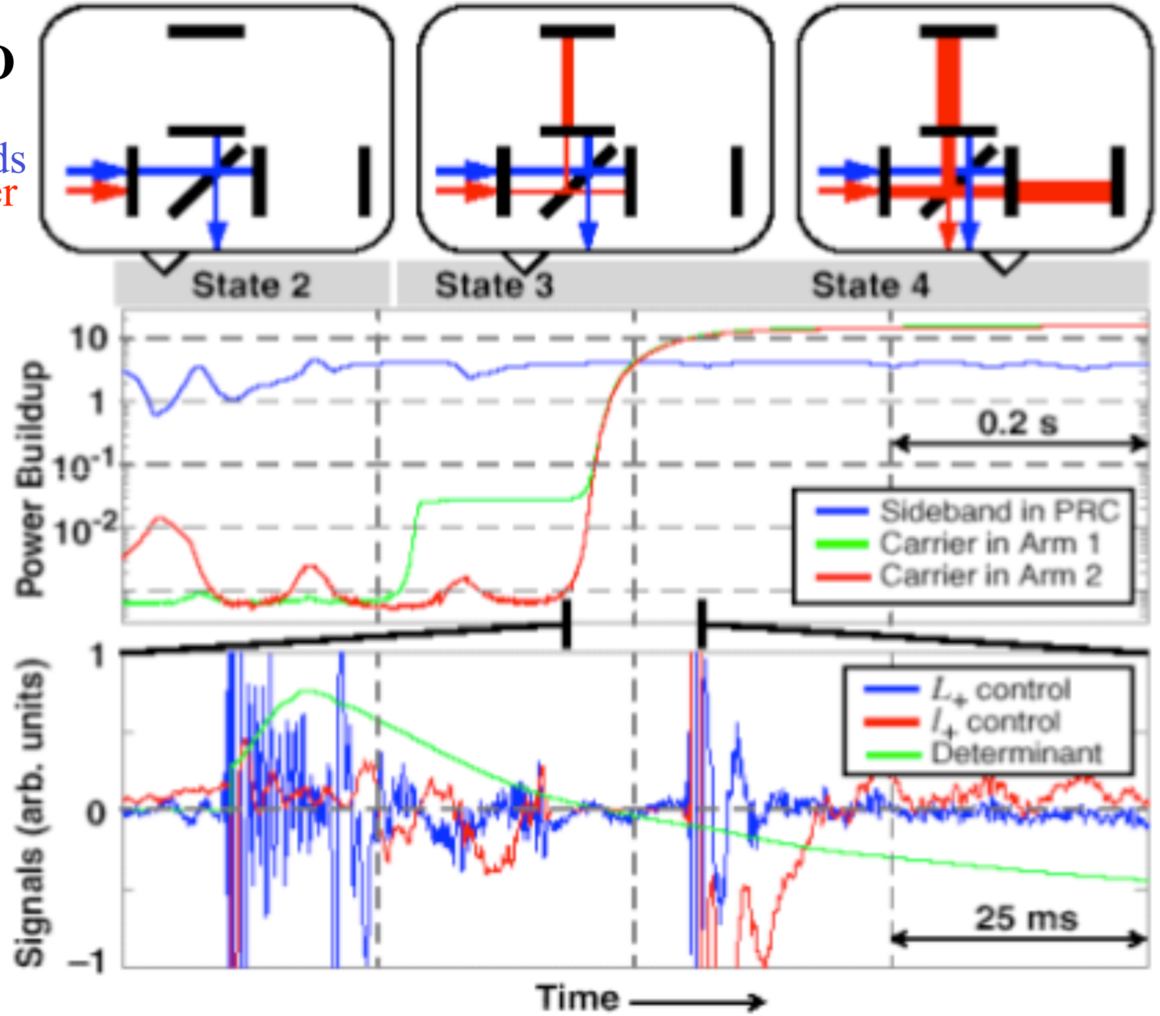

The process goes through unstable states

Faster is better

Power Recycling cavity has not autoalignment at the beginnings

Faster is better

Unachievable with LF Virgo-like suspensions

Control noise ➔ smallest forces close to test masses

- Required locking accuracy:
- $dL \sim 10^{-12}$ m
- Tidal strain over 3 km: $dL \sim 10^{-4}$ m
- Wide dynamic range to be covered without injecting actuation noise.
- Hierarchical Control
- 3 actuation points

<u>A note about hierarchical control:</u>

●Acting on Marionette from the last suspension stage, Superattenuator modes are excited (blue)

●Acting on Mirror from Reference Mass only, one longitudinal mode is excited (green)

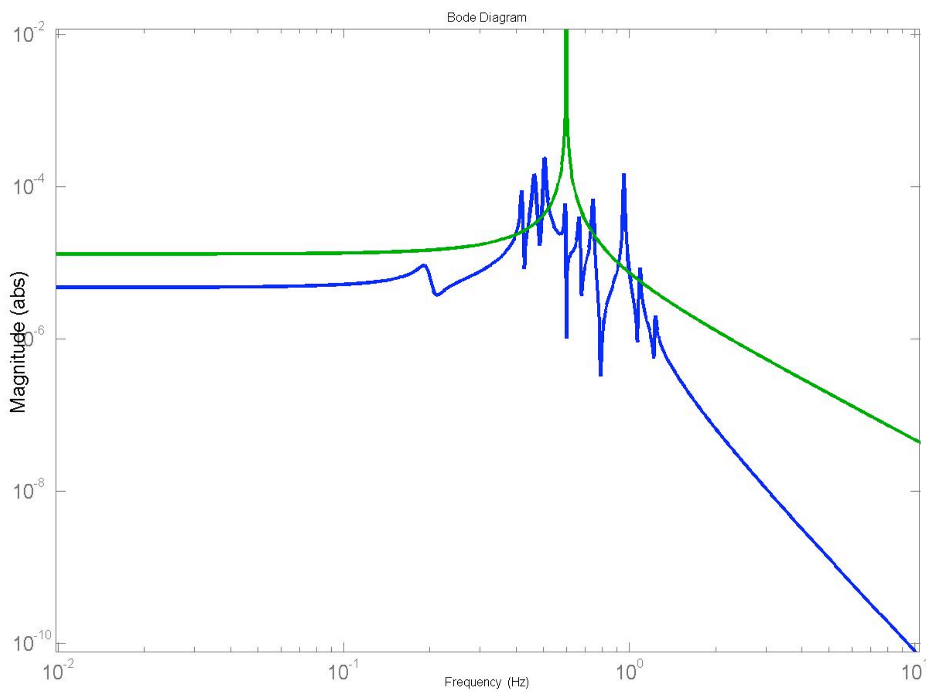

Actuation on the test masses: full hierarchical control

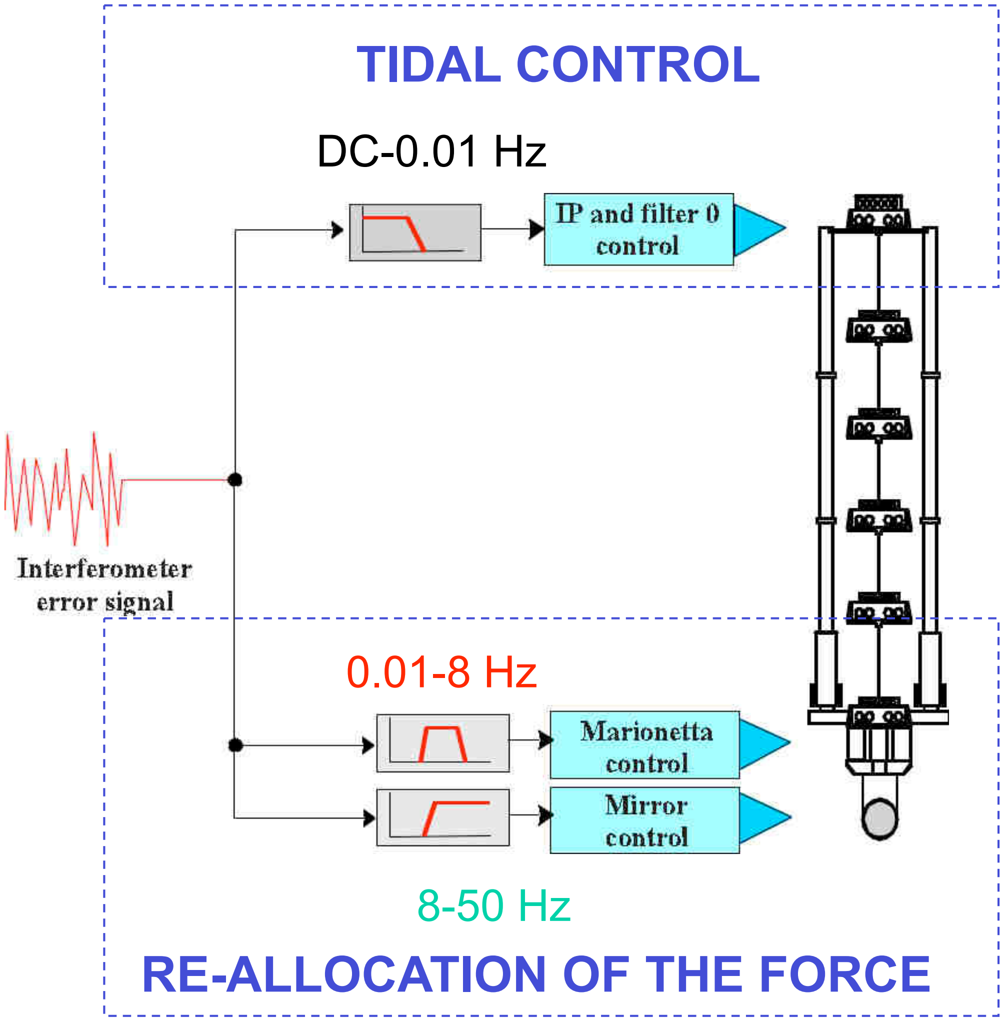

Corrections sent to the Marionette coil/magnets

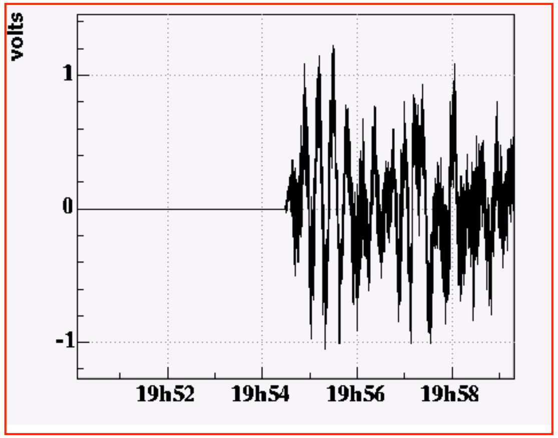

Corrections sent to the mirror coil/magnets

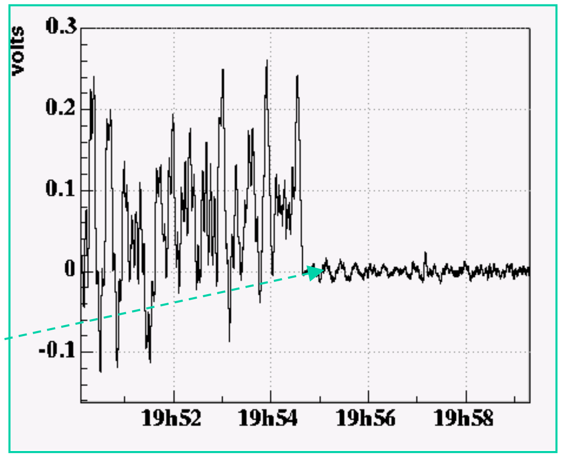

Magnetic actuation force on the mirror reduced
Switch to low noise coil drivers

Virgo Locking in 3 blocks

Basic concept: controlling the reflectivity of non-recycled interferometerby adding a **DC offset** on BS position.

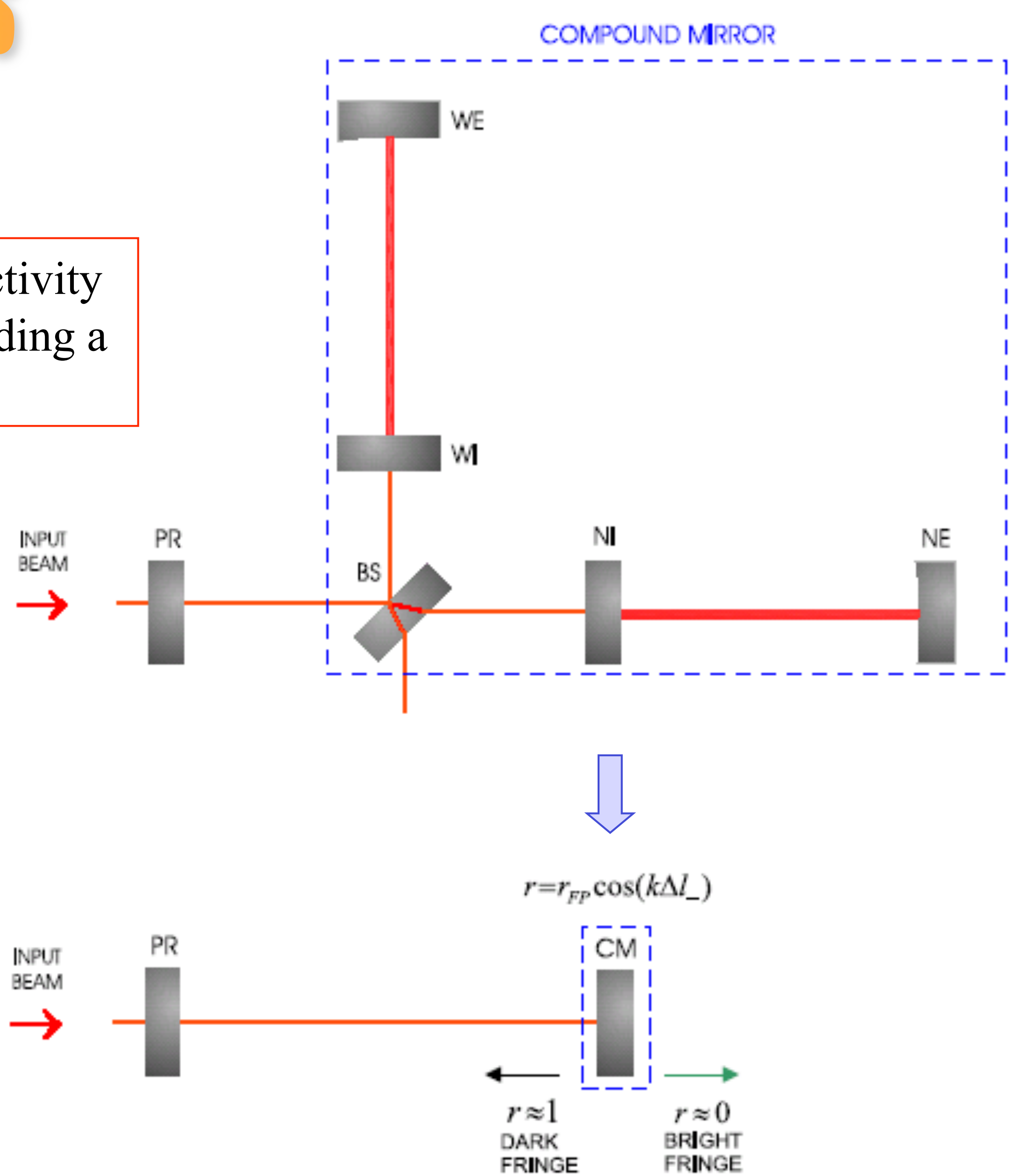

credits L. Barsotti

Concetto base: un piccolo ricircolo di potenza altera poco le risposte usate per controllare l'ITF

STEP 1

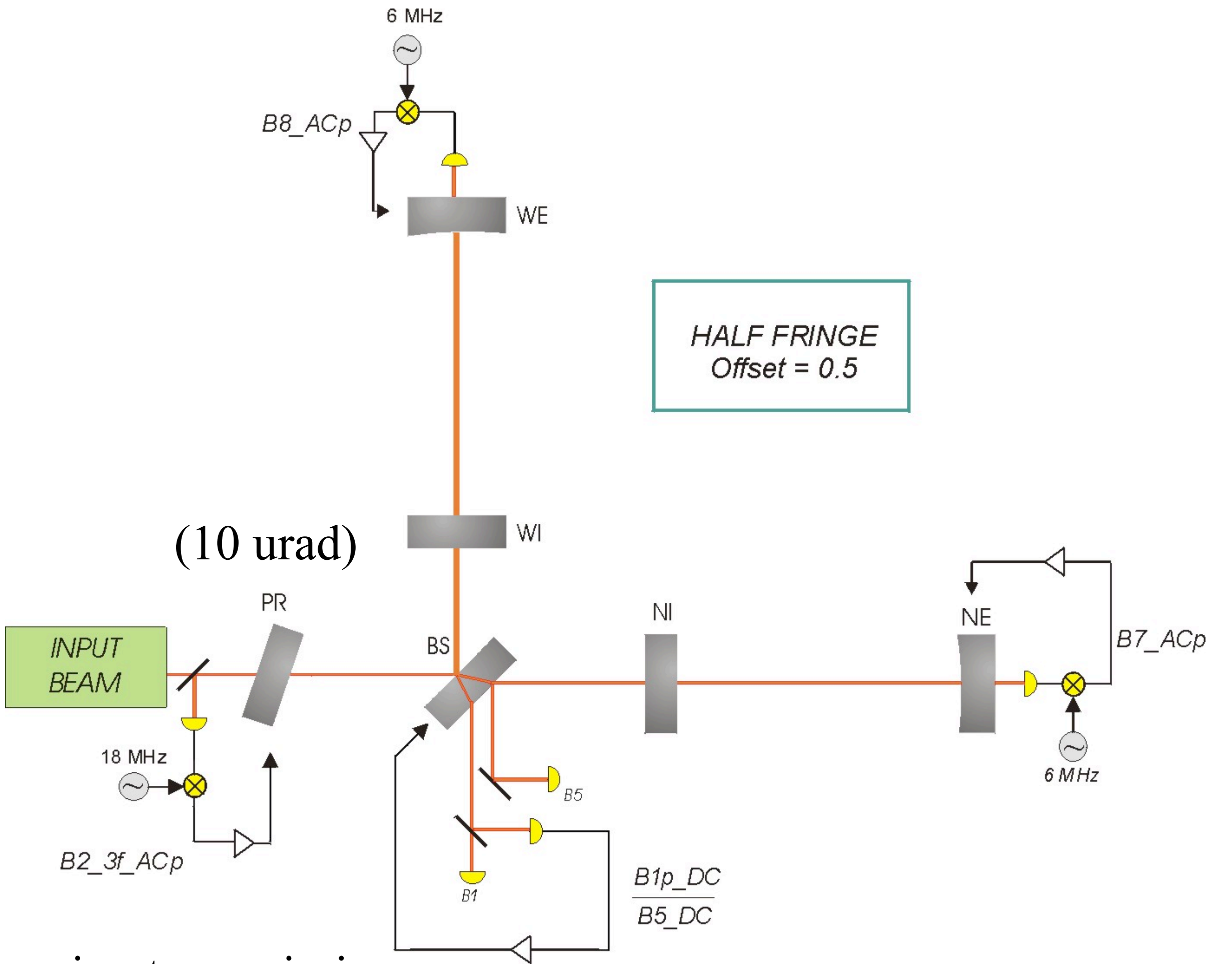

- long cavities independent lock using transmission
- PRCL resonant but mirror slitghtly **DC tilted** (3f used)
- MICH half free fringe
- CARM

Dalla frangia grigia alla frangia scura

STEP 2

LASER stab step 1 (CARM)

BS offset reduction

Offset = 0.2

Transmission differential signal used for DARM

PR realignment

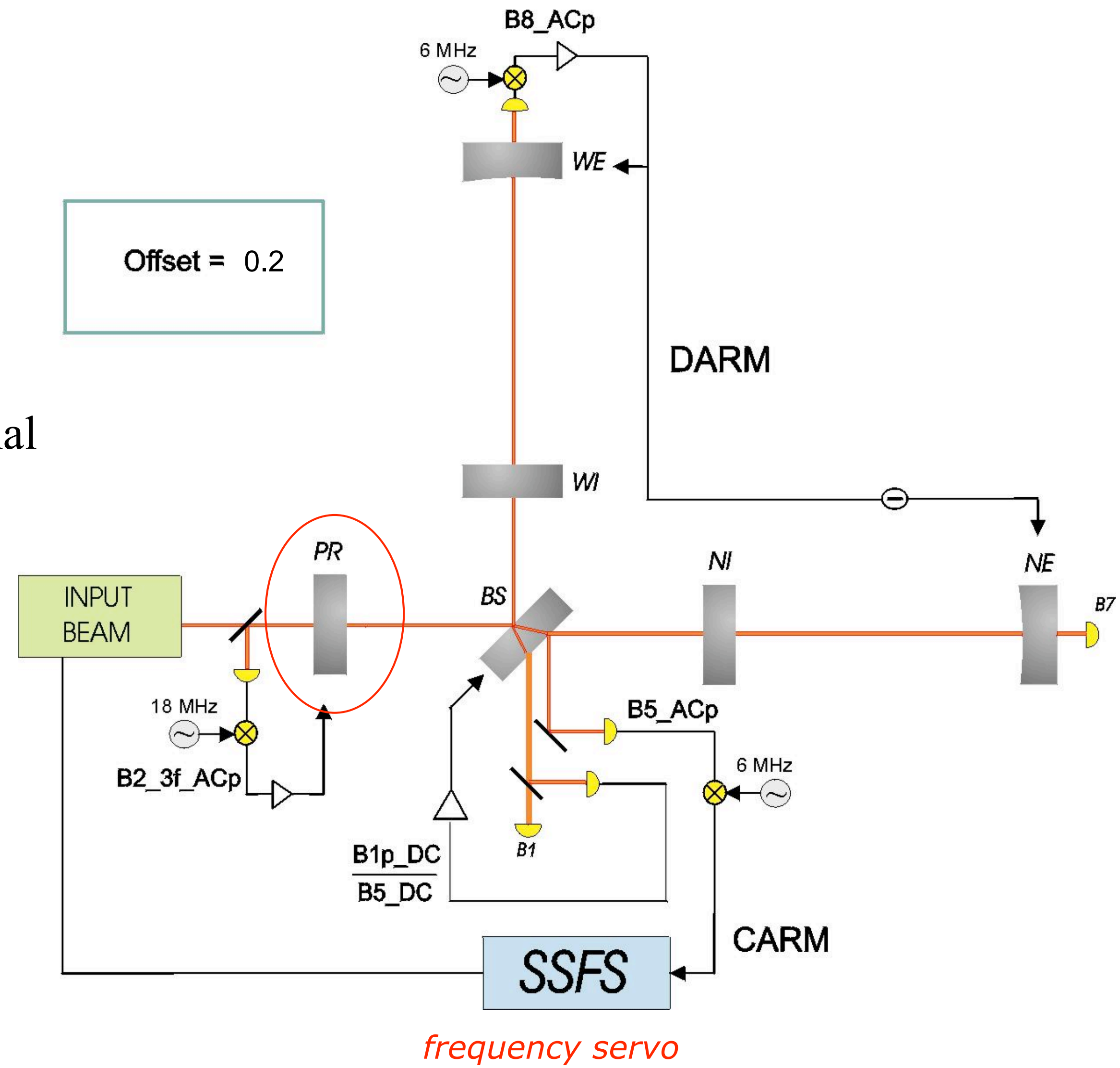

Final, dark dringe

STEP 3b

DF signal (dark fringe) to control DARM

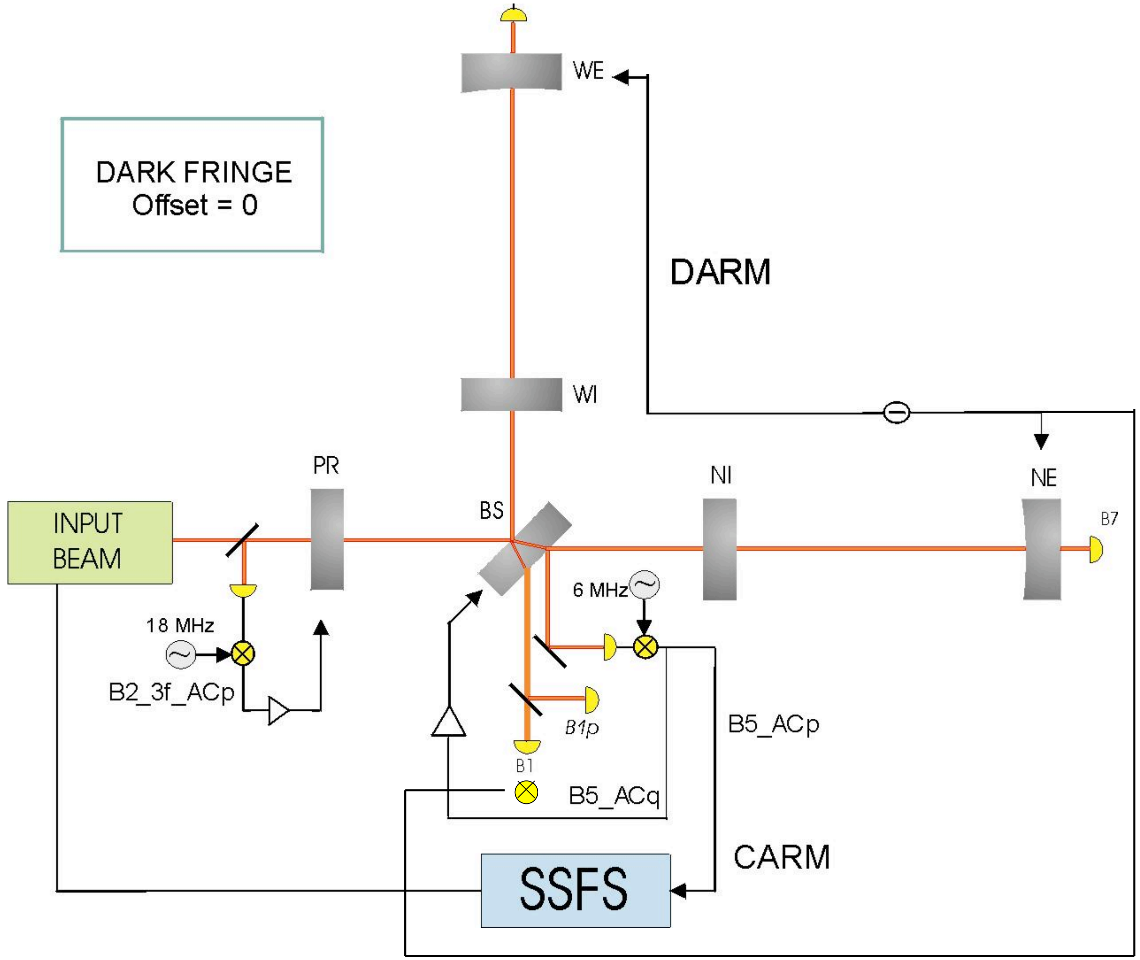

Overall locking is quite longer with respect to LIGO: LF suspensions imply several preparatory intermediate steps (11), however, the Virgo duty cycle is satisfactory.

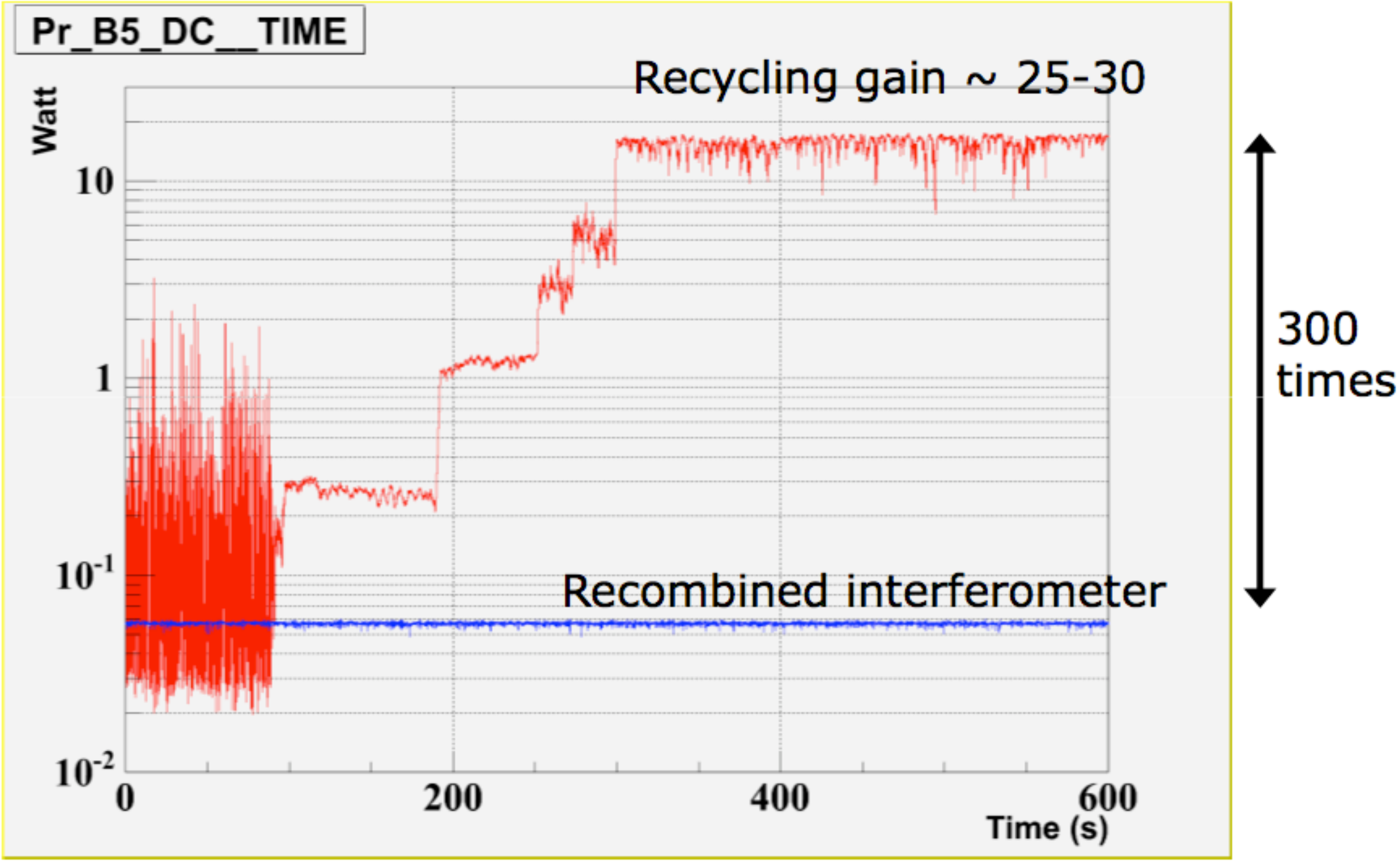

Thermal Compensation Scheme (concept): its operation is integrated with locking and compensates cavity power losses due to mirror deformation

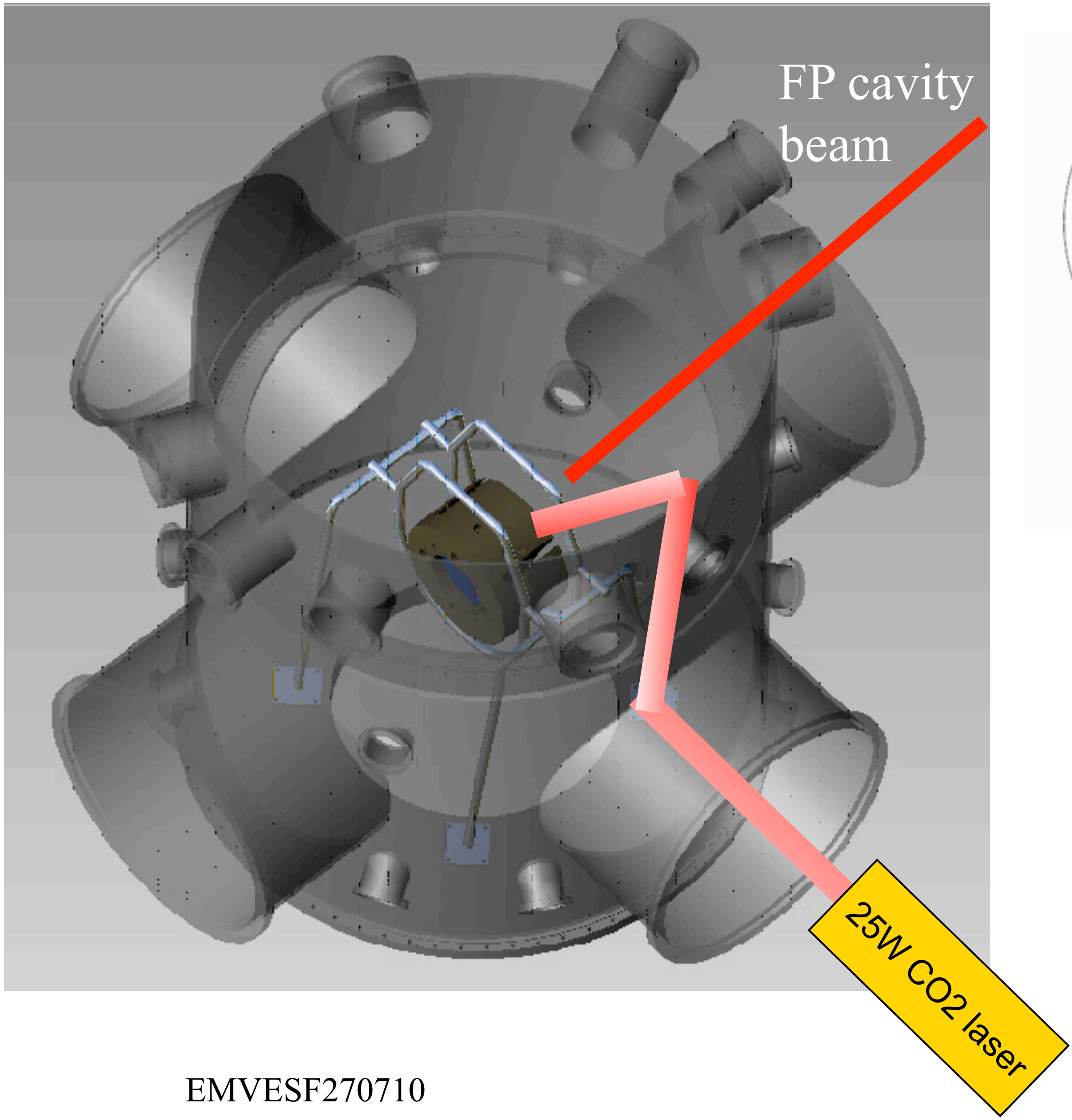

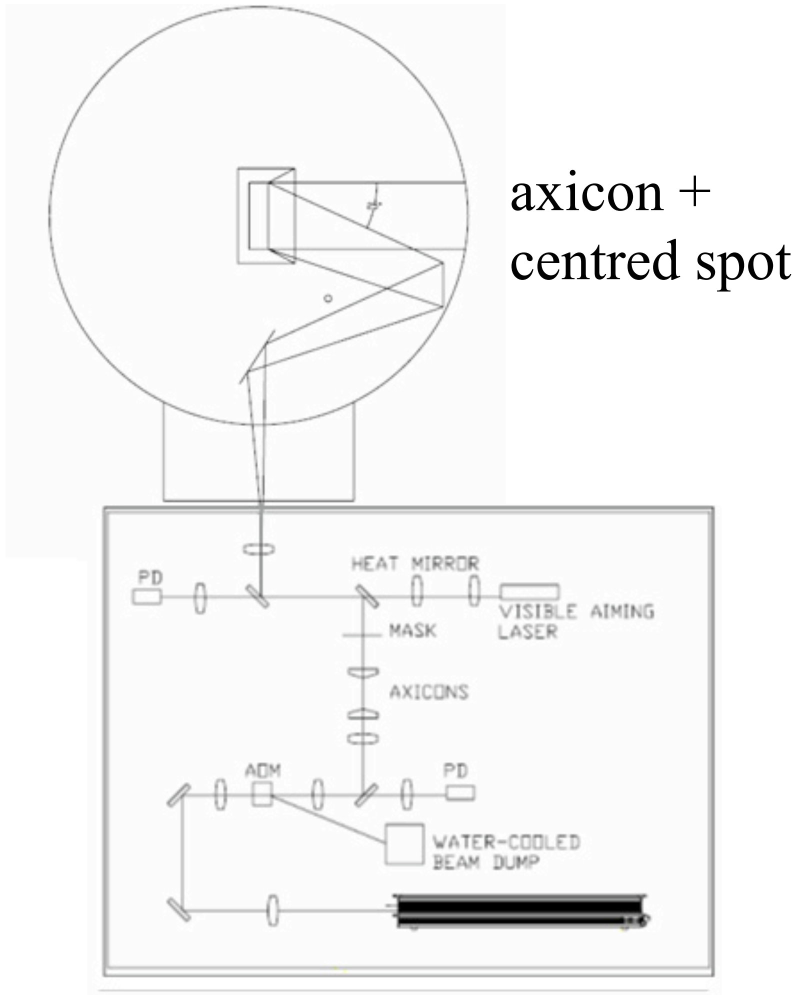

EMVESF270710

Thermal effects in the Virgo mirrors

(M. Punturo)

- The 3km Virgo arms are a long Fabry Perot cavity:

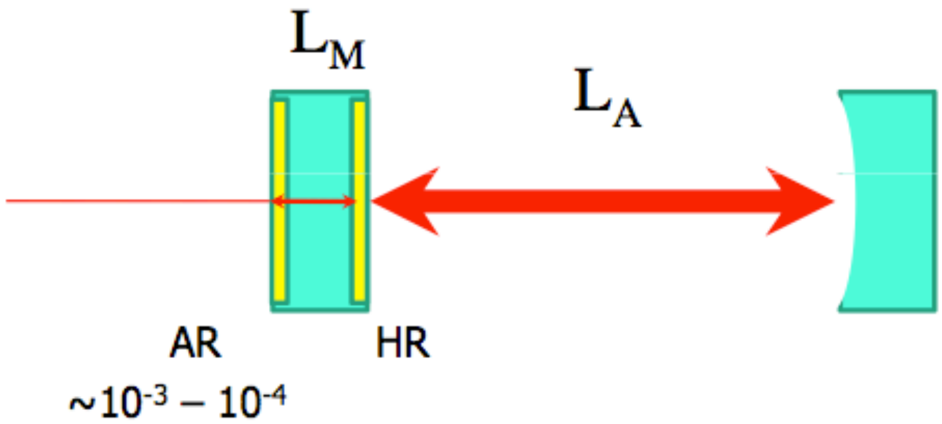

- Hence, actually, each arm is a double FP cavity:
  - Etalon effect $$r_M = -r_{AR} + \frac{t_{AR}^2 r_{HR} e^{-2ikL_M}}{1 + r_{AR} r_{HR} e^{-2ikL_M}} \qquad r_{FP} = -r_M + \frac{t_M^2 r_{end} e^{-2ikL_A}}{1 + r_M r_{end} e^{-2ikL_A}}$$

Etalon Effect

(M. Punturo)

- Hence, the Finesse of the cavity and all the fundamental parameters of the ITF are affected by the input mirror optical thickness variation
- But, why the mirror optical thickness fluctuates?

- Temperature!!

$$\phi = k \cdot x = \frac{2\pi}{\lambda} n \cdot x \rightarrow \Delta\phi = \frac{d\phi}{dT}\Delta T = \frac{2\pi}{\lambda}\left[\frac{dn}{dT}x + n\frac{dx}{dT}\right]\Delta T$$

$$\Delta\phi = \frac{2\pi}{\lambda} x\left[\frac{dn}{dT} + (n-1)\cdot\alpha\right]\Delta T$$

- Hence, knowing the mirror temperature it is possible to predict some of the ITF performances
- OK, but how to measure the mirror temperature?

Resonant mode technique

(M. Punturo)

- Obviously the resonant frequencies of a body depend on the temperature of the body
- For a Virgo mirror we evaluated this dependence with a ANSYS based FEM

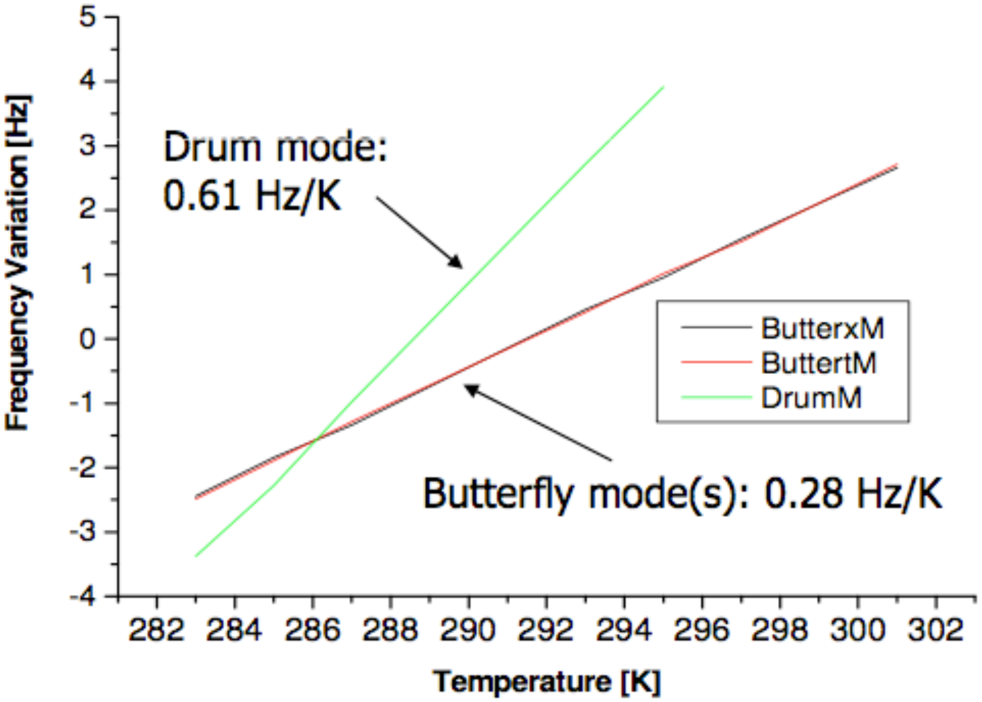

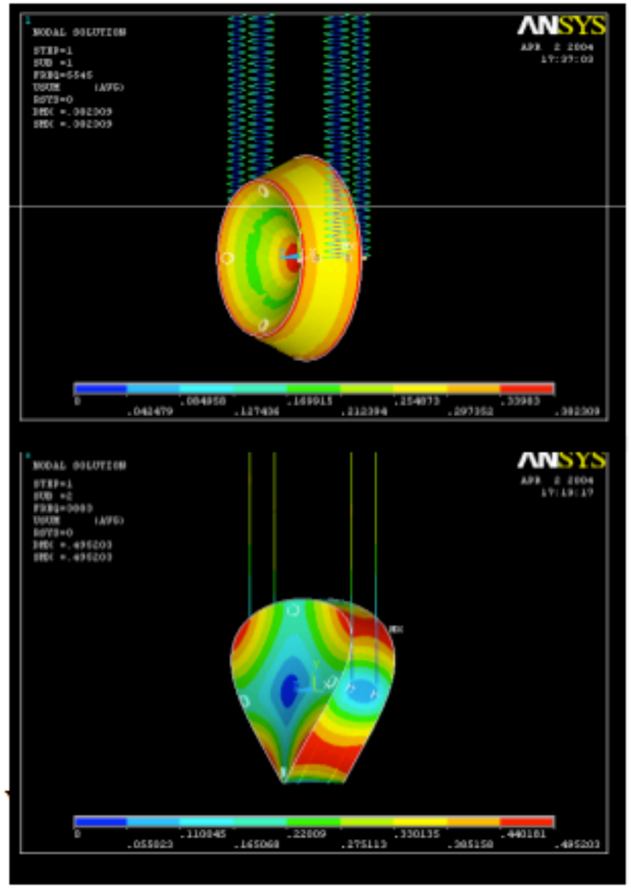

Cascina 5/26/2009

EMVESF270710

IV) Enjoying digital control in practice (with suspensions and interferometer together)

An example

LF disturbance

⇓

Big large feedback force at payload level (undesirable)

The example of inverted pendulum control

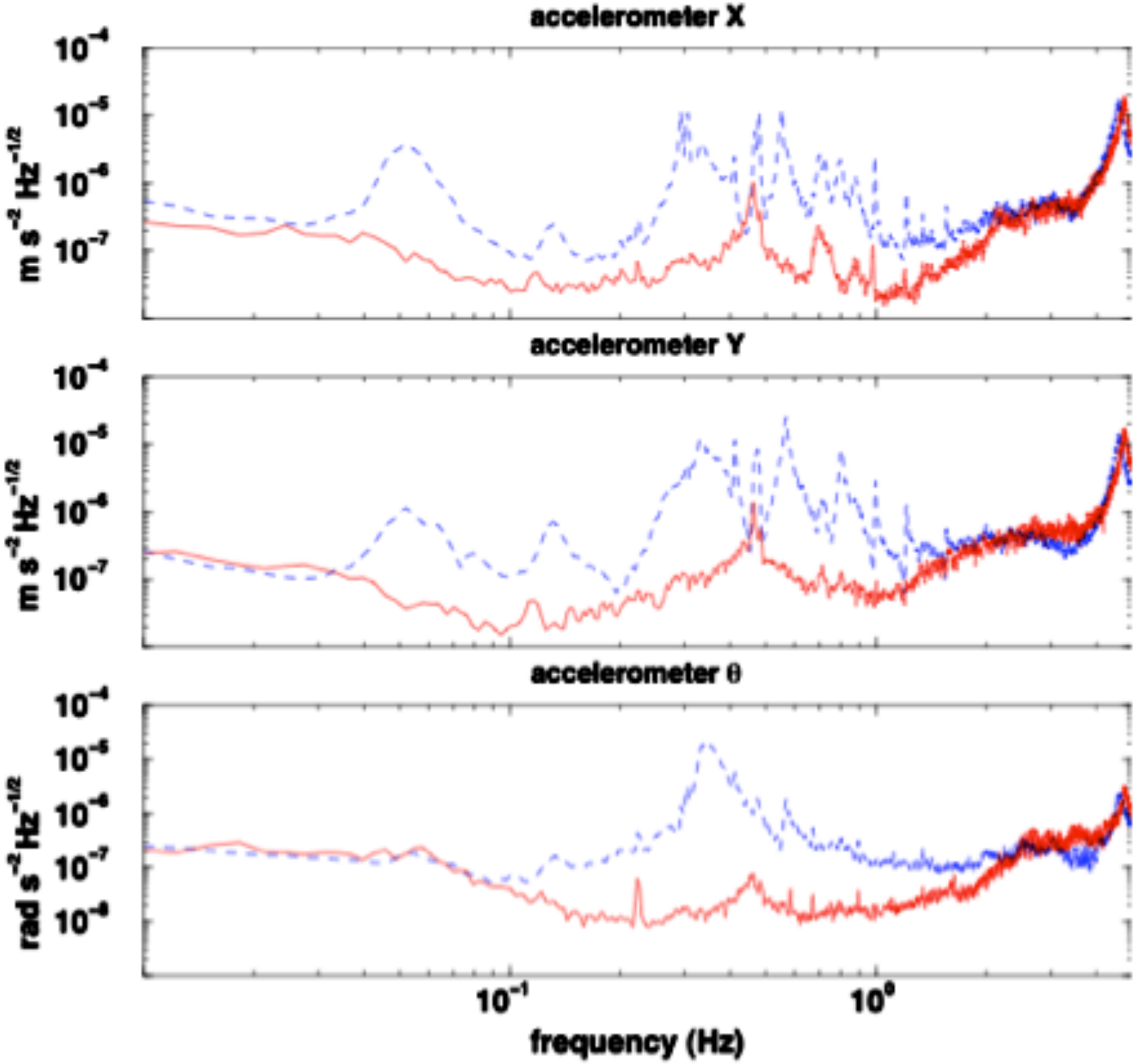

- 1 μm relative displacement
- 0.25 um/sec relative speed

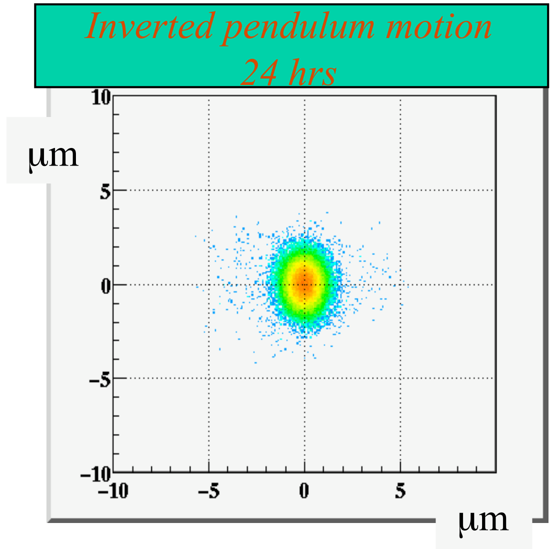

EMVESF270710

The case of Virgo is general for detectors aimed to low-frequency sensitivity

top-stage position RMS of actual inertial damping is affected by

- non-perfect sensing acceleration sensing

- Seismic reinjection through the control.

$$x_{RMS}(f) = \sqrt{\int_f^{\infty} \tilde{x}(\nu)\,d\nu}$$

error signal in-loop $\downarrow$ *position disturbance proportional to tilt* $\downarrow$

$$V_{acc} = \sigma(s^2 x - g \cdot \alpha) \approx 0 \Rightarrow x_{res} \approx \frac{g}{s^2}\alpha$$

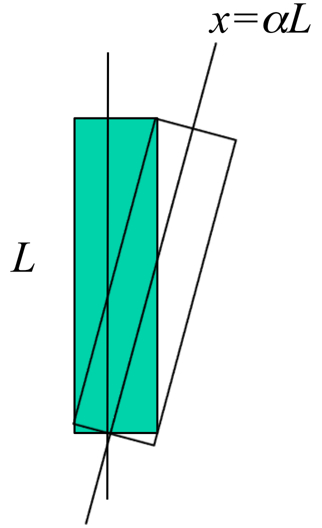

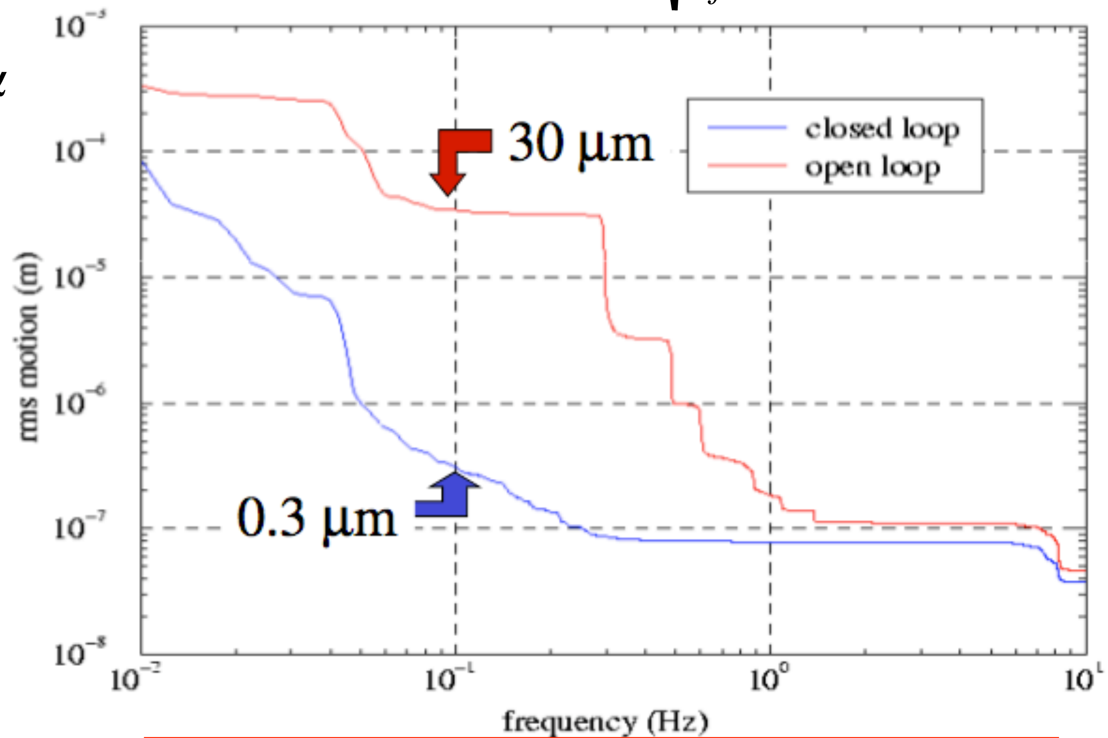

Tilt (wind): critical below 70 mHz !!

µseism (sea): critical at few hundreds of mHz

briefly… (sea activity versus quiet): combining sensors in order to reduce the impact of ground disturbance injected by suspension position sensor is important !

Micro-seism

Worse alignement

Worse sensitivity

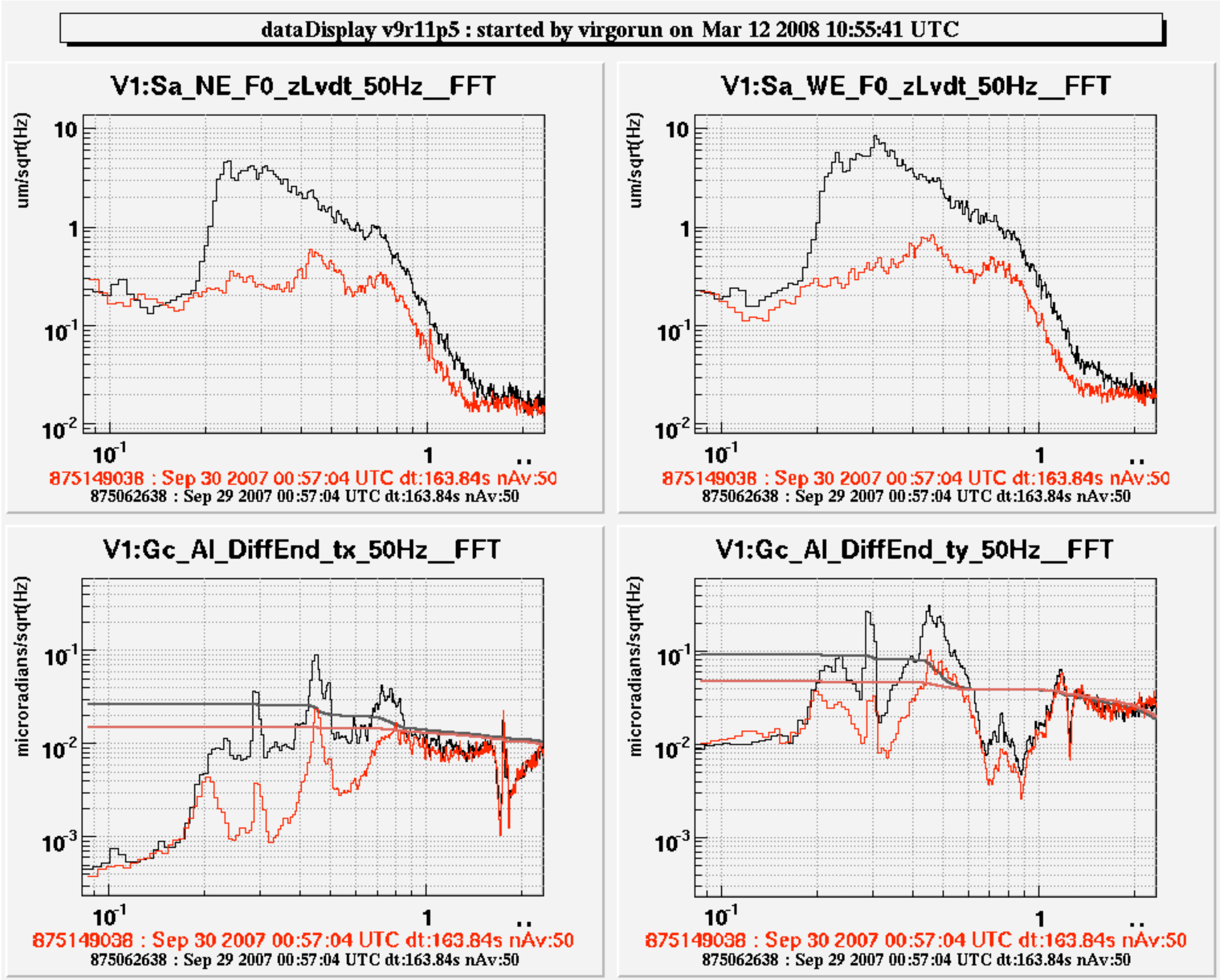

Position/Acceleration blending: suspension quasi-inertial damping

qi = quasi-inetrial
x_s = seism driven sensor reference

$$L(s)\cdot(x - x_s) + s^{-2}\cdot H(s)\cdot a_x(s) = x_{qi}$$

$$L(s) + H(s) = 1$$

$$x_{qi} = x - L(s)\cdot x_s$$

Increase L(s) slope — **Strategy A**

Reduce HP/LP crossover — **Strategy B**

"Reduce" x_s — **Strategy C**

A: two different crossover enabled in various environmental conditoins

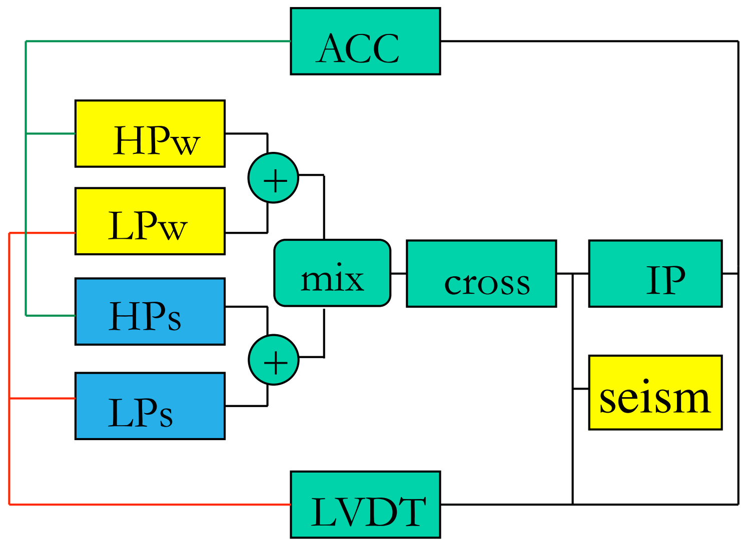

EMVESF270710

Position/Acceleration prefiltering for top-stage control

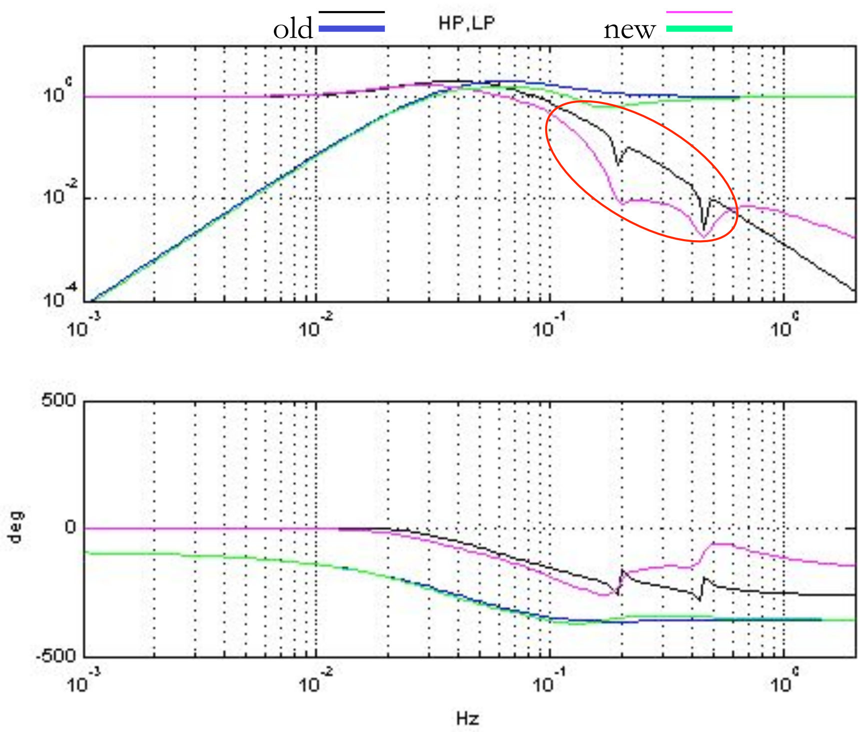

fx @ 50 mHz, 'trade-off' with improved features

two main issues

The problem of improving the system through independent optimization of each suspension:

wind-tilt noise
(through accelerometers, f < 70 mHz)

μseism sea disturbance
(through position control, 0.15-0.6 Hz)

Trade-off: **f_x=50 mHz**

Position/Acceleration prefiltering for top-stage control

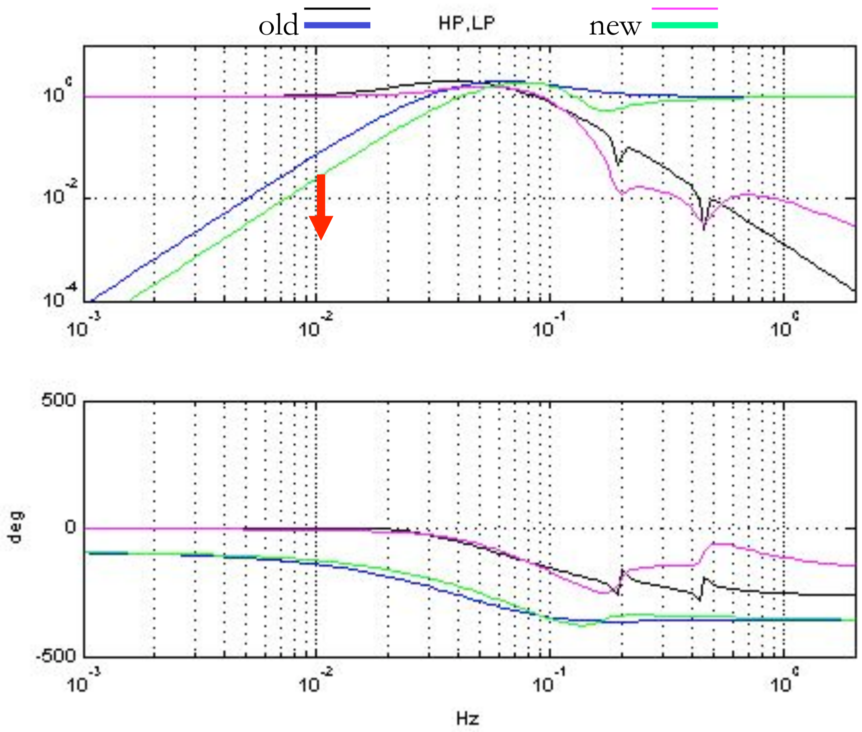

two main issues

The problem of improving the system through independent optimization of each suspension:

wind-tilt noise
(through accelerometers, f < 70 mHz)

µseism sea disturbance
(through position control, 0.15-0.6 Hz)

Trade-off: **f_x=50 mHz**

wind-earthqukes, f <70mHz: “aggressive” attenuation of accelerometer tilt noise.

Position/Acceleration prefiltering for top-stage control

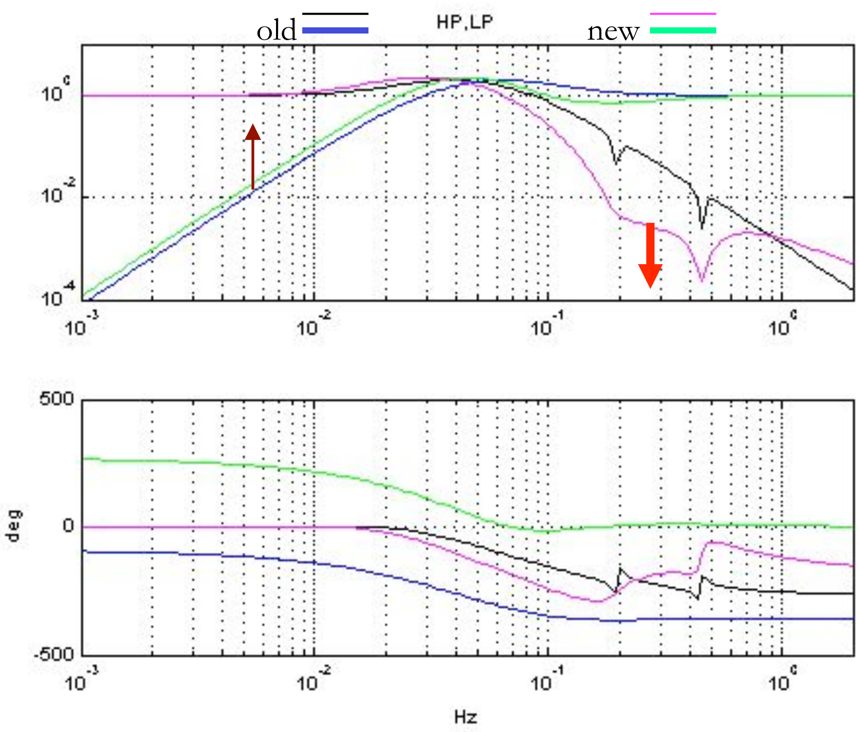

two main issues

The problem of improving the system through independent optimization of each suspension:

wind-tilt noise
(through accelerometers, f < 70 mHz)

µseism sea disturbance
(through position control, 0.15-0.6 Hz)

Trade-off: **f_x=50 mHz**

µseism, 150-600 mHz: "aggressive", slightly worsened against tilt noise.

μseism disturbance attenuated downstream
(➔the concept of Global Inverted Pendulum Control)

What would be the payload displacement due to sea μseism without VirgoSuperAttenuator ?

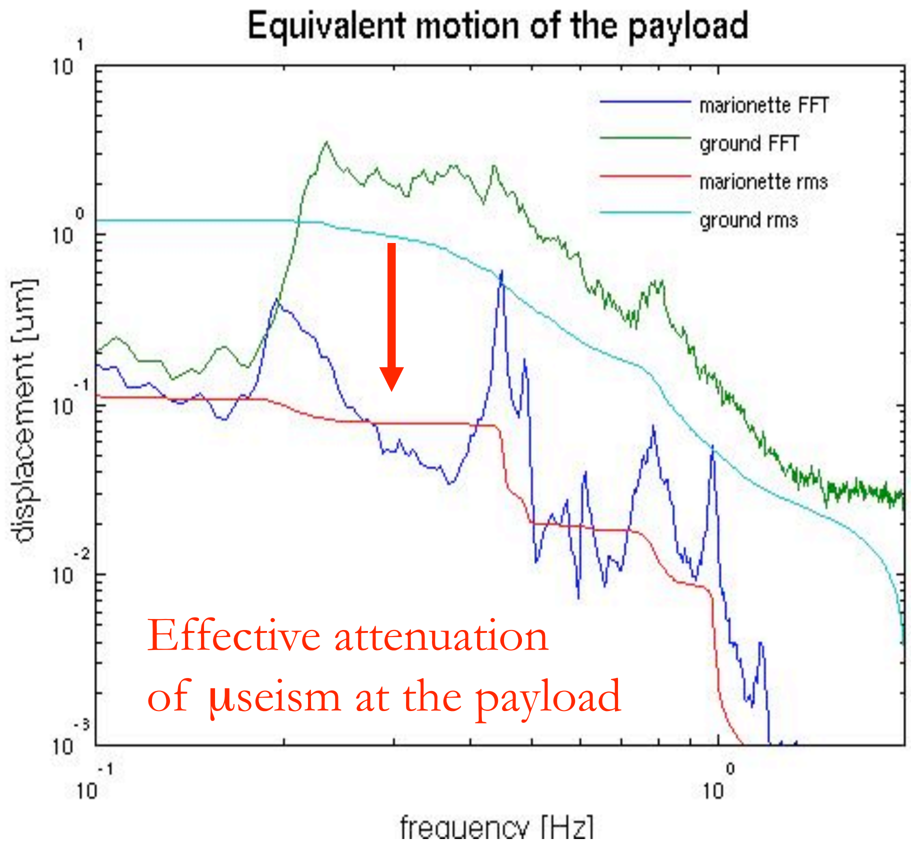

The lock force applied to the marionette corrects the residual payload motion, whose rms above 100 mHz is ~ 1 order of magnitude smaller than the ground motion.

A top-stage control position reference with smaller seismic noise allows to increase position/accel crossover without risks
HOW TO DO IT ?

µseism-free and Global Inverted Pendulum control

µseism is **incoherent**
along the arm baseline
=>µSeism reduced at
END suspension top-stages
by using position referred to
INPUT mirrors (GIPC);

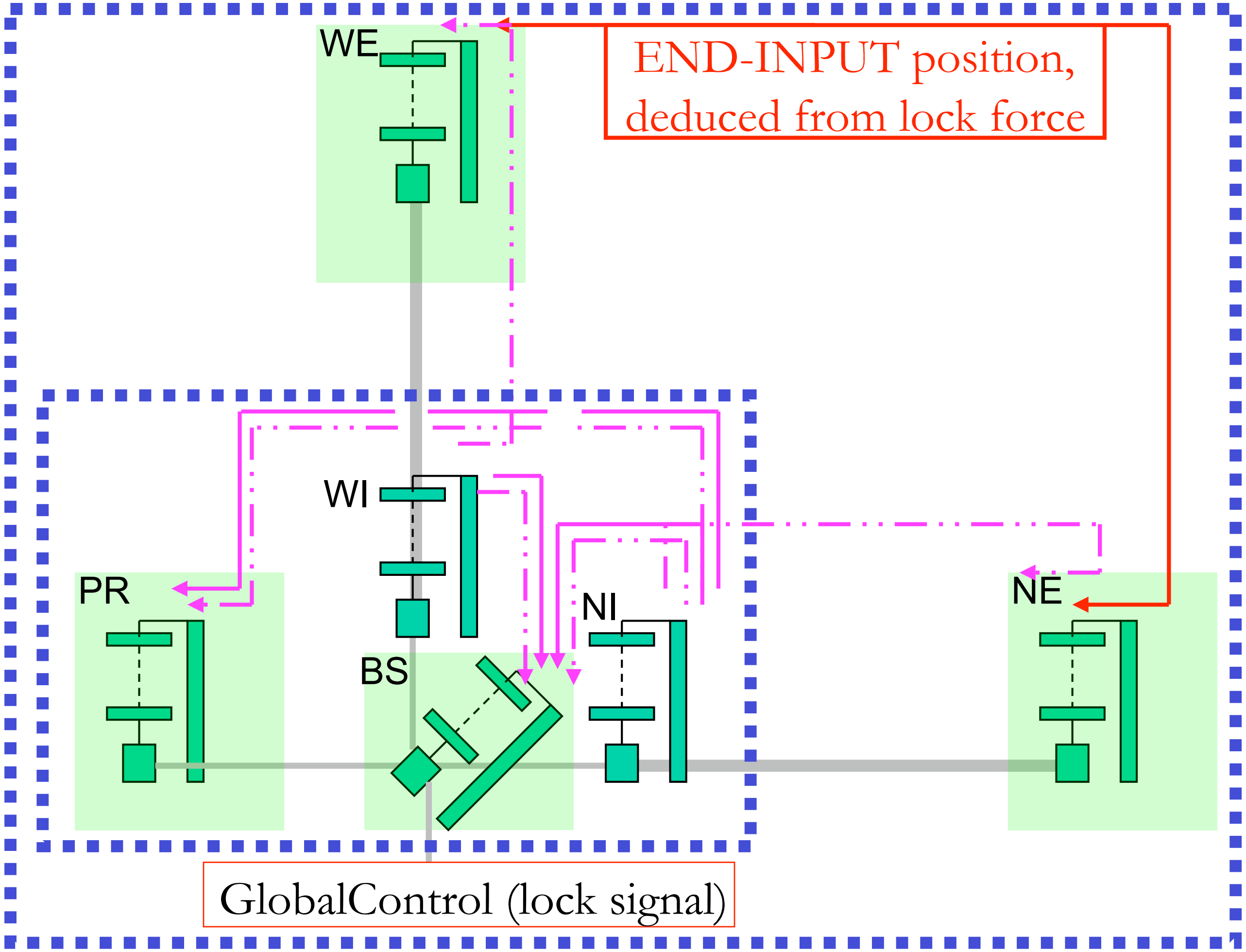

µseism is **coherent**
Among close suspensions.
µSeism-Free control signals
can be reconstructed with
respect to **INPUT mirrors (µSF)**

INPUT TOWERS USED AS REFERENCE ALLOWS TO USE microSEISMIC-FREE SIGNALS TO CONTROL ALL THE OTHER TOP-STAGES

VII) Noise hunting and performance

(4)

VSR2

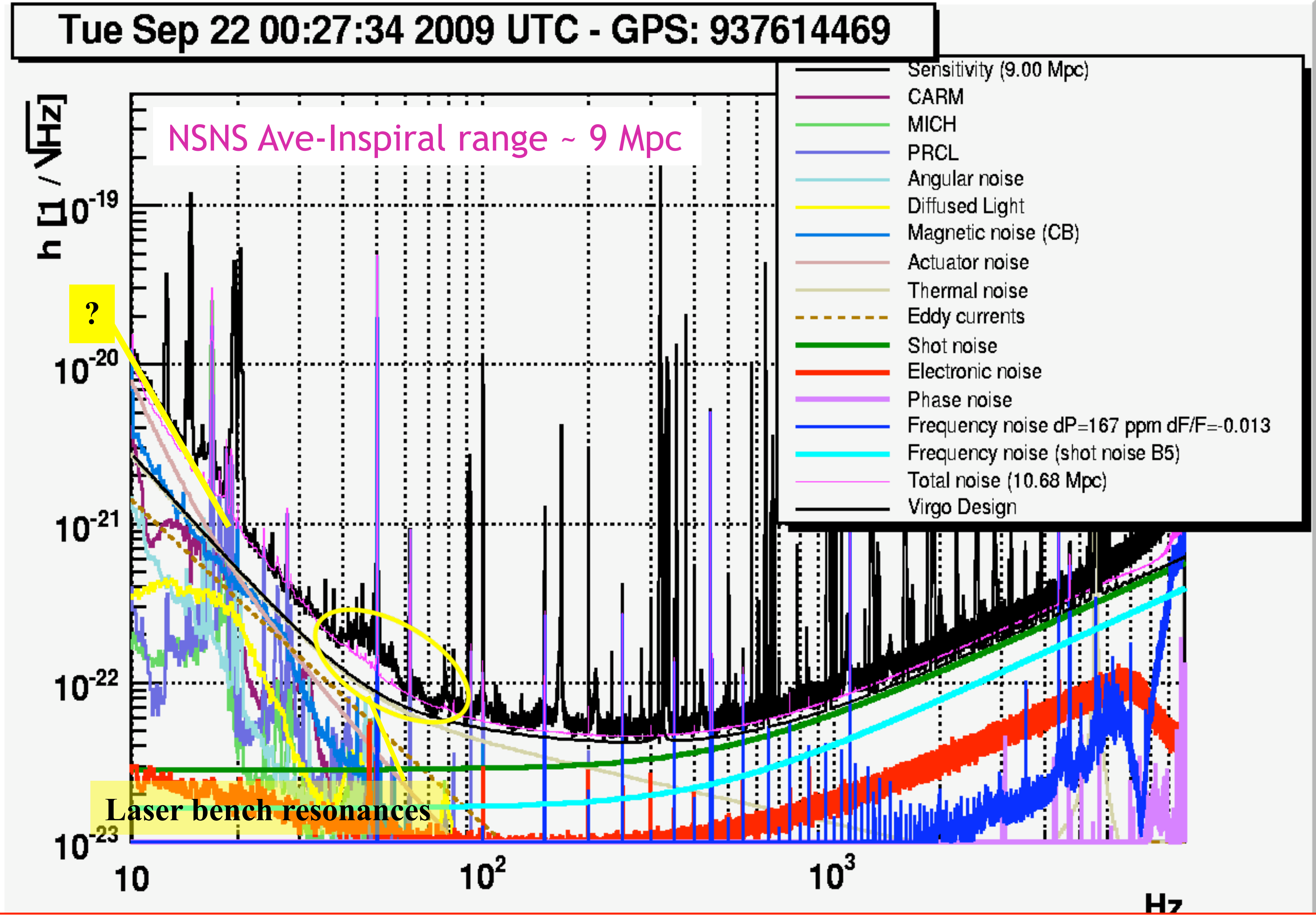

Virgo+ is being implemented gradually, noise hunting and modeling almost full.
V+ commissioning is interlaced with coincidence operation of *enhanced*-LIGO

VSR2

Science Mode duty cycle > 80%

Commissioning activities compliant with LIGO

Locked duty cycle > 85%

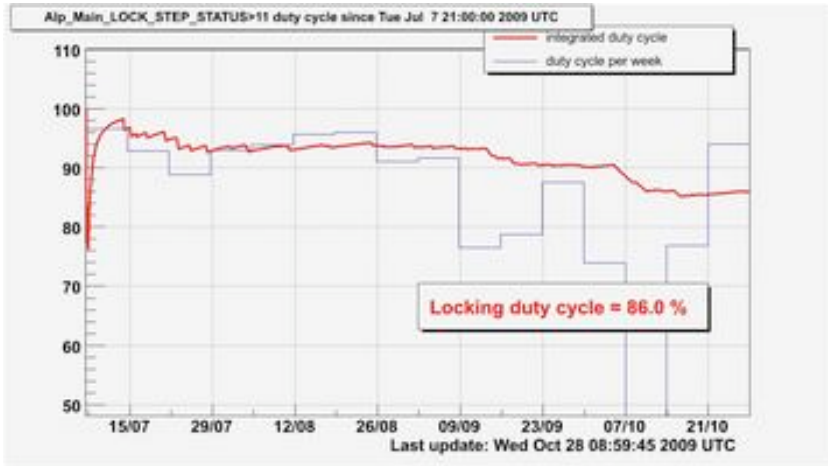

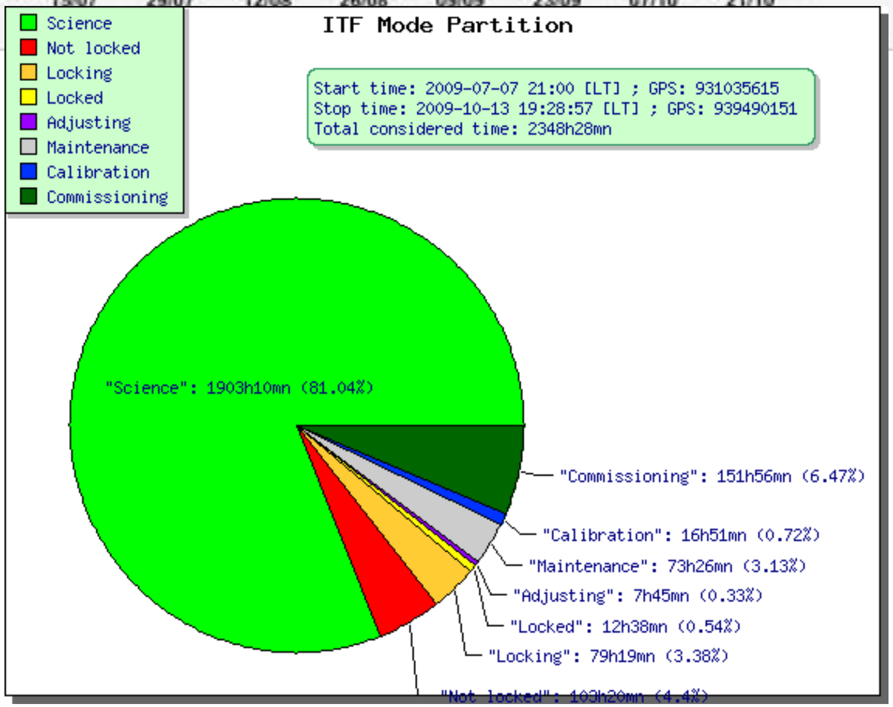

Interferometer working mode particion

Sensitivity improvements during commissioning and scientific runs

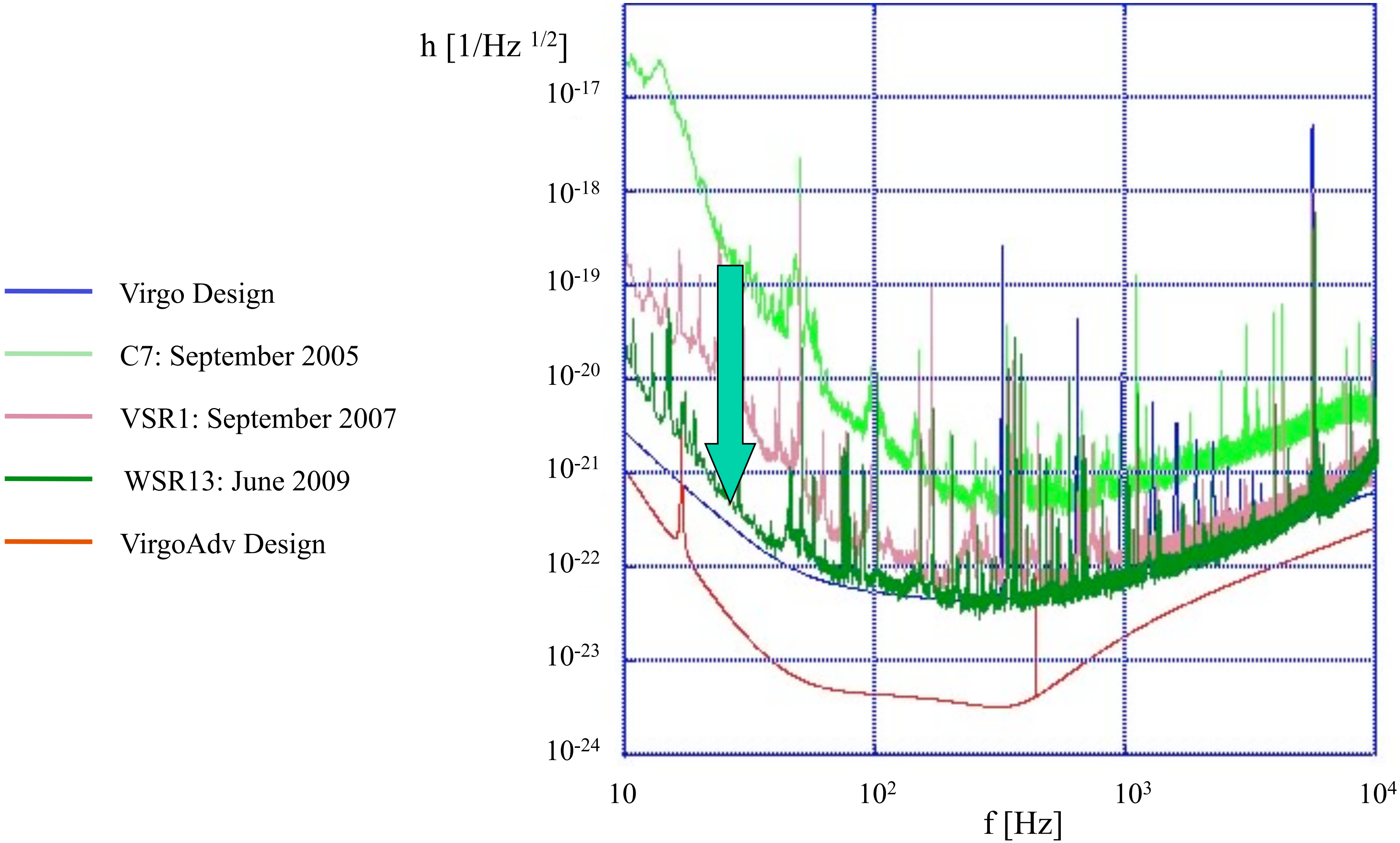

Background activity: four years spent to prepare preliminary Advanced Virgo design

Virgo+, first step towards Vadv: main improvements (many others underlaying)

Monolithic mirror suspension
(a new "payload")

low dissipation mirrors

Dedicated R&D to validate new test-mass payload (done!)

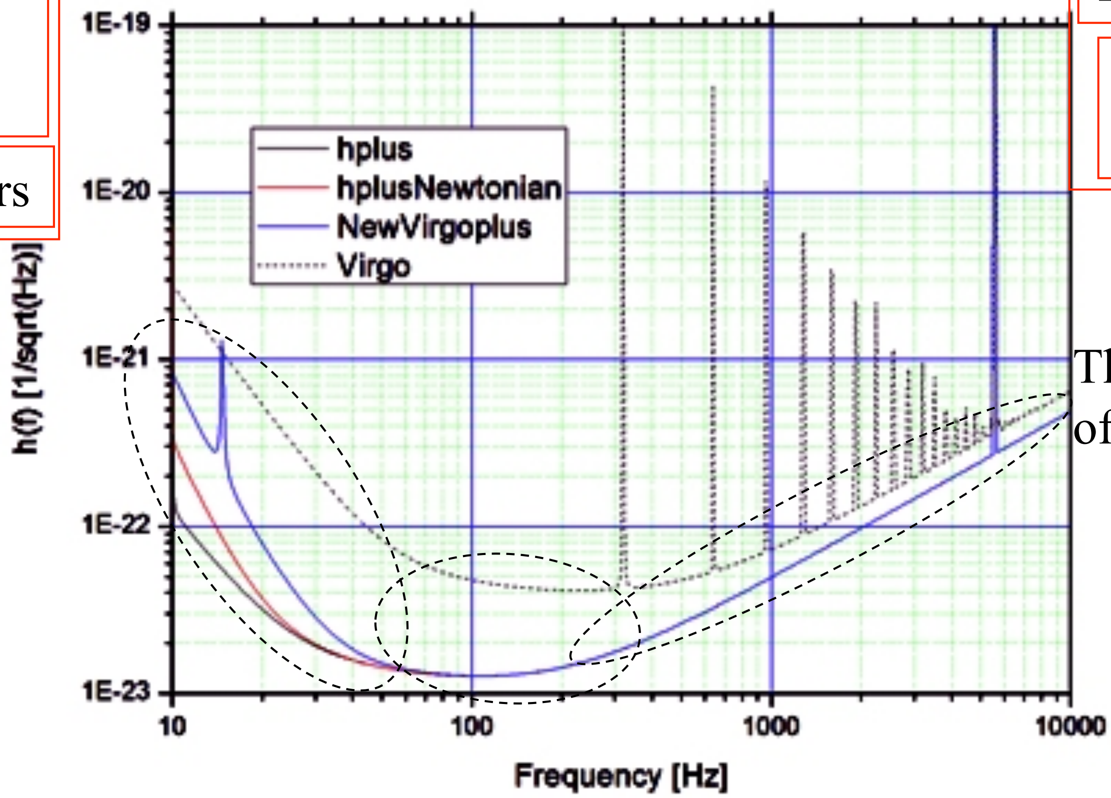

Powered injection

new mirrors (high-Finesse)

Thermal deformation of FP cavity mirrors

Thermal Compensation System needed

Thermal noise: new paylaod Virgo+ with monolithic suspension and high-finesse-high-Q mirrors (current commissioning)

VIII) Focus on monolithic suspension

(9+PICTS)

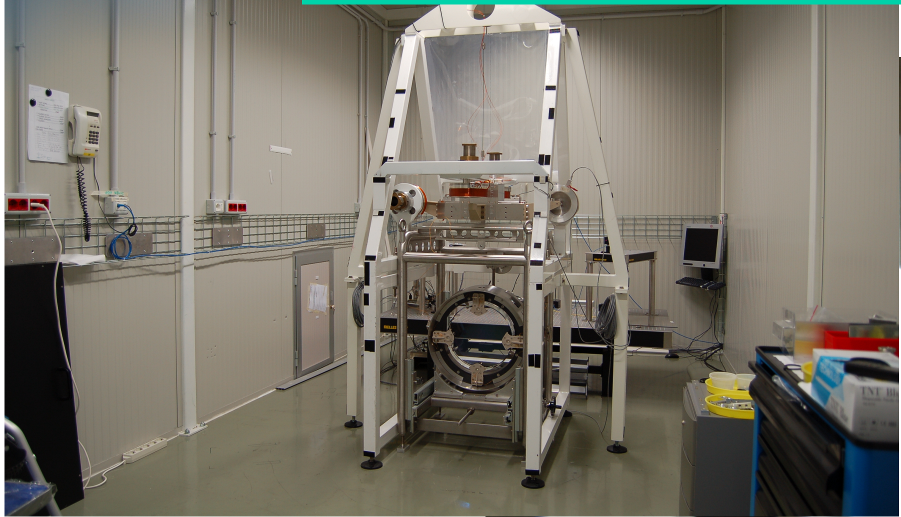

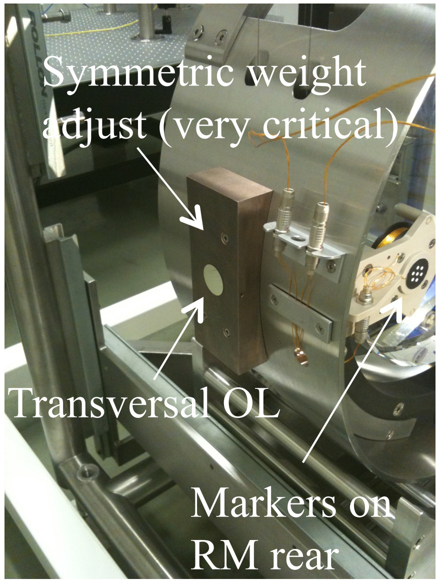

The old NE mirror, polished after the viewport breakdown

if $\Phi(\omega) = \Phi_o$

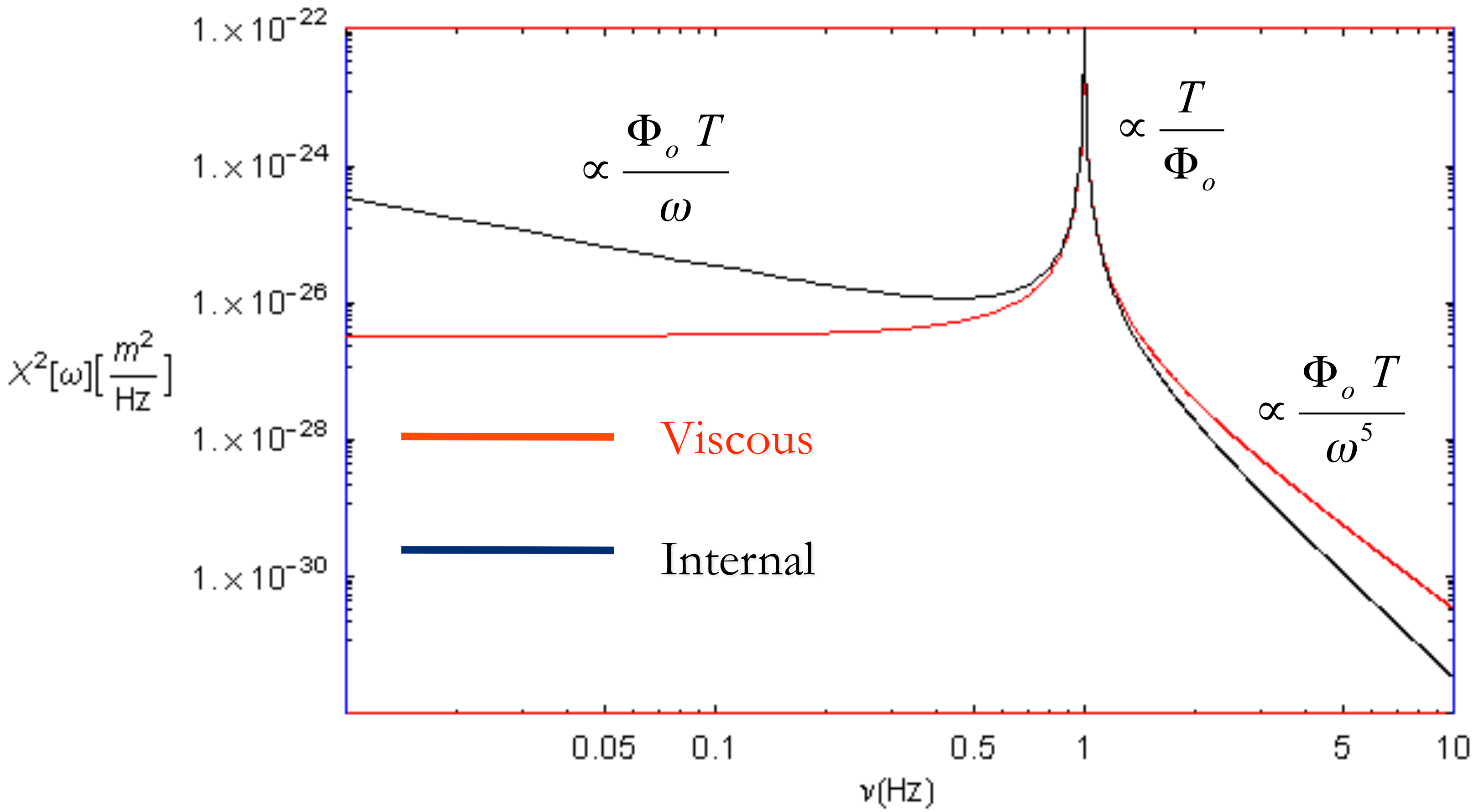

<u>All materials</u>

EMVESF270710

Dissipation measurements

$$Q_{meas} \equiv \frac{\omega_o}{\Delta\omega}$$

$$\mathbf{Q_{visc}} = \frac{\mathbf{m}\omega_\mathbf{o}}{\beta}$$

$$Q_{strut} = \frac{1}{\phi_{struct}}$$

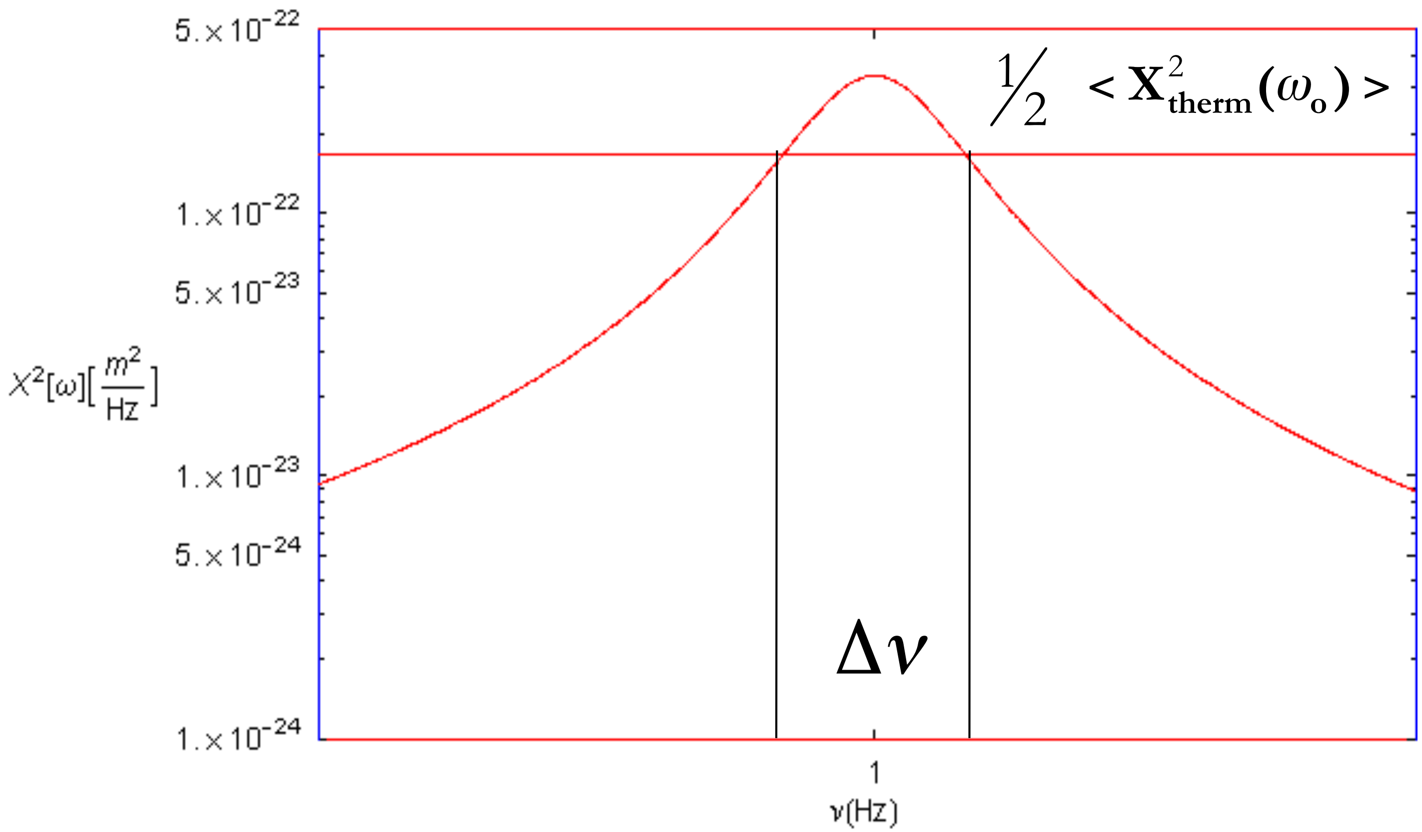

$$\Phi(\omega) = \frac{\omega}{\omega_o}\frac{1}{Q_{visc}} + \phi_{strut} = \frac{\omega}{\omega_o}\frac{1}{Q_{meas}} = \frac{\omega}{\omega_o^2}\frac{\beta}{m} + \phi_{struct}$$

High Q values
=> energy around the resonance (a benefit for any kind of detector of small forces)

Real pendulum with point-like mass

$$mL\ddot{x} + mgx + \boxed{\int_{-\infty}^{t} \tau(t-s)\frac{x(s)}{L}ds} = LF_{ext}$$

Restoring force moment

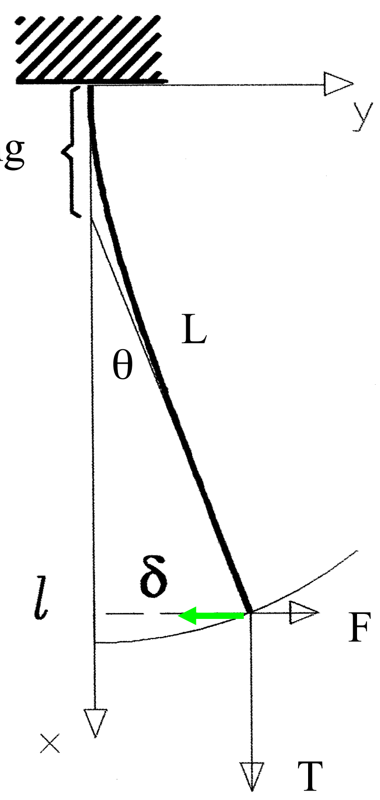

$$V_{el}(\omega) \approx \frac{1}{2}\left(\frac{T}{2L}\sqrt{\frac{YJ}{TL^2}}\right)\delta(t)^2$$

$$V_g(\omega) = \frac{1}{2}\frac{T}{L}\delta(t)^2 \approx V_{total}(\omega)$$

wire bending point

$$\phi_p(\omega) = \frac{< V_{el} >}{< V_g >}\phi_m(\omega) \approx \frac{1}{2L}\sqrt{\frac{YJ}{T}}\phi_m(\omega)$$

The pendulum loss-angle is reduced by a "dilution factor"

Y Young m.
r_w wire radius
T wire tension
J moment of wire section

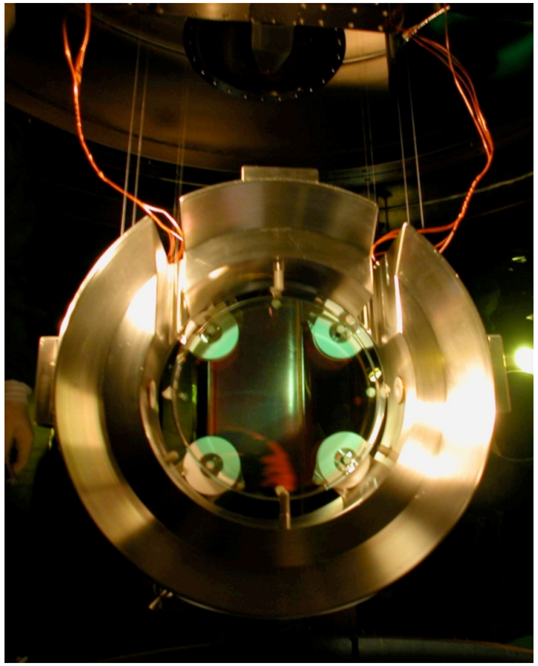

$$k(\omega) = k_e(1 + i\phi_s(\omega)) \;\; ; \;\; k_e = \frac{\sqrt{TYJ}}{L^2} \;\; ; \quad J = \frac{\pi}{4} r_w^4$$

$$\omega_p^2 = \left(\frac{k_e}{m} + \frac{g}{L}\right) = \omega_g^2 + \omega_e^2$$

$$-\omega^2\theta + \frac{g}{L}\theta + \frac{k_e}{m}\left(1 + i\,\phi_s(\omega)\right)\,\theta = \frac{F_{ext}}{mL}$$ $\longrightarrow$ FDT…

Dissipation occurs around the wire bending point

thermoelastic losses (suspension wire bending)

$$\phi_{th}(\omega) = \frac{Y\alpha^2 T}{\rho\, C} \frac{\omega\,\tau}{1+(\omega\,\tau)^2}$$

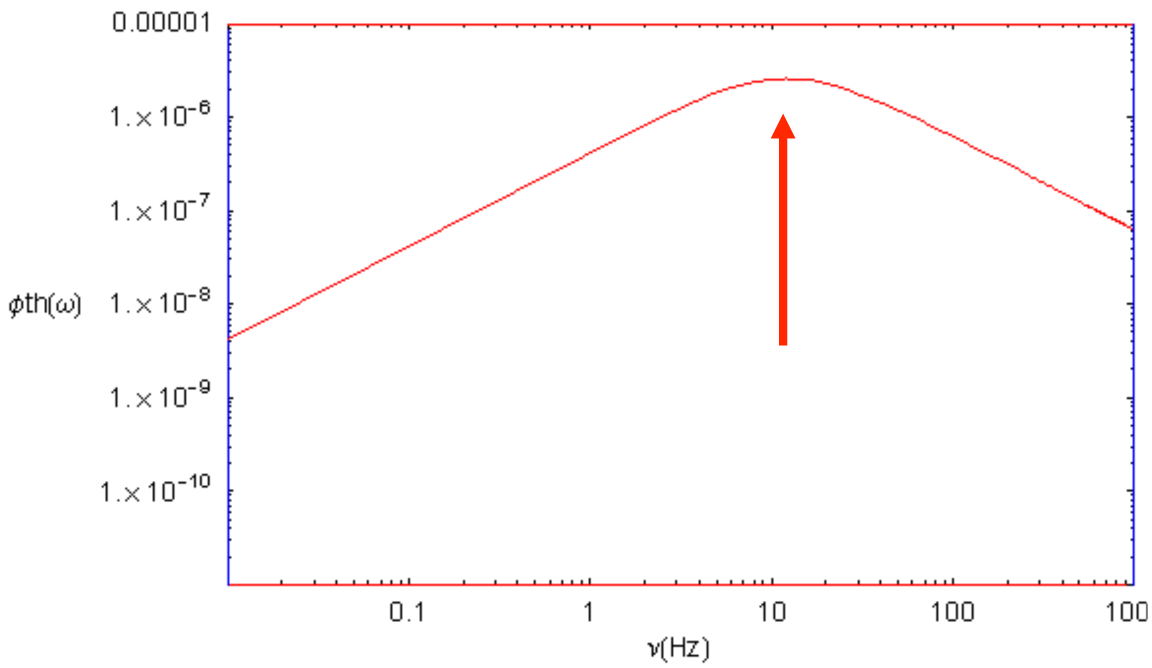

α linear thermal expansion coeff.
τ charact. time-of thermal diffusion
C thermal capacity

$\omega >> 2\pi/\tau$ ⇒adiabatic compression/expansion
$\omega << 2\pi/\tau$ ⇒isothermal compression/expansion
$\omega \approx 2\pi/\tau$ ⇒max

Objects with very asymmetric aspect ratios as fibers and membranes are critical

surface losses (wires,fibers,…clamping, mirrors)

$$\phi_{layer} = \frac{W_{surf}}{W_{tot}} \phi_{surf}$$

Inhomogeneity passing from the bulk to the surface causes elastic energy redistribution process.

$$\frac{W_{surf}}{W_{tot}} = \frac{\mu_w h_{sb} S_w}{V_w}$$

μ_w form factor (for a wire)
h_{sb} thickness of the layer
$S_w = 2\pi\, r_w\, L_w$ external surface considered
$V_w = \pi\, r_w^{\,2}\, L_w$ volume

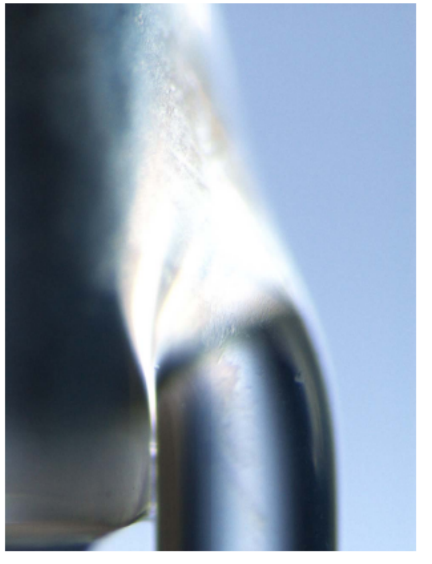

EMVESF270710

Internal modes (mirrors a “sane”Brownian motion)

$$SX_{TN} = \frac{4k_bT}{\omega}\sum_i \frac{\omega_i^2\phi_i}{M_i}\frac{1}{\left(\left(\omega_i^2-\omega^2\right)^2+\left(\omega_i^2\phi_i\right)^2\right)}$$

Naive model, ok around resonance peaks

$$M_i\,;\quad \frac{1}{2}M_i\omega_i^2X^2 = E_i$$

equivalent mass of mode *i*

$$\phi_i = \phi_{str} + \phi_{coat}$$

coating losses important

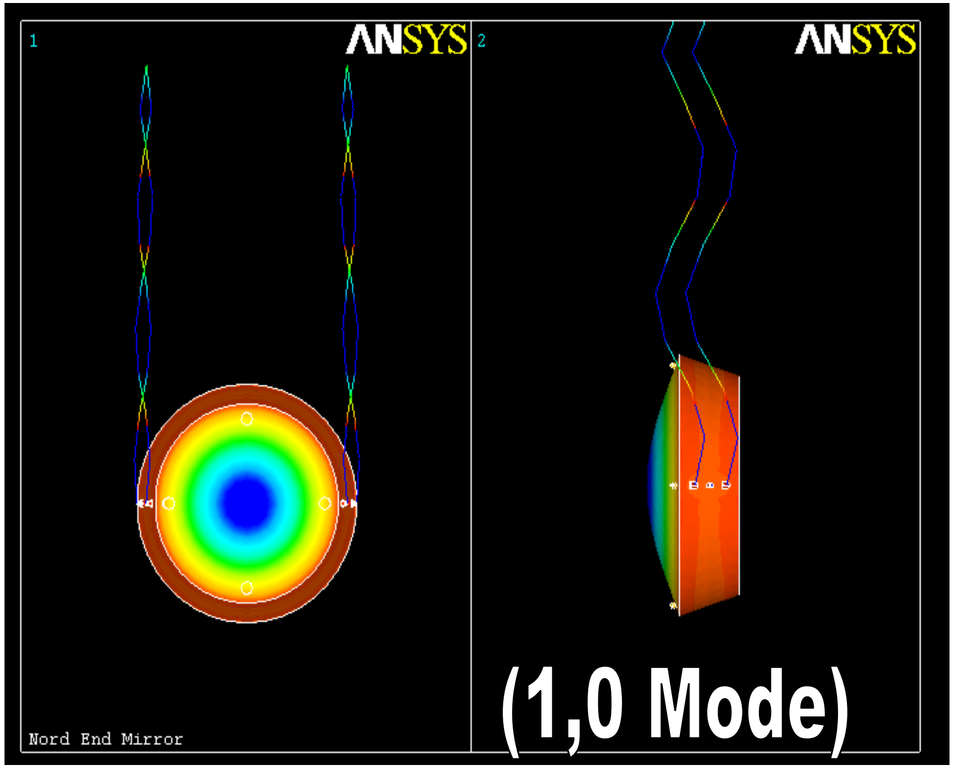

Simulation	Measured
NI/WI: 5584.9 Hz	NI: (5585.7 ± 0.5) Hz
	WI: (5583.5 ± 0.5) Hz
NE/WE: 5546.1 Hz	NE: (5543.2 ± 0.5) Hz
	WE: (5545.6 ± 0.5) Hz

TN versus coating

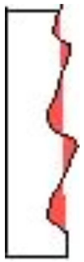

$$\varphi_{inc}$$

$$\varphi_{inc} e^{i2ku_z(t,x,y)}$$

$$< u_z(t) >$$

Equivalent displacement

Levin'sTh. Freq. domain,

$$u_z(t,x,y) = e^{i(\omega t - \Phi)} u_z(x,y)$$

Impedance definition Z(ω)

$$SX_{\substack{surface\\profile}} = \frac{4kT}{\pi f} \Phi U$$

Computation of the deformation balance given a beam wavefront (Vinet et al..)

$$\boxed{SX_{TN}^{\mathrm{TEM}_{00}} = \frac{4k_B T}{\pi f} \Phi \frac{1-\sigma^2}{2\sqrt{\pi} Y w}}$$

Poisson r.

e.g. for Virgo

$$SX_{TN}^{1/2} = 10^{-19} \sqrt{\frac{100}{f}} m / \sqrt{Hz}$$

EMVESF270710

A relevant issue for AdV detectors !

Virgo, mechanical TN

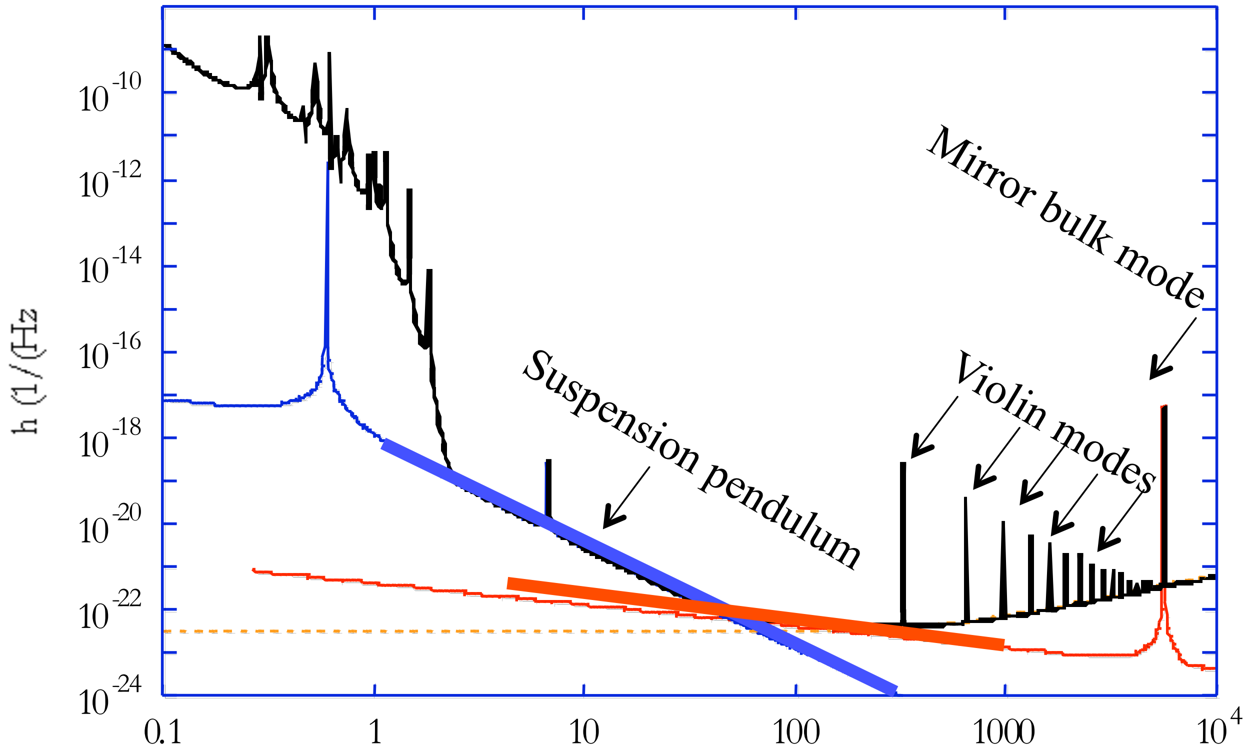

$$X_{tot}^2 = X_{pend}^2 + X_{mirror}^2 + X_{viol}^2$$

HW experiments !

ASSEMBLING PAYLOAD WITH MONOLITHIC SUSPENSION AND QUASI-FLOATING MARIONETTE.

$$\lambda = \sqrt{\frac{EJ}{T}}$$ Marionette wire bending

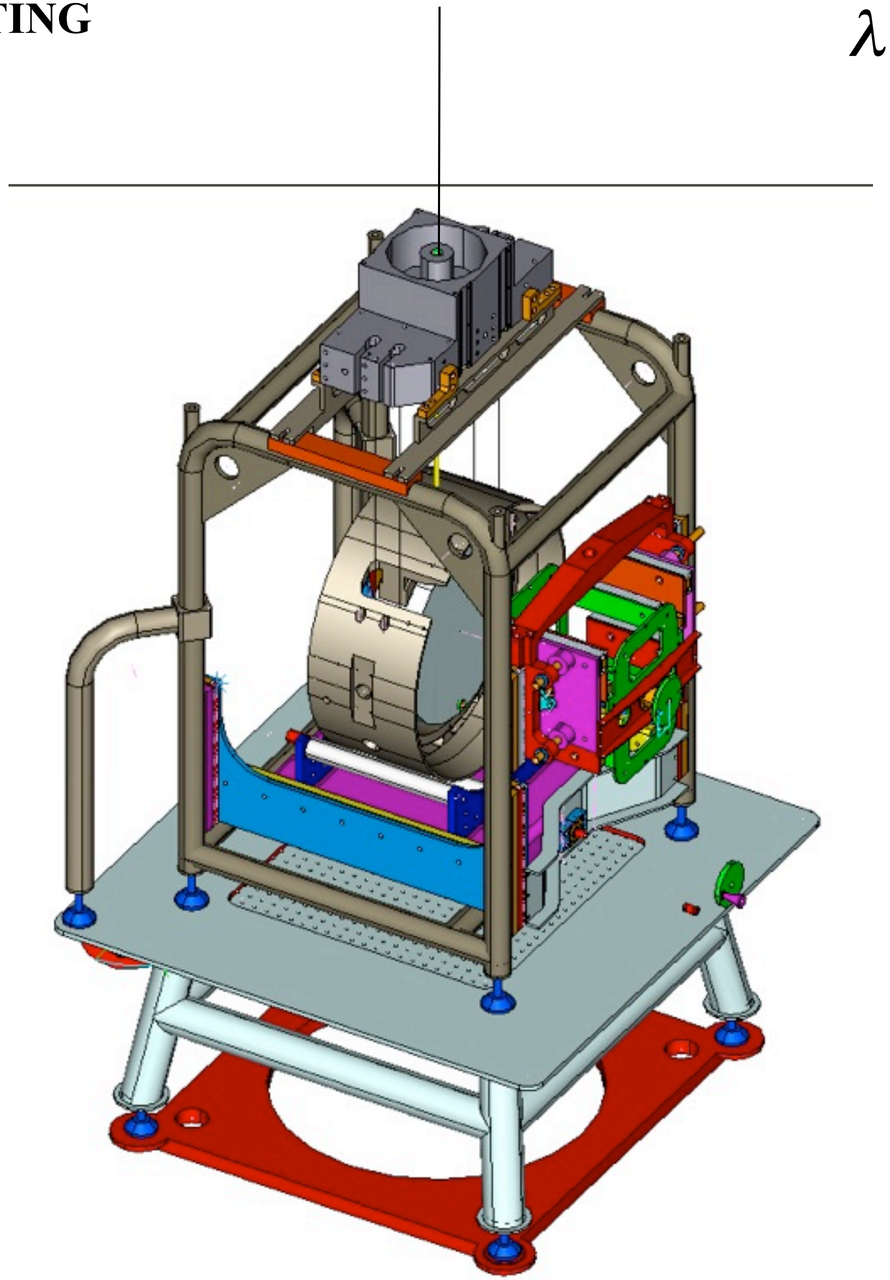

Transparence effects

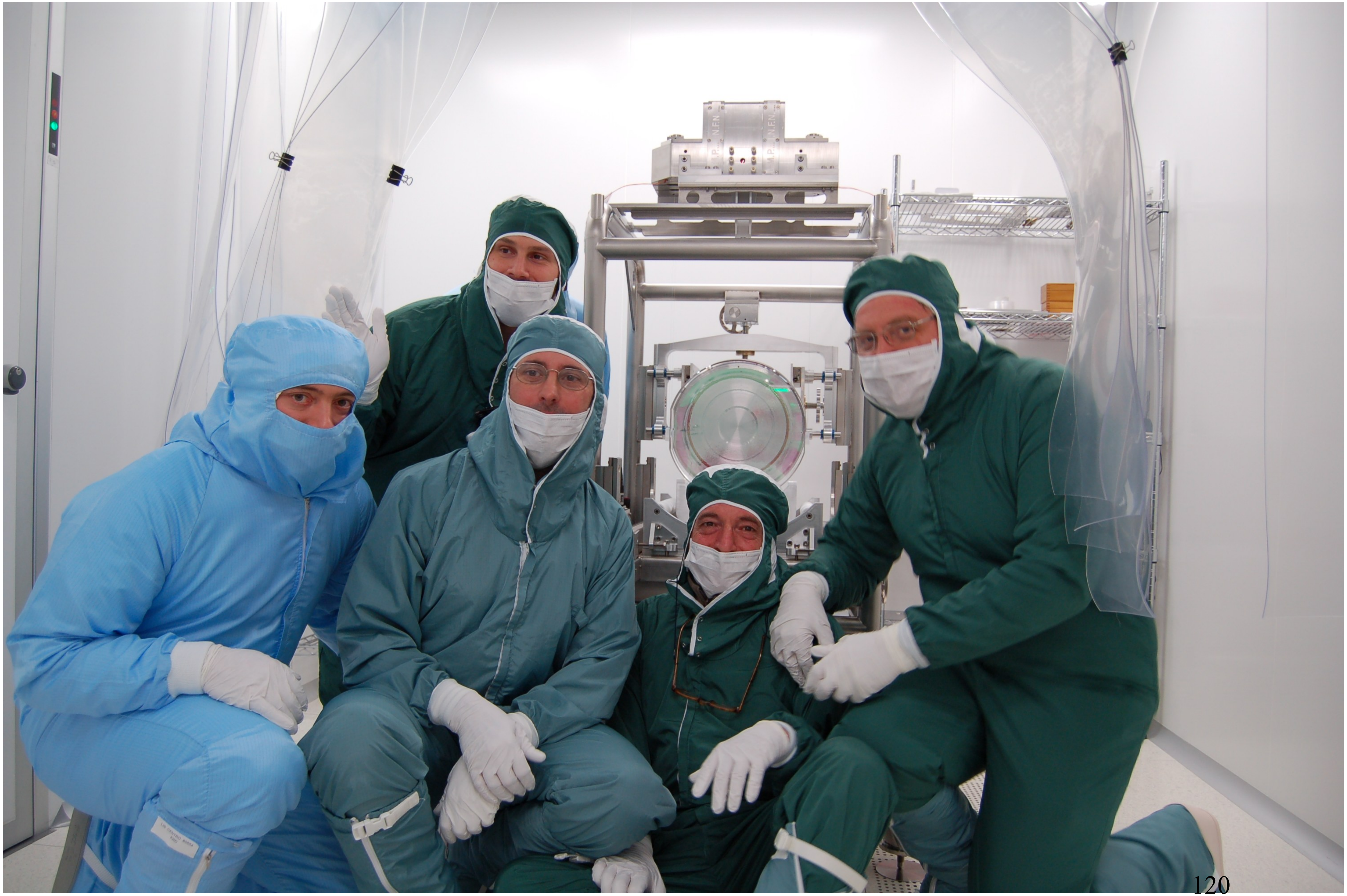

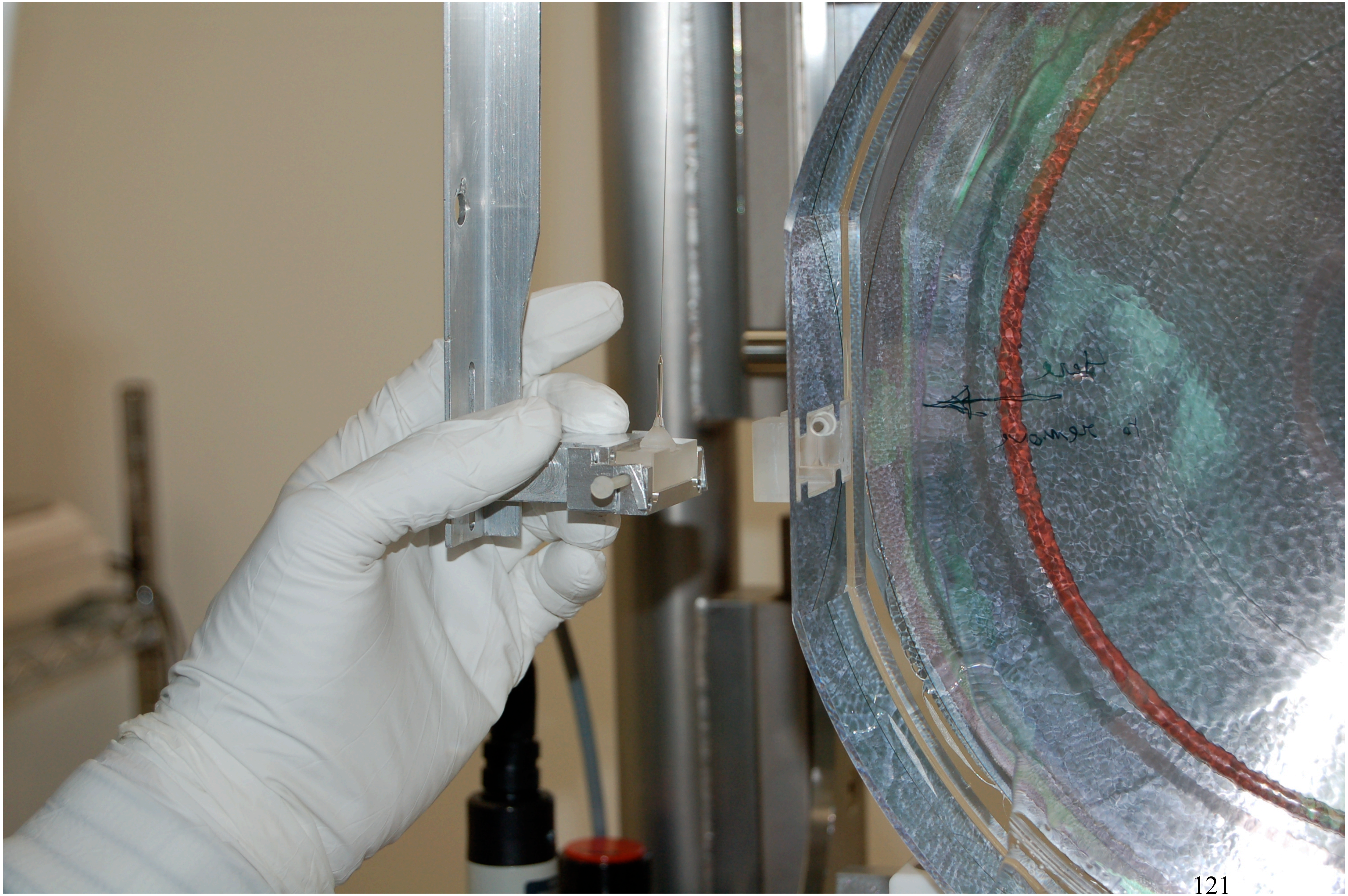

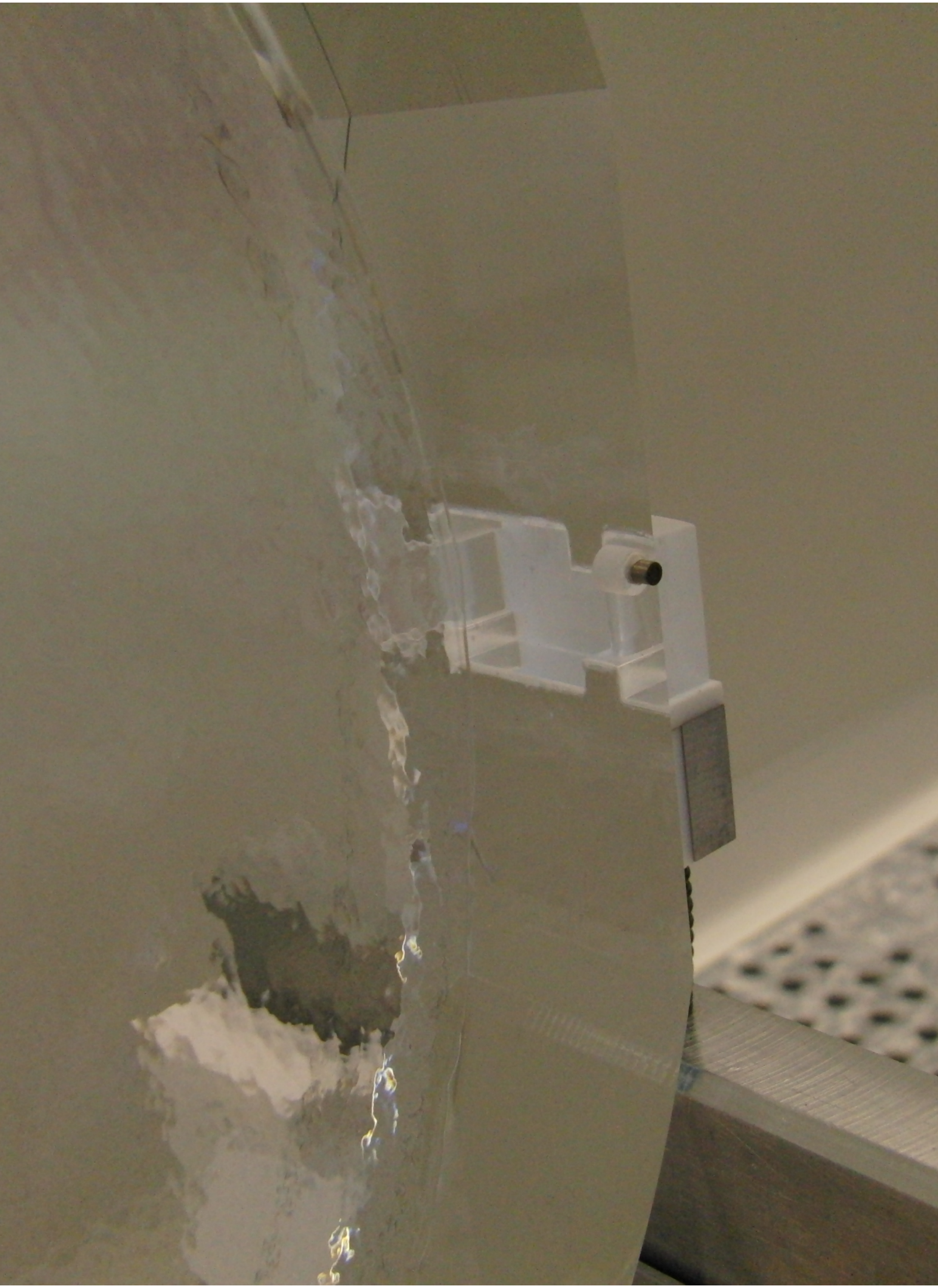

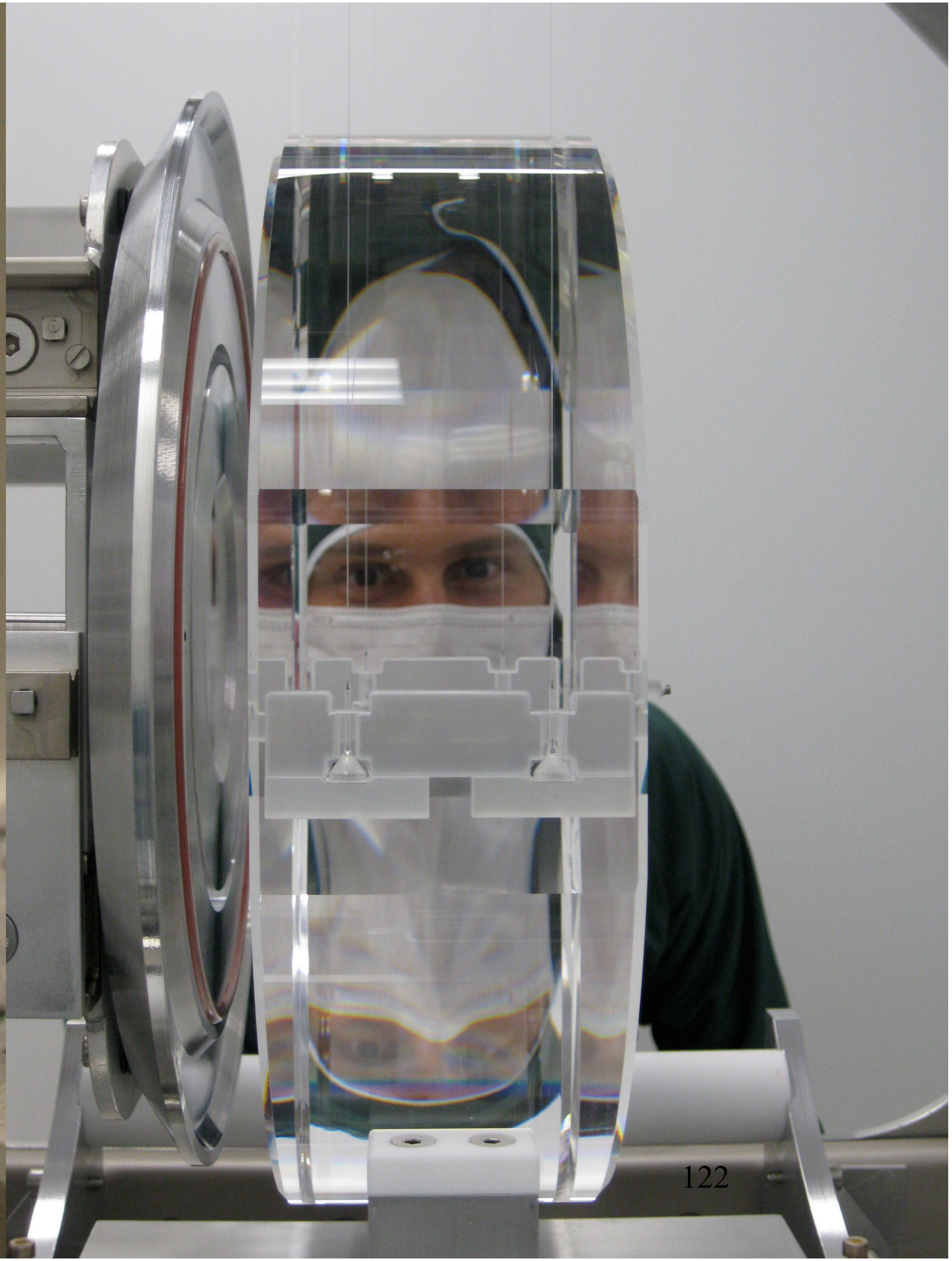

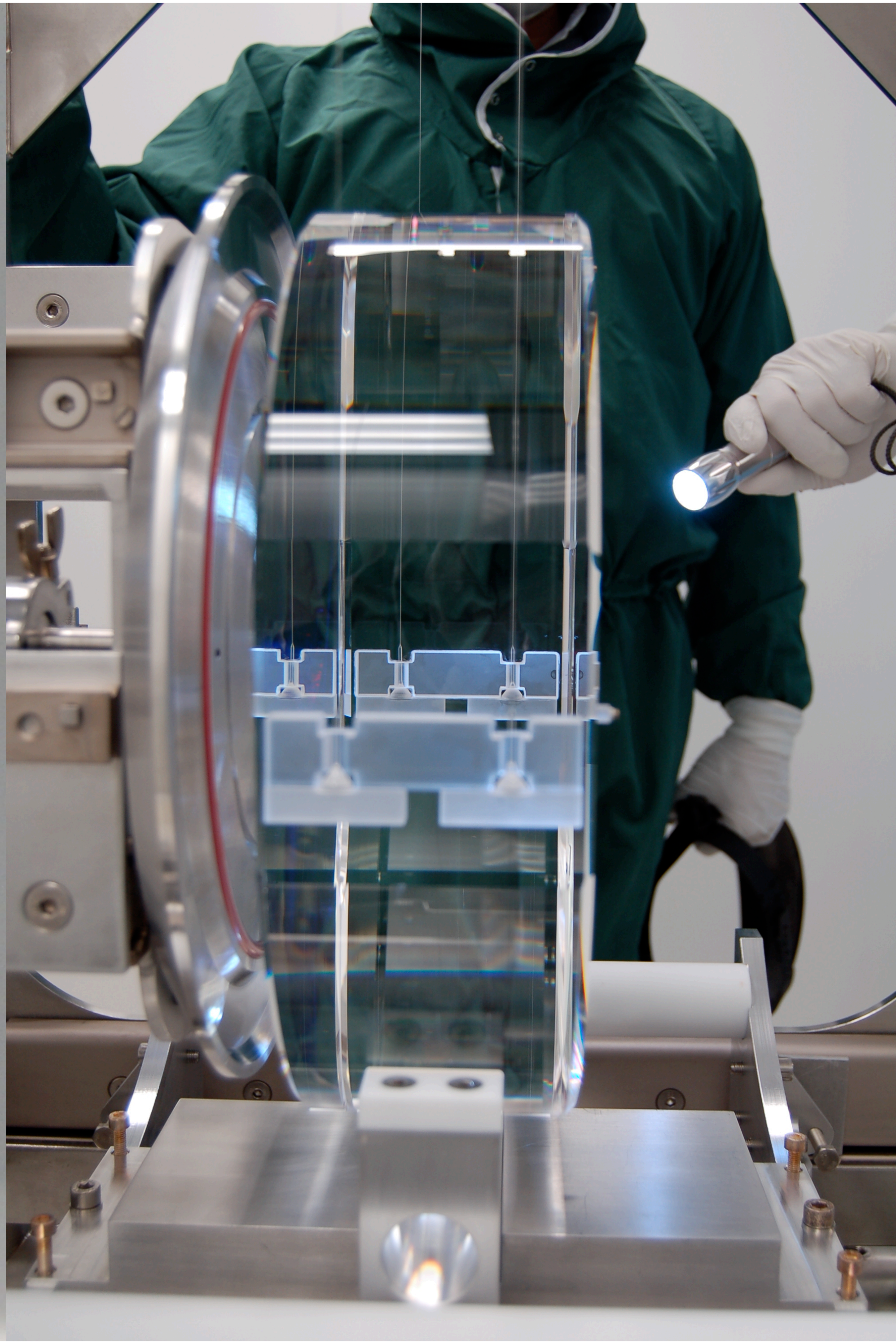


- Active-suspensions in the trolley !
- Data-logger to monitor humidity and temperature
- H-V accelerometers

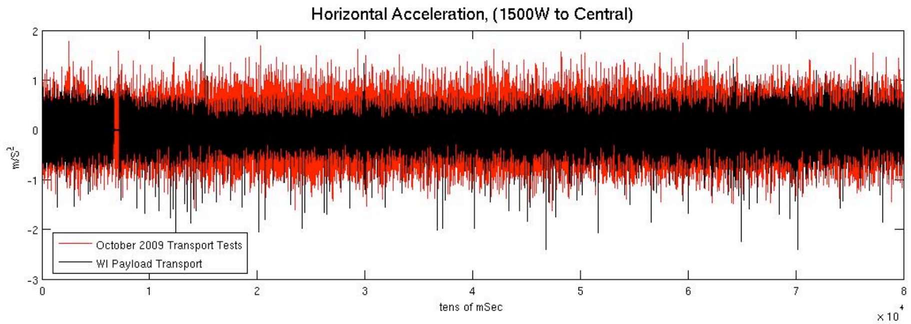
Horizontal Acceleration, (1500W to Central)
m/S^2
October 2009 Transport Tests
WI Payload Transport
tens of mSec
$\times 10^4$

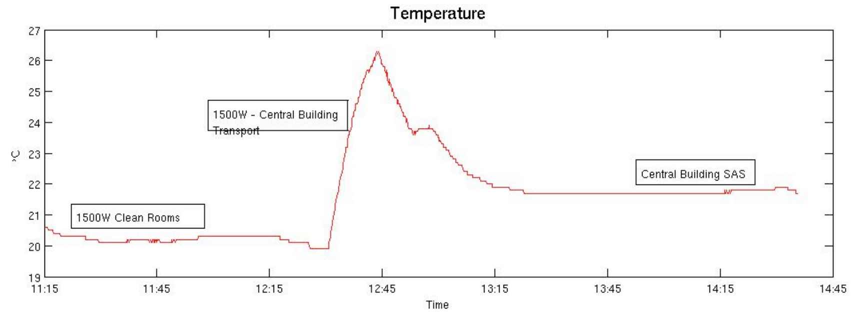
Temperature
°C
1500W - Central Building Transport
Central Building SAS
1500W Clean Rooms
Time

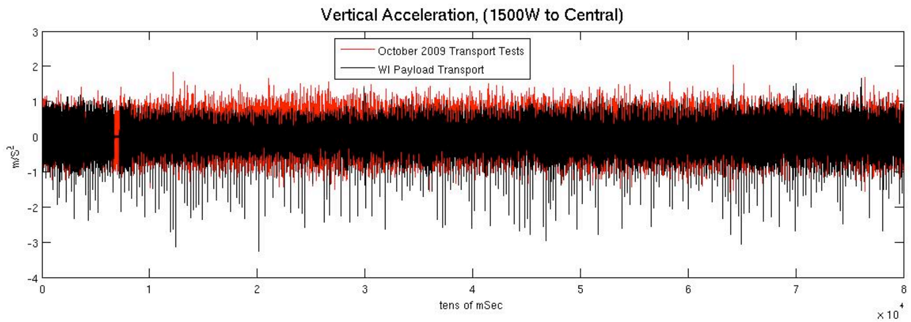
Vertical Acceleration, (1500W to Central)
m/S^2
October 2009 Transport Tests
WI Payload Transport
tens of mSec
$\times 10^4$

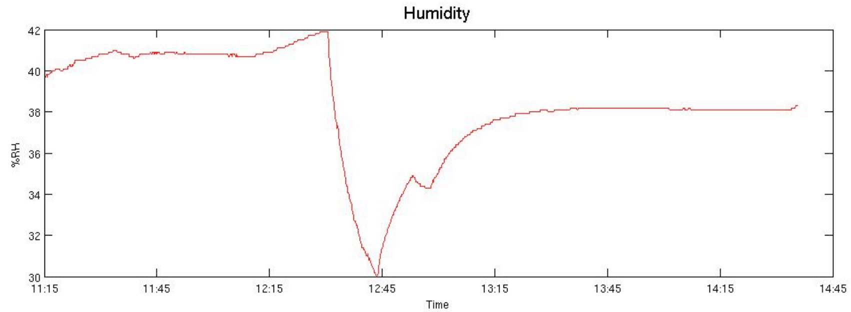
Humidity
%RH
Time

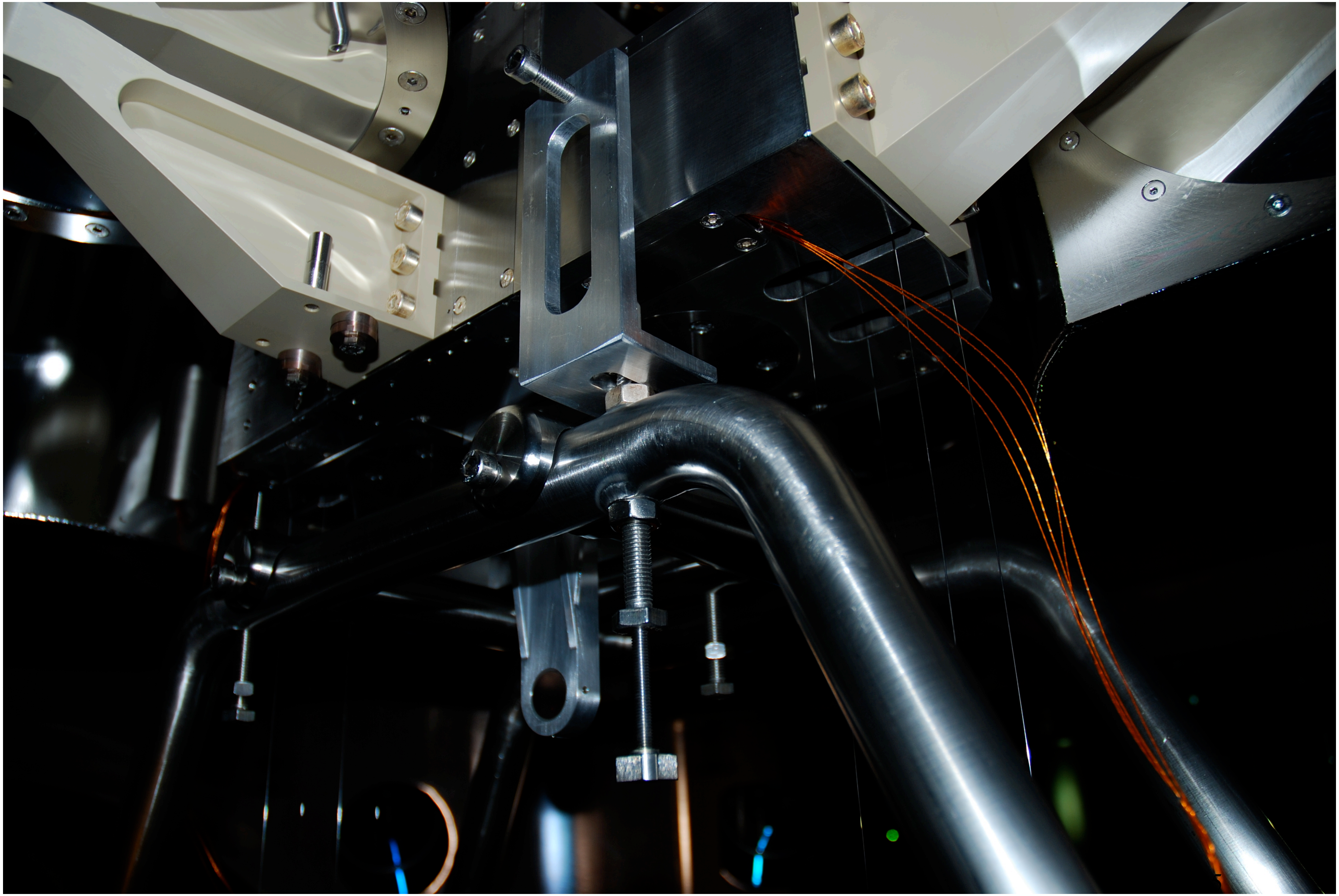

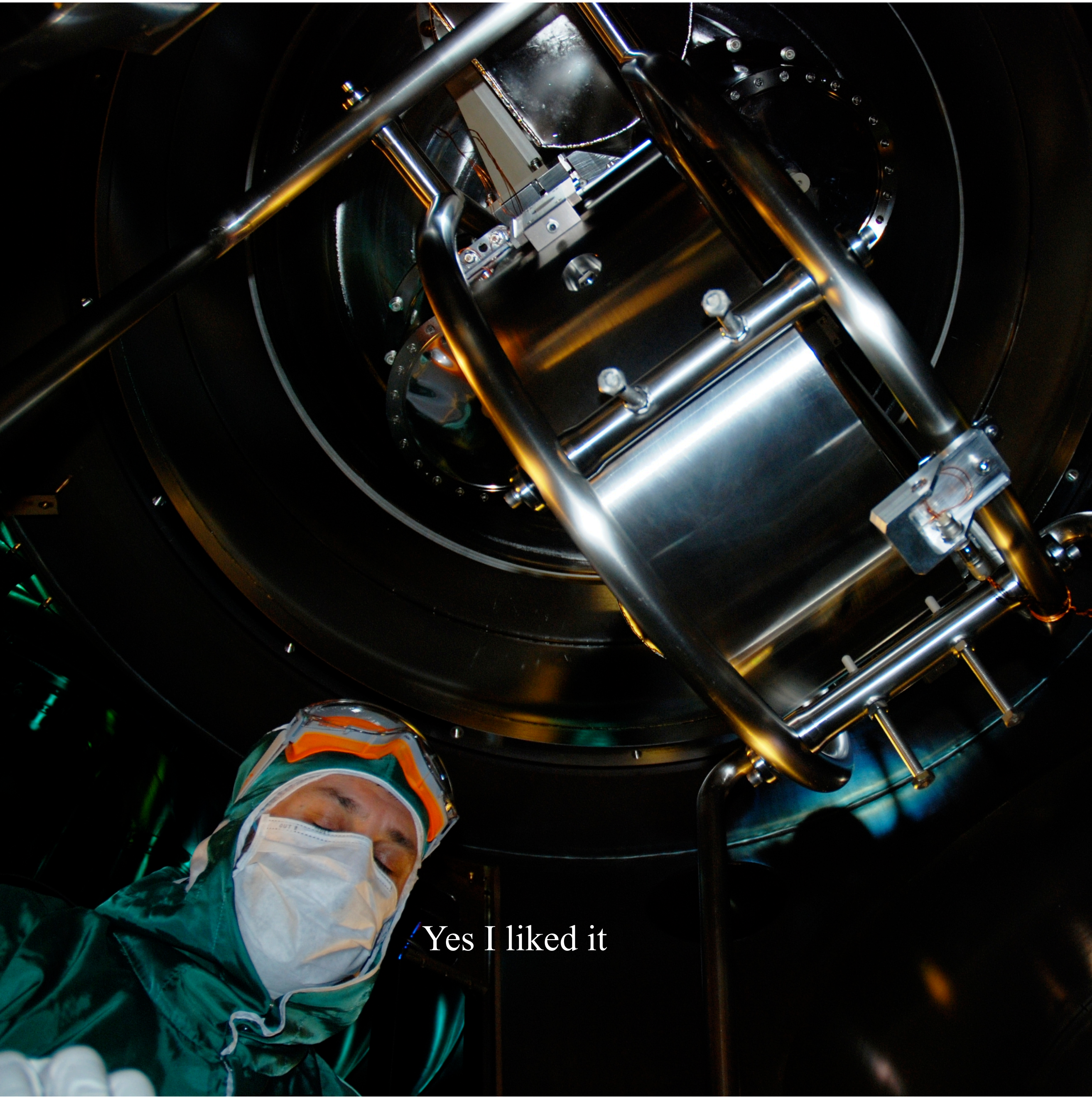
Yes I liked it